GAMMA DETECTION AND NEUTRON INDUCED RADIOACTIVITY

JOCHAN JOSEPH

DEPARTMENT OF PHYSICS
SCHOOL OF PHYSICAL SCIENCES
NEHU

A DISSERTATION

SUBMITTED
IN
PARTIAL FULFILMENT OF THE REQUIREMENT OF THE DEGREE OF

MASTER OF PHILOSOPHY

To

THE NORTH-EASTERN HILL UNIVERSITY

SHILLONG

INDIA

1992

in memory of
my
loving sister

Phone :
Grams : NEHU

North - Eastern Hill University

Bijni Complex
Bhagyakul, Shillong - 793003 (Meghalaya)

Department of.....

M.Phil. Course Grade Certificate

This is to certify that Mr.JOCHAN JOSEPH has satisfactorily completed and obtained the following grades for his M.Phil. courses.

	COURSES	GRADES
1.	M.Phil. Nuclear Physics (Course No:543D)	O
2.	Nuclear Reactions-I (Course No: 606)	O
3.	Numerical Methods as Applied to Computers (School Level Course)	O
4.	French Language (University Level Course)	O

Dr. Raghuvir Singh
(Prof. & Head)
Physics Department

Professor and Head
Department of Physics
North-Eastern Hill University
Shillong-793003

Phone :
Grams : NEHU

North - Eastern Hill University

Bijni Complex
Bhagyakul, Shillong - 793003 (Meghalaya)

Department of.....

Dr. Raghuvir Singh
Professor, Physics Department

CERTIFICATE

This is to certify that the dissertation entitled "*GAMMA DETECTION AND NEUTRON INDUCED RADIOACTIVITY*" submitted by Mr. JOCHAN JOSEPH in partial fulfilment for the requirement of the degree of Master of Philosophy of North-Eastern Hill University, Shillong, embodies the record of bonafide research carried out by him under my supervision.

This work has not been submitted for any other degree to this or any other university or institute.

Date : 24/6/92
Place: Shillong

Dr. Raghuvir Singh
(Supervisor)

Acknowledgement

I take this opportunity, with immense pleasure to express my deep sense of gratitude and thanks to my respected teacher and supervisor, Dr.Raghuvir Singh, Professor and Head, Department of Physics, North-Eastern Hill University, Shillong, for introducing me to this subject and giving me constant encouragement, advice and guidance in undertaking this work, without which this work would have not been possible.

I also wish to acknowledge Dr.D.T.Khathing, Professor and Head, R.S.I.C, North-Eastern Hill University, Shillong and Prof.C.S.Shastry, Dean, School of Physical Sciences, North-Eastern Hill University, Shillong for their interest in the progress of my work.

I am extremely grateful to my senior labmates Dr.M.Sudarshan and Dr.V.R.Rao for the fruitful discussions and valuable suggestions which helped me in completing this work. I wish to thank Mr.S.Banarjee for providing the APPLE and LSF codes to our laboratory which helped me in doing my analysis.

This column remains incomplete if I forget to acknowledge my other close friends, Srinivas, Jayanta, Felix Basabadutta and Susan for their selfless help during this work. There are many other friends to be acknowledged whose names are not mentioned here. But I humbly thank them all.

I feel happy to acknowledge my uncle, C.T.Sakaria, and all my relatives for extending all possible help. A large debt

of gratitude is owed to late Rev.Dr.JOSEPH KARIMPALIL and to my teachers in St.Alosius College with whom I was associated.

Last of all, I would like to thank my grand parents, parents and all my family members for giving me continuous encouragement and help which enabled me to complete this work.

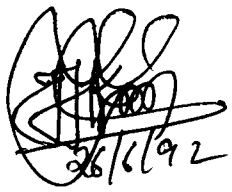

(JOCHAN JOSEPH)

CONTENTS

Chapter I		Introduction	1-6
Chapter II		Gamma detection - A Review	7-37
	II.1	Introduction	7-9
	II.2	Types of Gamma Detectors	9-33
	II.3	Determination of gamma ray intensities	33-34
	II.4	Relative merits of NaI(Tl) and Ge(Li) gamma ray spectrometers	34-35
Chapter III		Neutron Activation Analysis (NAA) and Full Energy Peak Efficiency (FEPE) of $157cm^3$ HPGe and 2"x2" NaI(Tl) detectors	38-88
	III.1	Introduction	38-39
	III.2	Neutron Activation Analysis (NAA)	39-59
	III.3	Determination of the Full Energy Peak Efficiency (FEPE) of a $157cm^3$ HPGe and a 2"x2" NaI(Tl) detectors	60-69
	III.4	Employment of a new method for calibrating the HPGe detectors	70-74
	III.5	Least Squares Fit of the FEPE data of a 2"x2" NaI(Tl) detector to the Analytical Functions	75-80
	III.6	Variation of measured resolution with gamma energy	81-84
	III.7	Concluding Remarks	85-86

Chapter I

INTRODUCTION

The information concerning the nuclear structure and nuclear forces was obtained mainly from the study of radioactive decays and nuclear reactions. Slowly the main interest in nuclear physics shifted from the investigation of nuclear force to that of nuclear structure. Gamma ray spectroscopy is often used in the field of radioactivity and several developments in nuclear theories were ushered in by the low energy phenomena occurring in this field. The absorption and scattering of nuclear radiation in matter leads to the study of phenomena which branch out in many directions. Most of the nuclear physics research depends on the measurement of the energy of radiations emitted by nuclei undergoing energy transitions. As a result, nuclear structure

investigations greatly depend on the techniques of accurate energy measurements.

Scintillation counting, one of the oldest radiation techniques, was outdated by the rapid growth and development of electronic counting techniques with the gas filled chambers. But it regained its former dominating role with the availability of the sensitive photomultiplier tube (PMT). On the other hand semi-conductor detectors with their outstanding progress more or less replaced the gas filled counters because of their increased stopping power and occassionally the scintillation counter by their excellent energy resolution in many nuclear science applications of high energy resolution gamma ray spectroscopy.

A brief review of gamma ray spectroscopy with thallium activated sodium iodide (NaI(Tl)) and germanium detectors (both Ge(Li) and HPGe) alongwith their characteristic properties like response function, linearity, resolution and detection efficiency etc., is given in chapter II. Scintillation spectroscopy began with the discovery and development of high efficiency NaI(Tl) detectors [1]. The availability of multichannel analysers developed them from an instrument for detection of radiation to a device for measuring the energy and intensity of that radiation. Along with the properties of this detector, the necessity and advantages of using large NaI crystals are also mentioned in the same chapter.

The development of semi-conductor materials for radiation detection boosted the gamma ray spectroscopy and have replaced NaI(Tl) detectors in many investigations due to their

excellent energy resolution. It was demonstrated that by an ion drifting technique, large size germanium detectors could be manufactured. Initially the available detectors were of comparatively smaller size having lower efficiency. Therefore, Freck and Wakefield [2] (see ref [1]), through the process of Lithium compensation on p-type germanium, developed lithium drifted Germanium (Ge(Li)) detectors for gamma ray spectroscopy. Moreover a major contribution to semi-conductor gamma ray spectroscopy was the development of high purity germanium resulting in fabrication of thick germanium detectors without lithium compensation [1,3].

Since the gamma ray interactions are identical in the case of Ge(Li) as well as HPGe detectors, the characteristic properties are the same for both detectors of same size and shape. This is discussed in chapter II alongwith the methods for continuum reduction. A discussion on the determination of gamma ray intensities with gamma detectors has also been given in the last part of this chapter. The relative merits of NaI(Tl) and germanium gamma ray spectrometers are also discussed in the end of this chapter.

Neutron Activation Analysis (NAA), as a technique, was developed by Hevesy and Levy [4] and it is based on the interaction of neutrons with an isotope of interest giving rise to a radioactive product nuclide whose concentration can be estimated by measuring the characteristic radiations emitted by the product(s) using suitable detectors (see ref [5]). The study of nuclear reactions induced by neutrons yielded significant

contributions to our knowledge of nuclear force, nuclear reaction mechanism and practical applications of nuclear physics. In short NAA is based on the quantitative detection of gamma rays produced in samples by neutron induced radioactivity.

This technique has been employed for measurement of half-lives of short lived isotopes such as ^{116m}In, ^{27}Mg, ^{51}Ti and ^{28}Al obtained by bombarding ^{115}In, ^{27}Al, ^{51}V and ^{28}Si respectively with neutrons. A study of elemental analysis of some samples (such as SRM 1633a and coinage metal) has been done by making use of this technique. A reinvestigation of the relative intensities of gamma rays emitted by ^{116m}In has also been done. A detailed description of the experimental procedure for the above applications of NAA are given in chapter III alongwith the description of the 5 Ci ^{241}Am-Be neutron source, and the 157 cm^3 HPGe coaxial detector with its associated electronics.

For many purposes the accurate determination of photon intensities can be of greater value than the determination of energies. Precise measurement of the gamma ray intensities with gamma detector necessitates an accurate determination of the Full Energy Peak Efficiency (FEPE). Therefore, its determination with a high degree of accuracy is very important. The experimental determination of FEPE at discrete energy values is a simple but tedious procedure with accuracies within a few percent. This could be done by employing a set of calibrated standard gamma sources of known strengths which cover a wide range of energies. The determination of the FEPE of a 157 cm^3 co-axial HPGe detector and that of a 2"x2" NaI(Tl) detector has been discussed in this

chapter. It is also possible to calculate (empirically) the FEPE of the germanium detectors by knowing its dimensions and the required absorption co-efficients. Ray Gunnik [6] developed a method for determining the FEPE of co-axial germanium detectors by using manufacturers specifications. We employed this method for the determination of FEPE of our 157 cm^3 HPGe co-axial detector.

The experimental determination of FEPE is somewhat complicated as one needs to maintain good and reproducible geometry and to account for the absorption effects. The semi-empirical approach provides a reasonably accurate way to obtain the FEPE in which all geometrical and relative scaling factors may be treated empirically. An investigation regarding the validity of analytical functions for the FEPE of a 3"x3" NaI(Tl) detector has been done recently by Sudarshan [7]. We have also discussed the validity of some analytical functions for representing the FEPE data of a 2"x2" NaI(Tl) detector in the energy region ranging from 59.5 to 1408.03 KeV. Along with this, the variation of the measured resolution with photon energy for the 157 cm^3 HPGe coaxial detector and two NaI(Tl) detectors (3"x3" and 2"x2"), are described in the same chapter.

References

1. S.S.Kapoor and V.S.Ramamurthy, "*Nuclear Radiation Detectors*", Willey Eastern Ltd. New Delhi
2. D.V. Freck and J. Wakefield, Nature, 193 (1962) 669
3. W.L.Hansen, Nucl.Instr.and Meths., 94 (1971) 377
4. G.V.Hevesy and H.Levy, Kgl.Danske.Videnskab.Mat.Fys.Medd., 14 (5) (1936) 3
5. V.R.Rao, Ph.D Thesis "*Study of an external beam irradiation system for liquids in charged particle activation analysis*", NEHU, Shillong (1990) (unpublished)
6. Ray Gunnick, Nucl.Instr.and Meths., *Physics research*, A299 (1990) 372
7. M.Sudarshan, Ph.D Thesis "*Bulk Elemental Analysis by Neutron Inelastic Scattering and Efficiency of Gamma Detectors*", NEHU, Shillong (1991) (unpublished)

CHAPTER II

GAMMA DETECTION - A REVIEW

II.1 INTRODUCTION

In the early 1950's high resolution gamma ray spectrometers, like crystal diffraction spectrometers and the external conversion magnetic spectrometers, were developed as tools for doing gamma ray spectroscopy. Both had fairly good resloution but due to low efficiency their applicability was limited. The discovery of scintillators, especially the thallium activated NaI crystals, revolutionised the gamma ray spectroscopy of that period with high efficiency and moderately good resolution. The spectrometer gap, between the high resolution instruments, whose applications were limited due to low

efficiency, and scintillators, whose applications were limited due to low resolution, was bridged with the advent of semi-conductor detectors which started a new era in the modern gamma ray spectroscopy. In the following sections we shall briefly review the subject of gamma detection.

Detection of nuclear radiations and measurement of their characteristics constitute the fundamentals of experimental nuclear physics. Their detection is possible only through their interactions with matter. The methods of detection are, in general, based on the process of excitation and ionization of atoms in the material as a result of the passage of radiation. But the gamma detection depends on the interactions in which all or a part of the gamma ray energy is transferred to the electron in the absorbing material because the gamma ray is not able to initiate such process by itself due to its neutral nature. The information about the incident gamma rays is provided by these fast electrons created in the interaction process because the primary gamma ray photons are "invisible" to the detection material.

Among the interaction mechanisms only three have real significance in gamma ray spectroscopy. They are (i) photoelectric effect, which is predominant in the low energy gamma ray region, and leads to the production of an electron by complete absorption of the incident photon energy leaving only x-rays from the residual atoms; (ii) pair production process, which is predominant in the high energy gamma ray region, and leads to the production of an electron-positron pair by the absorption of a photon only if the energy of the photon is greater than twice the rest mass

energy of electron; (iii) Compton scattering, which is the most probable process in the intermediate energy range, leads to the production of a recoil electron and a scattered gamma ray photon. This scattered photon may escape from the material or may further be absorbed. Complete absorption of the gamma rays takes place in the case of materials of high atomic number (Z) because the first two processes increase rapidly relative to the Compton effect with increase in Z leaving only x-rays from photoelectric process and 511 keV photon from pair-production process. The Compton scattering process sometimes results in hard photons leading to a possibility of escape of some of the gamma ray energy.

For a detector to function as a gamma ray spectrometer it should be a good conversion medium (for incident gamma to fast electrons) and also be a conventional detector for the secondary electrons. For efficient detection of gamma rays, the stopping power of the detector material should be high (in view of the low absorption coefficients of gamma radiation). Gamma ray spectroscopy is entirely based on two types of detector materials - scintillators and semi-conductors and their performance depends mainly on the energy resolution and detection efficiency.

II.2 TYPES OF GAMMA DETECTORS

Except for crystal diffraction spectrometers most of the devices and techniques used for the measurement of the gamma rays actually respond to or analyse the secondary electrons. Initially the detection of gamma rays was carried out using devices such as

Ionisation Chamber, Proportional and Geiger Müller Counters.

The other technique employed for the gamma ray spectroscopy was crystal diffraction spectroscopy, in which gamma rays were analysed directly by Bragg's reflection and detected with ordinary counters. Its applications are limited because of low efficiency. After the discovery of scintillators, the most widely used device for the detection and measurement of gamma rays were scintillation counters. The process of flourescence is the basis of the operation of a scintillation detector. The most widely used inorganic scintillators are NaI and CsI activated with thallium. The NaI(Tl) detectors have relatively good resolution and therefore, have been employed more often. In fact, till the advent/availability of the semi-conductor detectors NaI(Tl) detectors had been most widely used. We shall discuss these detectors in detail in the following sections.

II.2.1 NaI(Tl) Detector

The discovery and development of NaI(Tl) detector marked the begining of scintillation spectroscopy of gamma rays which was introduced by Hofstadter [1] and Hilne [2] (see ref [3]). The NaI crystal is water clear and hygroscopic whose emission spectrum overlaps with its absorption spectrum. Therefore, an activator, thallium (Tl) had been added in melt for shifting the emission spectrum to a longer wavelength side to avoid absorption and thereby rendering large scintillation light output. This discovery led to the modern gamma ray spectroscopy. The most appreciable

property of NaI(Tl) detector is its excellent light yield and its response to gamma rays which is more or less linear in a wide range of energy. Generally this detector is operated at room temperature.

Properties of Scintillation Gamma Ray Spectrometers

The technical refinement of the instrumental components and the availability of multichannel analysers (MCA) have developed the scintillation counter from an instrument for detection of radiation to a device for measuring the energy and intensity of that radiation with a relatively fair degree of accuracy. The performance of the gamma ray spectrometers depends on the following properties.

(i) Response Function

The fundamental property of the detector output to get an information about the incident radiation is the pulse height distribution. The availability of the NaI crystals in large sizes resulted in high interaction probabilities for gamma rays. The three interaction processes mentioned earlier may contribute to the response function. Because of the high atomic number of iodine a large part of the interaction will result in complete absorption of gamma ray energy (finally decided by the size of the NaI crystal and gamma energy) and thereby the fraction of the events lying under the full energy peak (FEP) in pulse height spectra is greatly increased. Even though the other materials, like CsI and BGO, have higher density and effective Z, NaI(Tl) have dominated

scintillation spectroscopy because of relatively high light output and shorter decay time.

The factors that influence the shape of the response function and its importance were given by Müller and Maeder [4] (see ref [5]). There are many events that influence the response function. If the secondary electron ranges are larger than the detector size a large number of electrons may leak from the detector material without full absorption of their energy and contribute to Compton continuum. Sometimes these secondary electrons might lose energy by the radiation of bremstrahlung photons. In photoelectric absorption the x-ray photons may also escape if it is taking place near the surface of the detector. With these escapes different categories of events are created and collected at the output of the detector system with an energy equal to the original gamma ray energy minus the escape energy. The secondary radiations like annihilation radiation (created when the positron from pair-production process comes to rest and annihilates with electron), the bremstrahlung emission (resulting from the decay of gamma ray sources by β^- emission), the back-scattered gamma rays (produced from the surrounding material), and other secondary radiations influence the recorded response function to a large extent.

(ii) Resolution

The energy resolution of a detector is conventionally defined as

$$\text{Resolution, } (R) = \frac{\text{FWHM}}{H_o}, \qquad (1)$$

where FWHM : full width at half maximum of the FEP and

H_o: mean pulse height corresponding to the same peak (i.e. the peak position)

The primary factor affecting the resolution of the detector is the line broadening due to the statistical fluctuations in the conversion process of incident gamma ray energy into free electrons. Statistical broadening of the peaks of mono-energetic gamma ray can be calculated by considering each conversion process as a Poisson process. By assuming Gaussian shape of the peak, the resolution is given by Poisson statistics as

$$R \approx 2.35/N^{1/2}, \qquad (2)$$

with N as the number of charge carriers created. But the carefully measured value of R usually turn out to be less than the predicted minimum value given by eqn.(2). This observed variance in statistical fluctuation is accounted for by introducing a factor 'F' defined as

$$F = \frac{\text{observed variance}}{\text{Poisson predicted variance}}$$ in the number of charge carriers.

This factor, F is known as the fano factor. Therefore, R becomes,

$$R = 2.35\ [F/N]^{1/2}, \qquad (3)$$

F = 1, for scintillation detectors

F << 1, for proportional counters and semi-conductor detectors.

Considering the dominance of statistical broadening of peak among the potential sources, the variation of the resolution with photon energy can be declared by saying that FWHM of the peak is directly proportional to the square root of photon energy and

the average pulse height produced is proportional to the photon energy. With this information eqn.(3) can be written in another form (using eqn.(1)) as

$$R = \frac{K}{E_\gamma^{1/2}}. \qquad (4)$$

Taking logarithm on both sides

$$\ln R = \ln K - (1/2)\ln E_\gamma. \qquad (5)$$

Fig.II.1 gives a plot of experimental value of R as a function of E_γ for a NaI(Tl) detector [6]. From this figure it is clear that non-statistical potential sources also contribute to the peak broadening because the slope is not as steep as predicted. So eqn.(4) has to be modified to represent the measured data as follows.

$$R = \frac{(\alpha + \beta E_\gamma)^{1/2}}{E_\gamma}, \qquad (6)$$

where α and β are constants which depend on the scintillator-photomultiplier combination.

(iii) Linearity

In all scintillators the amount of light generated per unit energy loss (dL/dE) depends on the type of particle and its kinetic energy. In fact dL/dE is a constant, independent of particle energy for an ideal spectrometer. Therefore, the response function of the scintillator is linear, as the light yield is directly proportional to the incoming particle energy. Fig.II.2 depicts the differential linearity measured for a NaI(Tl) detector [5]. In gamma ray spectroscopy, mono-energetic gamma rays produce a cluster of secondary electrons with different energies. Therefore, there will be some non-linearities with photon energy,

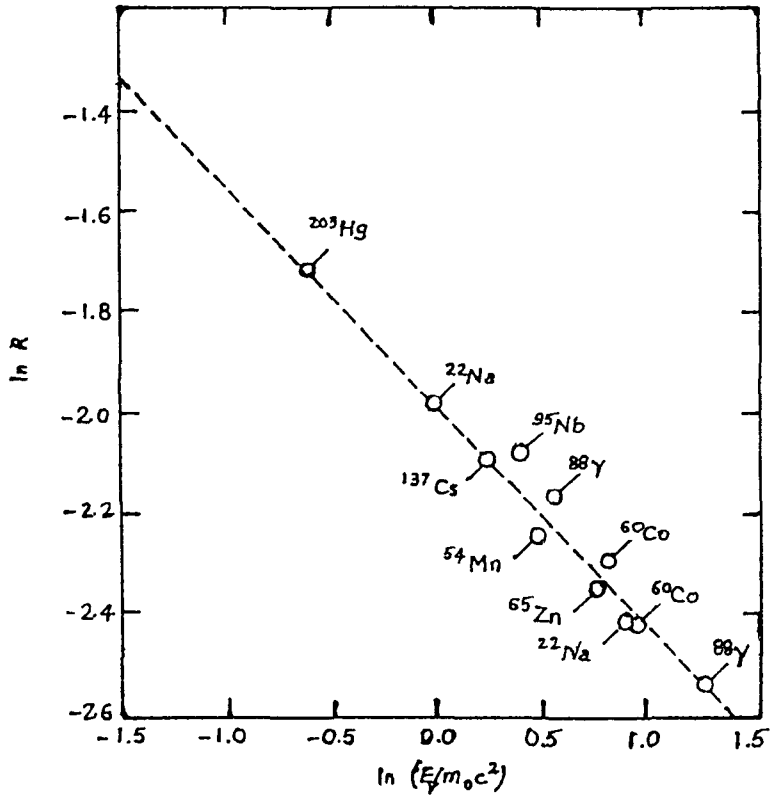

Fig.II.1 Experimentally measured resolution R for various gamma ray energies E_γ from a NaI(Tl) detector.

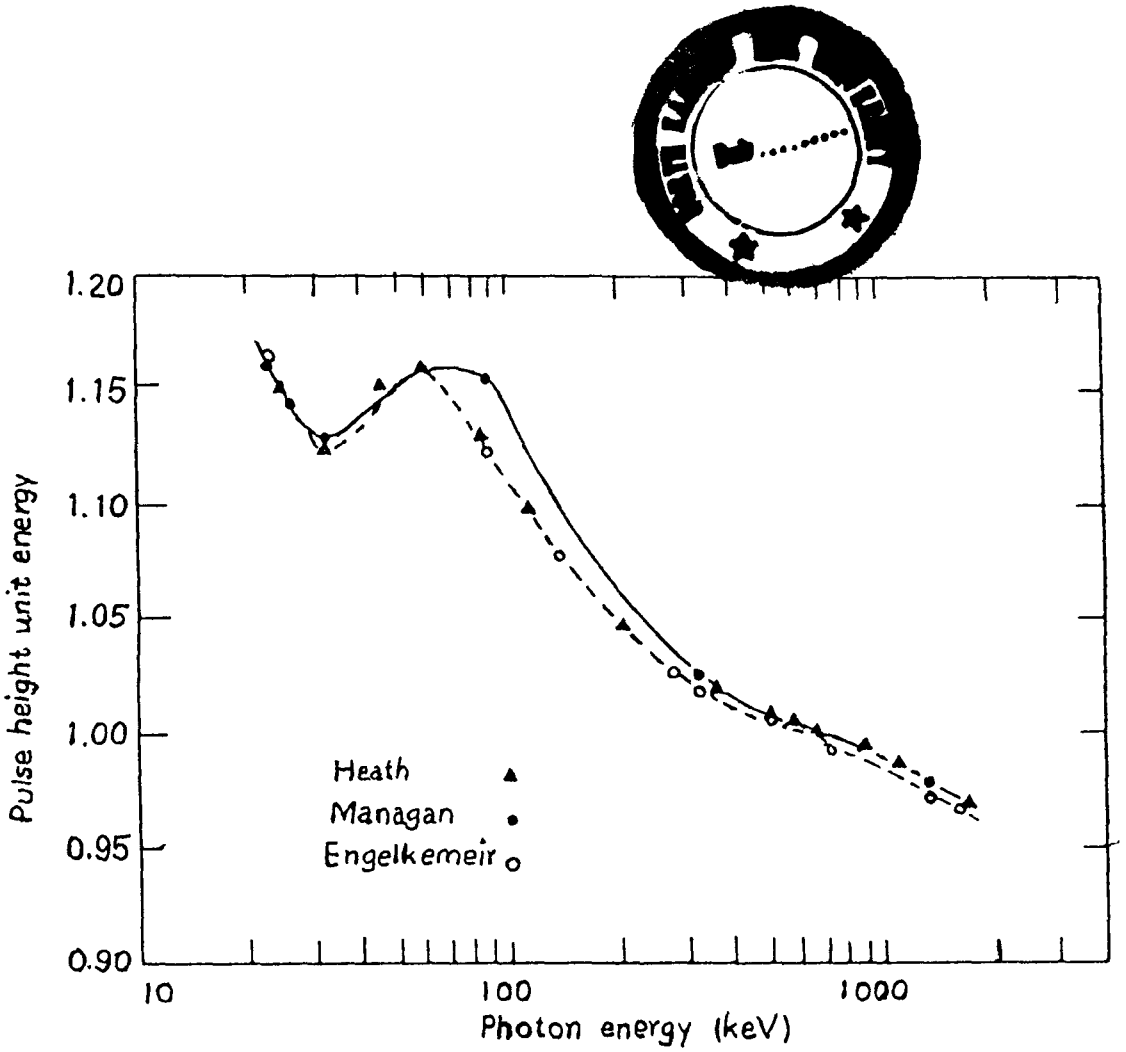

Fig.II.2 Differential linearity measured for a NaI(Tl) detector.

but it is closer to being linear.

(iv) Detection Efficiency

For a given detector the gamma detection efficiency depends on the cross section for the three processes (photoelectric, compton scattering and pair-production) via which the gamma rays interact with the detector material. The detection efficiency of the scintillator of thickness 'd' and linear absorption coefficient 'μ' (when gamma rays of a certain energy are incident on it) is given by (which is the gamma ray interaction probability)

$$\varepsilon = 1 - \exp(-\mu d), \qquad (7)$$

Total intrinsic efficiency is obtained by integrating eqn.(7) analytically over all path lenghts 'd' for simple geometry. This analytical calculation is not so easy because of the complexity of the interaction events which contribute to the FEP. However, with Monte Carlo calculations the efficiency determination is possible. Such a calculation simulates the absorption of gamma ray photon with the knowledge of the probability of interaction process.

Experimental determination of the efficiency of the detector is a simple but tedious process. The absolute efficiency of the detector is given by

$$\varepsilon_{abs} = \frac{\text{Number of pulses recorded}}{\text{Number of radiation quanta emitted by source}}$$

But the intrinsic efficiency is given as

$$\varepsilon_{abs} = \frac{\text{Number of pulses recorded}}{\text{Number of radiation quanta incident on the detector}}$$

Intrinsic and absolute efficiencies are related through the solid

angle factor, and is given by

$$\varepsilon_{int} = \varepsilon_{abs} \left[\frac{4\pi}{\Omega} \right], \qquad (8)$$

with Ω as the solid angle subtended by the detector at the source and is given by

$$\Omega = \frac{\pi r^2}{d^2},$$

where r is detector radius and d is the source-detector distance.

The determination of efficiency is explained in detail in section III.3. The size and the physical nature of the source, and the absorption of the gamma rays in region between the source and detector affects the counting efficiency. NaI(Tl) is an important tool in the field of gamma ray spectroscopy because of its high detection efficiency, due to the availability of large size and high density. The absolute total efficiency for a 5.08cm x 5.08cm cylindrical NaI(Tl) detector at different positions of the source as a function of gamma ray energy [5] is given in Fig.II.3.

II.2.2 Large NaI Crystals

Developments in NaI(Tl) have taken place basically in the fields of increased crystal sizes and the reduction of impurities in the crystal itself. The interaction probabilities for gamma rays are quite high in case of NaI crystals due to the availability of large sizes and high density of the material.

If the mean path of secondary gamma radiation produced by the interaction of the original gamma rays is larger than or of

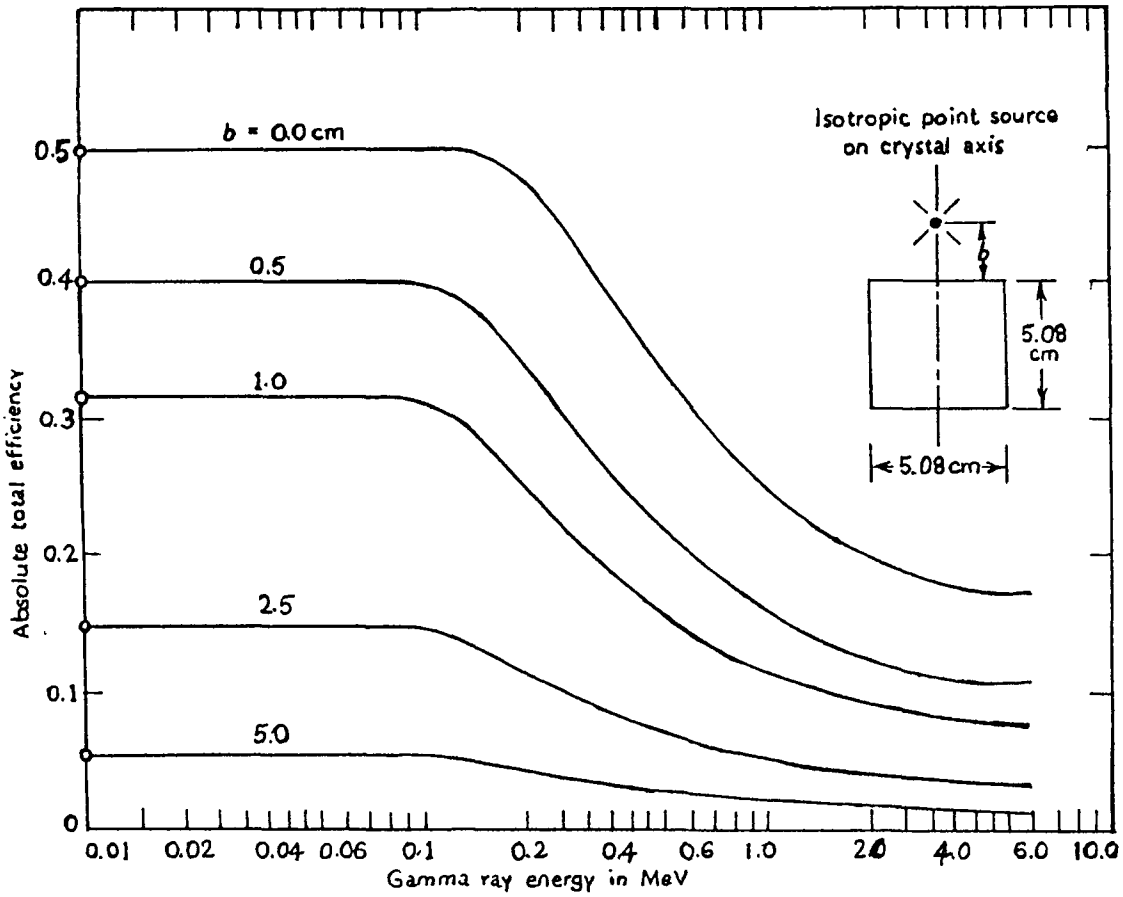

Fig.II.3 The calculated absolute total efficiency for a 5.08cm x 5.08cm cylindrical NaI(Tl) detector at different source locations.

the order of the crystal dimension there might be the possibility of escape of all the secondary radiations like Compton scattered gamma rays and annihilation photons (including the escape of one or both the annihilation photons) from the surface of the crystal without further interaction. That is why it is important to use large crystals to prevent the possibility of these types of escaping events,thereby rendering complete absorption through multiple interactions. These escape peaks can be further reduced by introducing the gamma rays at the centre through a column on the axis of the crystal. Further improvement can be made by using larger crystals [5] as shown in Fig.II.4 .

As regards the size of the crystals, it is now possible to prepare crystals of 13.5" diameter (or even greater) by crystal growth and this type of crystals can be utilised as anti-coincidence shields to reduce the background of smaller crystal assemblies. Perkins [7] has described a large annulus of NaI(Tl) 11.5" diameter by 12" high which contains two 6" diameter by 4" high NaI(Tl) crystal assemblies. For the detection of high energy gamma rays, NaI crystals, which consist of one or more single crystals of cylindrical shape can be used. The details of the interaction process of high energy gamma rays in matter, are discussed in refs. [8-10]. There are criteria to determine the dimension of the crystal for large absorption. It is observed that crystals 25 to 30 cm in length and about the same size in diameter can fully absorb most of the incident energies.

The merits of the large NaI(Tl) detectors are the large solid angle and the high detection efficiency. For large crystals

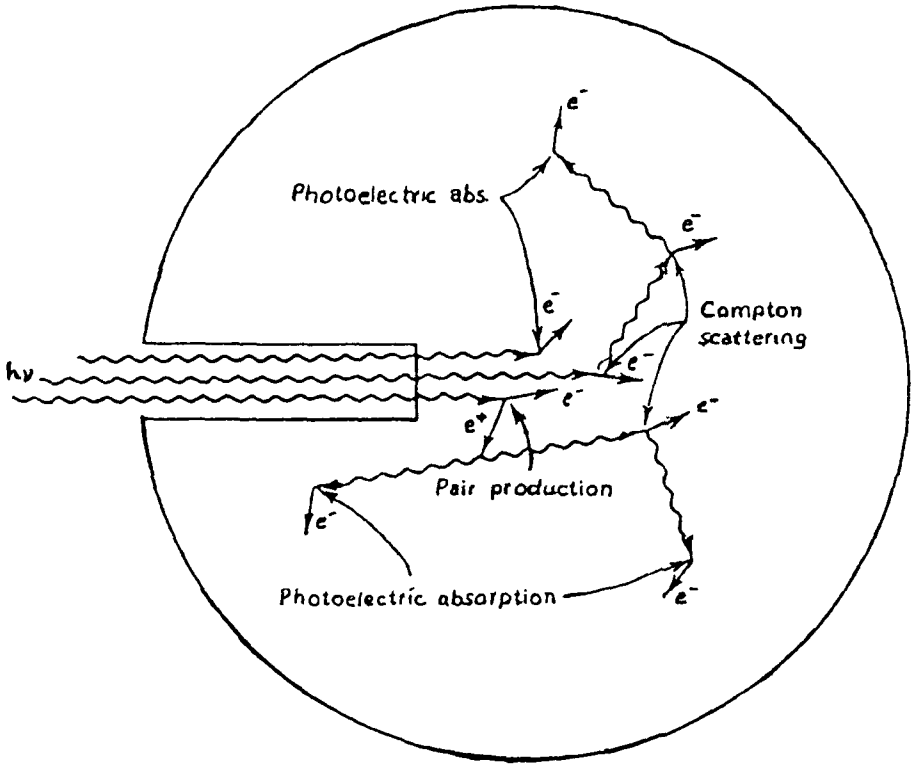

Fig.II.4 A represantative gamma ray interaction process in large crystals.

the resolution depends on its homogenity and uniformity of the output for each event in the crystal. Large NaI crystals need bulky shieldings around them which results in increase in the overall size of the detector.

II.2.3. Semi-Conductor Detectors

The development of semi-conductor materials for radiation detection boosted the modern gamma ray spectroscopy. Now a days NaI(Tl) detectors are being replaced for many investigations in gamma ray spectroscopy by semi-conductor detectors because of their excellent energy resolution. However, the high efficiency and large size of NaI(Tl) detectors will ensure their continued use. The disadvantage of smaller size and lower atomic number of semi-conductor materials is compensated to a great extent by its superior energy resolution. The combination of superior energy resolution and capability of recording simultaneous energy spectra enabled semi-conductor detectors to play a dominant role in many areas of nuclear physics as a tool for gamma ray spectroscopy.

To behave as an efficient detecting medium the semi-conductor material should have the following properties: (a) The average energy, (W), required to produce an electron hole pair and the fano factor, (F), which measures the fluctuation in the produced electron hole pairs, should be small. (b) Collection of the free charge carriers should be complete. This requires the carrier collection time to be less than its life time, and the

trapping length to be larger than the physical dimension of the detecting medium. (c) Application of the high electric field for collecting charge carriers produces large leakage current which prevents the measurement of tiny signals from transient currents thereby ruling out the use of conducting material and suggests the use of the insulating material. But these insulating materials do not satisfy the above two properties. So the use of high resistivity semi-conductors was recommended. All these requirements for semi-conductor detecting medium are satisfied by silicon (Si) and germanium (Ge). Leakage current can be reduced for these semi-conductors by providing "blocking contacts".

The semi-conductor detecting medium for an ionizing radiation should be devoid of free charge carriers. The necessary conditions for this purpose can be obtained by a reverse biased semi-conductor p-n junction which sweeps all the free charge carriers away from the junction. The electron hole pairs formed at the junction due to the interaction of incident radiation are immediately swept by the applied voltage and give rise to a current in the external circuit which can be considered as a measure of the energy of the ionizing radiation. This is the basic principle behind the working of a simple semi-conductor p-n junction detector.

Development of the Semi-Conductor Gamma Ray Detectors

It is not so easy to say when or under what circumstances semi-conductors were first employed to study the

behaviour of gamma rays. The diversity of common semi-conductor radiation detectors extends over two materials (Si and Ge) and over a wide range of resistivities and operating temperatures. The development of semi-conductor radiation detectors started in early 1956 with an examination of germanium surface barrier detector. But this had to be kept at liquid nitrogen temperature to reduce the noise due to leakage currernt from thermal excitations. A solution for this was reported by Davis [11] by introducing an analogous device with silicon which could function at room temperature since it has a larger band gap (1.1eV) than Ge (0.7eV). But in the sixties and seventies several types of semi-conductor detectors were developed, such as diffused junction detectors, fully depleted detectors and position sensitive detectors, which found their use in nuclear physics research, especially as charged particle spectrometers. The applications of the above mentioned detectors were restricted due to the non-availability of large size crystals.

The fabrication of the detector with much more thickness was demonstrated by Pell [12] (in 1960) by ion-drifting and this drift technique was exploited to fabricate the lithium drifted silicon detectors (Si(Li)) for gamma ray spectroscopy. Thereafter Freck and Wakefield [13] (in 1962) developed lithium drifted germanium, Ge(Li), detectors for gamma ray spectroscopy through the process of lithium compensation on p-type germanium [3]. The idea to construct a co-axial structure of a large volume Ge(Li) detector was proposed by Miller [14] in 1963 . Later in 1965 this idea was transformed by Tavandale [15] by constructing the large

volume Ge(Li) detector . As the atomic number of Si (Z=14) is less than that of Ge (Z=32) the requirement of good photo-electric absorption for gamma ray is met only by Ge (because photo-electric cross section varies as Z^5). So in high resolution gamma ray spectroscopy Ge(Li) detectors are preferred over Si(Li) detectors. Cooled Si(Li) detectors are useful in high resolution x-ray spectroscopy, where extremely low leakage currents are acceptable.

A major development in semi-conductor gamma ray spectroscopy was the development of high purity germanium (HPGe) detectors. By this development thick germanium detectors could be fabricated without lithium compensation [16]. With more efforts in material improvement, detector fabrication technology and electronic amplifying circuits made high resolution gamma ray spectroscopy a success in various areas of experimental nuclear physics. To discuss the exact behaviour of all semi-conductor detectors is a task too large for this review work. Therefore, we shall discuss only the high resolution germanium detectors (both Ge(Li) and HPGe).

II.2.4. Ge(Li) Detector

The gamma ray spectroscopy was indeed revolutionised by the advent of germanium semi-conductor detectors. Because of its high resolution, the analysis of gamma ray spectra in nuclear physics research and several applied areas in nuclear science are indebted to it. It is very difficult to achieve a depletion depth beyond 2-3 mm for Ge materials, with highest available

resistivity, by the application of a reverse bias near the breakdown.

Due to the nonavailability of large size germanium detectors its efficiency does not come to the expected value. So an attempt was made by Pell [12] to increase the active volume by fabricating germanium detector of large thickness through ion drifting. The basic principle behind this process is to create a thick region of compensated material in which a balance between acceptor and donor impurities is satisfied. To accomplish the desired compensation donor atoms must be used, as Ge material available with high purity is found to be p-type. In this regard Li is selected for the drifting process as it tends to form interstitial donors in Ge crystals. Moreover Li has favourable properties such as small ionic radius, high mobility and low ionization energy in Ge. The drifting of Li is possible, under the influence of strong electric field to the ionised Li atoms which are mobile at an elevated temperature. Germanium detectors fabricated by drifting Li in Ge crystals are called Ge(Li) detectors and these detectors have been in use for the past three decades or so.

The fabrication procedure of Ge(Li) detector was proposed by Hansen and Jarrett [17] and developed by Freck and Wakefield [13]. The fabrication process begins by evaporating Li on to or diffusing Li on the surface of the p-type Ge crystal at $425^{o}C$ for about 5 minutes so as to outnumber the original acceptors and to form an n-type region at the exposed surface. The resulting $n^{+}p$ diode obtained ($\sim$ 0.5 mm thick) is reverse biased

to about 500V by keeping the drifting temperature between 20 - 50^{o}C to obtain a sufficiently thick detector. The actual time for drifting is variable in practice. The width of the compensation zone is given by

$$d = (2\mu_L Vt)^{1/2}, \qquad (9)$$

where d : width of compensation zone (cm),

μ_L : mobility of Li ions (cm^2/V-sec),

V : applied voltage (V),

t : drift time (sec).

The geometrical configuration of germanium detectors commonly used are shown in Figs.II.5 & II.6 in which, co-axial geometry is used for high energy gamma ray measurements where high efficiency is important, while planar geometry is used for low energy gamma ray measurements [18]. Ge(Li) detectors are operated at liquid nitrogen temperature in order to reduce the thermally generated leakage current to as low a value as possible. Extreme care must be taken for the maintenance of Ge(Li) detector by keeping it at liquid nitrogen temperature even when they are not in use. This is because at room temperature, due to the high mobility of Li in Ge, detector structure might be damaged by the precipitation of Li, causing loss of compensation.

In gamma ray spectroscopy Ge(Li) detectors are found in common use rather than Si(Li) detectors. It is mainly due to the following factors associated with the Ge when compared to Si like high atomic number, ease of drifting very thick devices (because of the high mobility of Li in Ge) and the lower energy required to produce an electron-hole pair. More over, during fabrication,

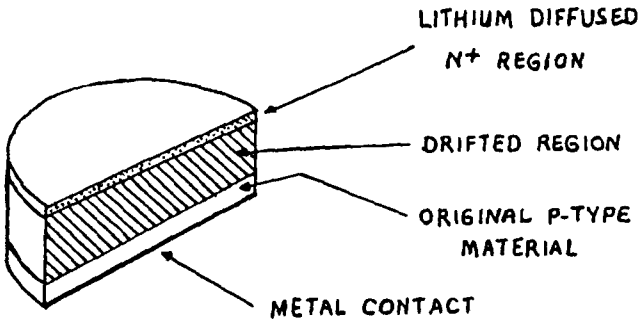

Fig.II.5 Common planar geometry for a germanium detector.

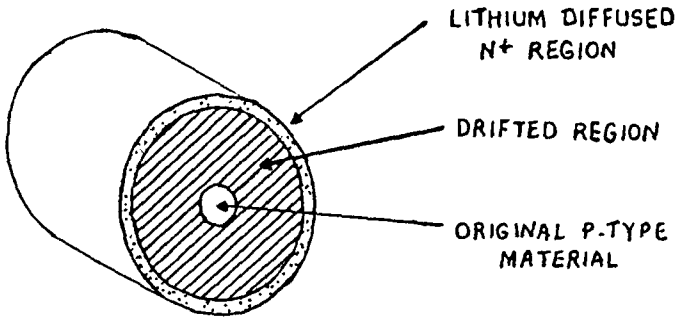

Fig.II.6 Common co-axial geometry for a germanium detector.

drift temperature for Ge(Li) detector is 20-50^{o}C due to the narrow energy band gap of Ge (0.7eV), while in Si(Li) detectors it is 120-140^{o}C (band gap of Si is 1.1eV). Heat must be supplied to Si(Li) detector while fabricating (because at 500V the current produced is 1mA) whereas in the case of Ge(Li) detectors one has to face difficulty in removing heat produced in it (because at 500V the current produced is 50mA) [1].

The performance of Ge(Li) detectors are really impressive and usually specified in terms of response function, resolution, linearity and detection efficiency which will be discussed later.

II.2.5. HPGe Detectors

Gamma ray spectroscopy has suffered for a long time due to a weak balance between resolution and detection efficiency till the advent of germanium, the most promising material for gamma ray spectroscopy. With the available purity of germanium a depletion depth beyond 2 or 3mm is dificult to achieve even by the application of bias voltage to its break-down level. For high energy gamma ray spectroscopy a detector with much more thickness is required and it is advisable to have a single crystal with large thickness so as to minimize the effect of factors that affect the detector performance. So one has to rely on various aspects of crystal growth.

To accomplish this goal of making detectors with large thickness one has to follow either of the following processes. The

first approach is to follow the method of ion drifting as discussed in the above section. The second approach is to use a refining technique which is capable of reducing the impurity concentration. A general solution for the thickness of the depletion region is given by

$$d = [2\ \varepsilon\ V\ /e\ N\ ]^{1/2}, \qquad (10)$$

Where, e : charge of electron,

ε : dielectric constant of the medium,

V : applied reverse bias voltage and

N : net impurity concentration in the semi-conductor material.

From this equation it is clear that to obtain a depletion depth of 10mm using a reasonable reverse bias voltage of 1000 volts the germanium crystal should be so pure as to have impurity concentration of $\sim 10^{10}$ atoms/cm^3. Using the advanced crystal growth technology, a detector can be fabricated from ultra pure germanium or high purity germanium which is available with impurity concentration $\sim 10^{10}$ atoms/cm^3. Thus it is possible to manufacture detectors with large active volumes without lithium compensation. These type of detectors are usually referred to as High Purity Germanium (HPGe) detectors.

The high purity germanium material is subjected to zone refining technique for accomplishing the above purpose. Since the impurities are more soluble in molten germanium, a melted zone is slowly introduced from one end to the other end of the sample which is locally heated for reducing the impurity level so as to transfer the impurity to the molten zone. Finally the transferred

impurity can be swept out from the sample. After a cycle of this process the required impurity concentration is found to be achieved. From this purified feed stock large crystals can be fabricated. HPGe detectors are produced in planar as well as in co-axial geometry [19].

The advantages in using HPGe detector over Ge(Li) detector is that, unlike Ge(Li) detectors, HPGe detectors, when not in use, can be stored at room temperature. The detector cryostat and dewar configuration for keeping the germanium detectors at liquid nitrogen temperature will be discussed in section III.2.1.

Characteristic Properties of Germanium Detectors

Detection of nuclear radiation and the measurement of their characteristics are greatly involved in various areas of nuclear physics research. The performance of germanium detector in gamma ray spectroscopy by its superior energy resolution enables it to explain the complexity of gamma ray spectra. This detector thereby functions as a key tool for gamma ray spectroscopy. Since the gamma ray interactions are identical in case of Ge(Li) as well as HPGe detectors, the following properties like response function detection efficiency etc., are same for both detectors of same size and shape.

(i) Response Function

Most of the devices and techniques used for the measurement of gamma rays actually respond to or analyze secondary

electrons. The fundamental property of the detector to get an exact information about the incident radiation is the pulse height spectra. Significant dissimilarities in the features of the pulse height spectra are observed between NaI(Tl) and germanium detectors due to the differences in atomic number and availability of sizes.However, the contribution to the response function for both detectors are same.

The intrinsic efficiency of a germanium detector is small compared to the corresponding NaI(Tl) detector of the same size due to the low atomic number of Ge which results in reduction of photoelectric cross section by a factor of $\sim$ 20. Because of its high resolution, peaks are prominent but the area under each FEP is much smaller. The major contribution to the FEP are from the events like multiple interaction and Compton scattering followed by photoelectric absorption. The contribution from single photoelectric event is very small which is clear from Fig.II.7(taken from [5]). Compton continuum is dominant in germanium detector spectra and due to its high resolution the continuum is raised near the compton edge. Most of the detected events lie in the Compton continuum rather than under the peak because the ratio of compton cross section to photoelctric cross section is large. Besides for these detectors, the probability of escape peaks are high due to its high transparency to the secondary gamma rays. The factors affecting the response function are the same as explained in the case of NaI(Tl) detectors.

For germanium detectors standard pulse height spectra are not available because of their diverse size and shapes. So

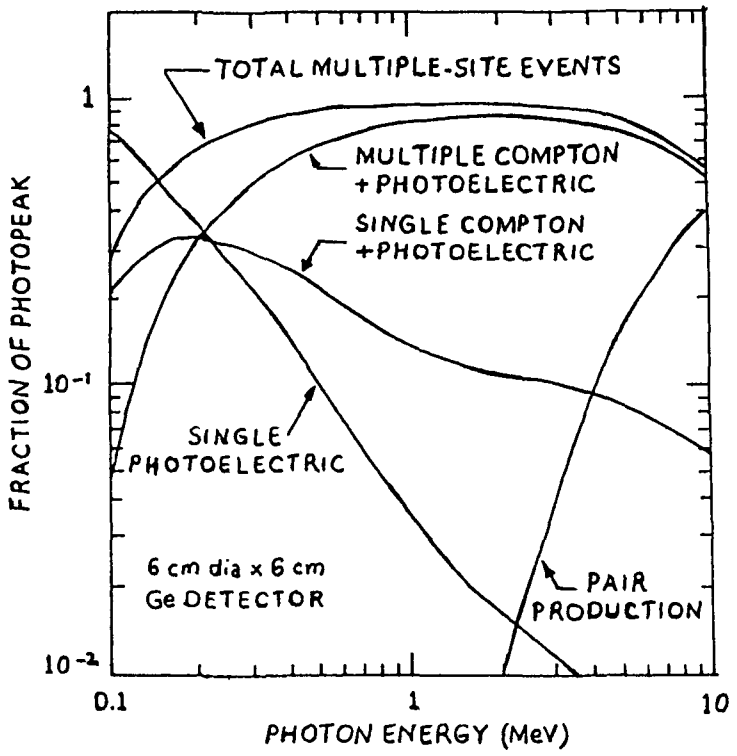

Fig.II.7 Fractions of full energy peak contribution in a 6cm x 6cm co-axial HPGe detector by different energy loss mechanisms.

Monte Carlo programme of Meixiner [20], which simulate the gamma ray photon with the knowledge of the probability of interaction process, is used for getting good results for the response function as shown in Fig.II.8. It is observed that Meixiner's calculated spectrum is in good agreement with the measured one.

Methods for Continuum Reduction

The diversity of continuum reduction in the case of germanium detector is significant because Compton continuum is prominent in its pulse height spectra. The reason for this is that the major fraction of the detected events lie under the Compton continuum rather than under the photopeak, as described earlier. So continuum reduction is essential for this detector to simulate the efficiency. The continuum reduction modes applied to NaI(Tl) detector can provide more benefits when applied to germanium detectors. This is due to the low photo fraction of germanium detectors as compared to NaI(Tl) scintillators.

The Compton rejection by anti-coincidence mode is achieved by keeping the germanium detector as the central detector and a surrounding detector, which should be able to capture most of the escaping photons. Usually large scintillation detectors like NaI(Tl) and BGO are used to meet this requirement. One disadvantage of this method is that it suppresses some FEPs of certain isotopes having complex decay schemes which are emitted in coincidence.

The principle of sum-coincidence mode for germanium

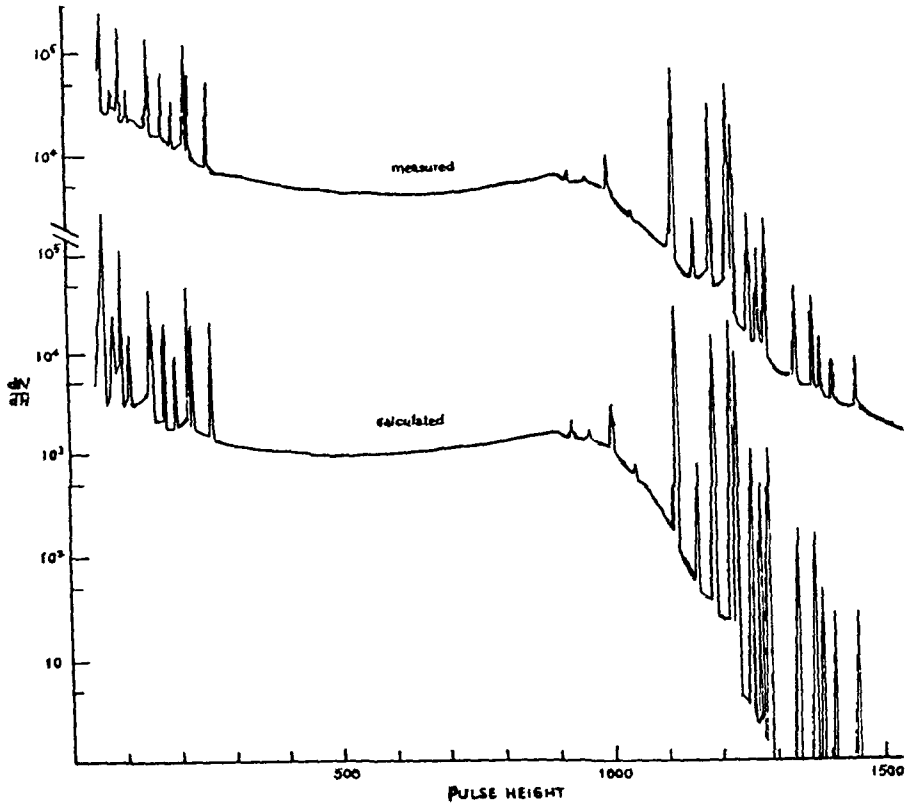

Fig.II.8 A comparison of the measured Ge(Li) spectrum for gamma rays from ^{182}Ta with a Monte Carlo calculated spectrum.

detectors is same as that for NaI(Tl) detector. Palms *et.al* [21] assembled a sum-coincidence spectrometer with two concentric co-axial germanium detectors (see ref [5]). They obtained the ratio of FEP to average Compton continuum larger by a factor of 5 compared with a single germanium crystal of same size. By this method Compton edges and escape peaks were greatly reduced at the expense of reduction in FEPE because the full energy absorption was not confined to a single crystal. The working principle behind the Compton spectrometer, is to select Compton events by establishing co-incidence requirements between two crystals. This spectrometer for germanium consists of a central germanium detector surrounded by scintillation detectors.

(ii) Resolution

The outstanding feature of germanium gamma detectors is their excellent energy resolution which has made a wide range of nuclear measurements possible, that were previously impractical.As mentioned in connection with the NaI(Tl) detectors, the detector resolution is conventionally defined as

$$R = \frac{FWHM}{H_o},$$

where FWHM : Full width at half maximum and

H_o : The position of peak (in terms of pulse height)

The excellent energy resolution of a germanium detector is mainly due to the low energy required for liberating an electron-hole pair and also due to the possibility of complete charge collection by the application of a suitable field without allowing the leakage current to increase. The factors that affect the

resolution are same for both germanium and NaI(Tl) detectors. The dominant factors which determine the resolution are statistical fluctuations in number of charge carriers, variation in charge collection efficiency and the contribution from electronic noise.

Therefore the FWHM of a typical peak (W_T) can be written as

$$W_T^2 = W_D^2 + W_X^2 + W_E^2 \qquad (11)$$

Where W values on the right hand side represent the expected peak width due to each effect mentioned above, respectively. Variation of the FWHM of the FEP of a 86 cm^3 HPGe detector with photon energy is shown in Fig.II.9 (taken from [22]).

(iii) Energy Calibration and System Linearity

One of the principal functions of gamma ray spectroscopy is the measurement of energies of gamma rays. The identification of various peaks in the gamma ray spectra can be done by calibrating the pulse height scale in terms of absolute gamma ray energy. Standard gamma ray sources are used for this calibration purpose. In many applications, gamma rays expected to appear are well known in advance and the gamma ray energies of the peaks in the unknown spectra can easily be identified, once energy calibration is done. After this calibration process a calibration curve of energy versus channel number is obtained. Since the degree of non-linearity is small in the case of germanium detectors the calibration curve is presented as a plot of deviation from perfect lineariry versus channel number and is depicted in Fig.II.10 (taken from [5]).

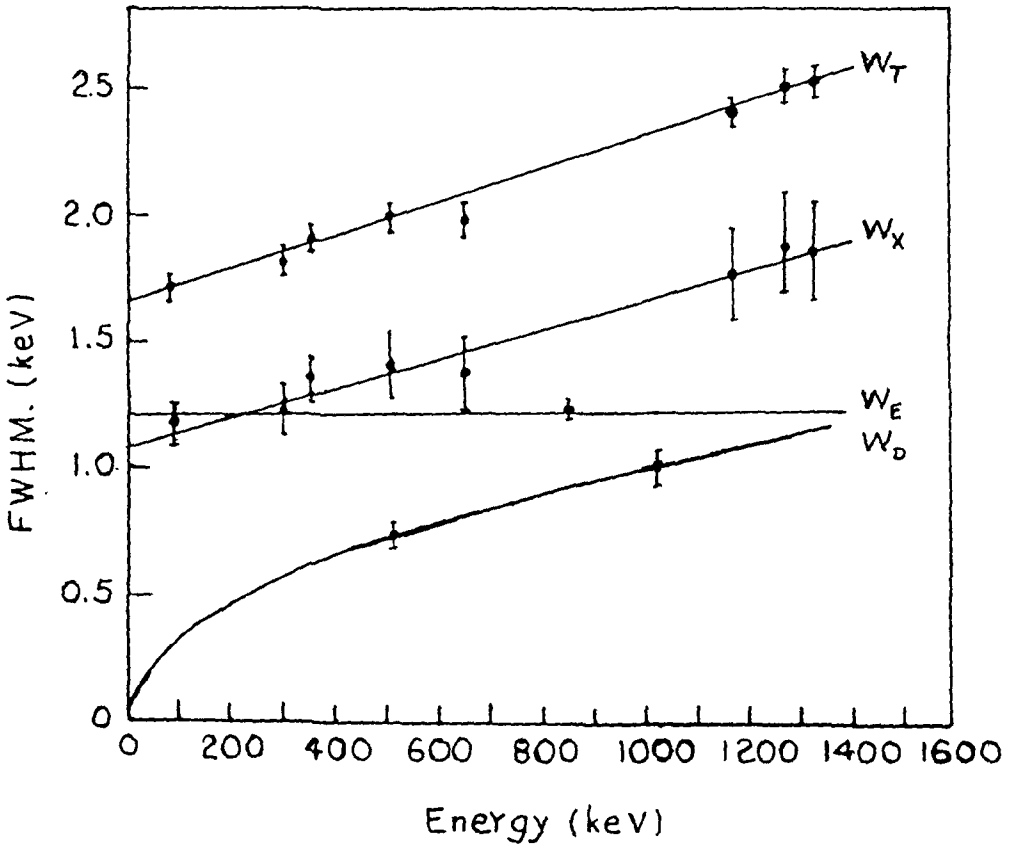

Fig.II.9 Variation of the FWHM of the full energy peak with gamma ray energy for a 86 cm^3 HPGe detector.

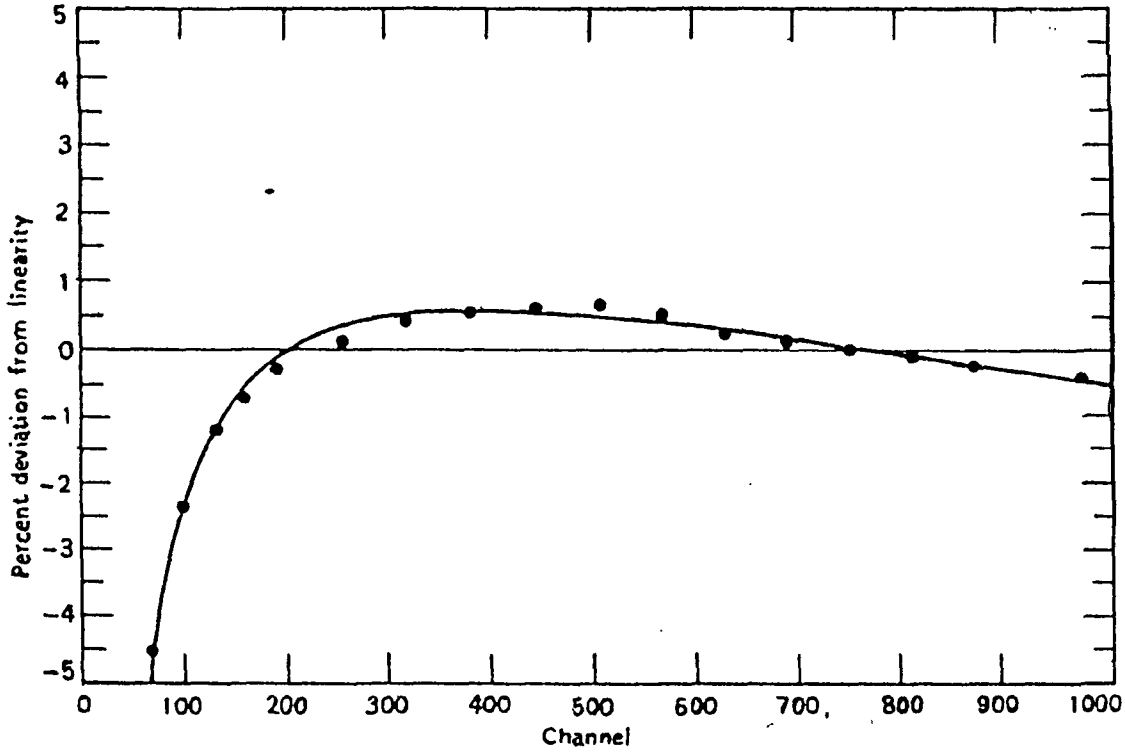

Fig.II.10 A typical differential linearity plot for a germanium detector system.

(iv) Detection Efficiency

An accurate determination of the FEPE of a germanium detector with high accuracy is very important because of the dependence of accurate measurement of intensity on the FEPE. The early germanium detectors suffered from low detection efficiency due to the inavailability of large sizes at that time. But the presently available germanium detectors (both Ge(Li) and HPGe) have the efficiencies that can be compared favourably with smaller NaI(Tl) detectors. The lower atomic number of Ge results in the lower intrinsic peak efficiency by many factors when compared with that of NaI(Tl) detectors having same active volume. It is not essential to use detectors with large sensitive volumes for gamma ray spectroscopy. But a detector thick enough to stop most of the incident radiation is certainly required for this purpose.

The ratio of Compton to photoelectric cross section is much larger for Ge. Therefore, most of the detected events lie within the so called Compton continuum rather than under the FEP. So the FEP area is much smaller and accordingly the efficiency is also lower. The exact determination of peak-to-total ratio is difficult, so it is measured as a ratio of the FEP height to the Compton distribution height. A crude estimation of the detection efficiency can be obtained from Fig.II.7. As the pair-production cross section increases monotonically with the energy, the single and double escape peak efficiencies are also found to be increased. Therefore, sometimes in germanium gamma ray spectroscopy, efficiency estimation is based on the area under single or double escape peaks instead of the area under FEP.

Calculation of the efficiency of germanium detectors requires precise definition of the geometry of the system, knowledge of photoelectric and Compton absorption coefficients and point-source approximation etc,. Due to these difficulties experimental approach is usually adopted in finding the FEPE of a detector and the procedure is discussed in chapter III. Since the boundaries of germanium detectors (HPGe) are diffused, the FEPE calculation (using Monte carlo technique) often does not give accurate results. Fitting of the FEPE data points can be done over an energy region of interest by using some empirical formulae or analytical functions. The best representation of FEPE for a planar detector was first obtained by Mowatt [23] using the equation,

$$\varepsilon = \frac{K\,[\tau + \sigma\, Q\, \exp(-RE)]}{\tau + \sigma}\,\{1 - \exp\,[-P\,(\tau + \sigma)]\}, \qquad (12)$$

with τ and σ as photoelectric and Compton absorption coefficients at energy E while K, Q, R and P as the parameters.

For a co-axial detector the best fit was obtained with a function proposed by McNelles and Campbell [24],

$$\varepsilon = (a_1/E_\gamma)^{a_2} + a_3\exp(-a_4E_\gamma) + a_5\exp(-a_6E_\gamma) + a_7\exp(-a_8E_\gamma) \qquad (13)$$

where a's are the parameters.

But Singh [25] modified this equation by dropping the last term and demonstrated that an equally good fit was posible for a 38 cm^3 co-axial Ge(Li) detector (see Fig.II.11). Validity of a number of semi-empirical formulae and analytical functions

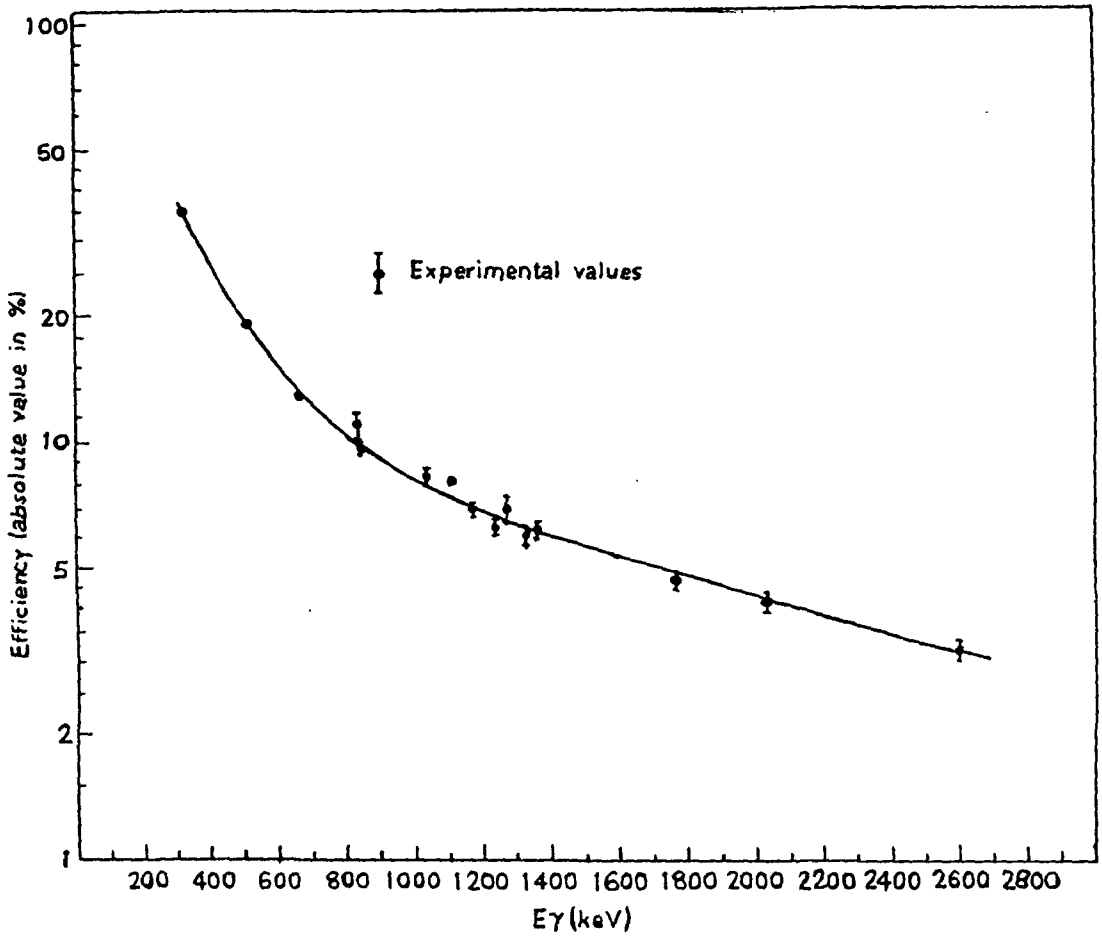

Fig.II.11 Measured intrinsic FEPE for a co-axial 38 cm^3 Ge(Li) detector as a function of gamma ray energy.

available in literature was tested by Singh [25] for both planar and co-axial germanium detectors. Now there are a large number of semi-empirical formulae and analytical functions available for carrying out such an analysis of the efficiency data (see chapter III and refs.12 & 16-21, for example).

II.3 DETERMINATION OF GAMMA RAY INTENSITIES

An accurate determination of the FEPE of a detector is essential for the precise measurement of the gamma ray intensities. For many purposes the accurate determination of photon intensities can be of greater value than the determination of energies. Thus an accurate determination of FEPE as a function of gamma energy is very important. The intensity of gamma rays is related to the total number of counts under the pulse height distribution through the total detection efficiency. An accurate determination of intensity is possible by measuring the area under the FEP and is not affected by the changes in resolution. In a complex spectral distribution, the amplitude of the maximum count in the FEP of each component gives an idea of the intensity.

For NaI(Tl) detectors a Monte Carlo type of calculation often gives accurate results for FEPE because a precise definition of size of the active volume is possible. Unlike NaI(Tl) detectors such accurate results (from Mote Carlo calculations) for FEPE is not possible for Germanium detectors (HPGe) because of the impossibility of the precise definition of size due to diffused boundaries. Moreover at high energies escape probabilities of

electrons are high because of the transparency of Ge crystals for secondary electrons. All these difficulties combined together make it extremely difficult to calculate the intrinsic efficiency of Ge detectors with any degree of precision. Because of these reasons intrinsic peak efficiencies are determined experimentally by a technique using calibrated standard gamma ray sources. Intensity of gamma rays can be determined by knowing the FEP area and the FEPE. The procedure is discussed in section III.2.4.

II.4 RELATIVE MERITS OF NaI(Tl) AND Ge(Li) GAMMA RAY SPECTROMETERS

The developments in nuclear physics research and several applied areas in nuclear science really depend, to a large extent, on the performance of gamma ray spectrometers. The gamma ray spectroscopy has long been dominated by two categories of detectors known as NaI(Tl) scintillation counters and the Ge(Li) detectors. Although there are many other potential factors but the choice of the spectrometer for gamma ray studies depends mainly on the yield of gamma radiation and the complexity of the gamma ray spectrum.

The excellent energy resolution of the germanium detectors, as discussed earlier, over NaI(Tl) detectors helps to reveal the hidden truths behind almost all nuclear properties to a great extent by separating many closely spaced gamma ray energies. To differentiate between the pulse height spectra of NaI(Tl) detector and Ge(Li) detector, a comparative spectra from the decay

of ^{110m}Ag and ^{108m}Ag are given for both detectors in Fig.II.12 with identical incident gamma rays (taken from [5]). From this figure it is clear that the gamma ray peaks which are not resolved by NaI(Tl) detectors can be seen separately with the help of germanium detectors. This way the explanation of complex decay scheme is possible with germanium detectors.

While, considering the detection efficiency of both detectors it is observed that the efficiency of NaI(Tl) detector is many factors greater than that of germanium detector of same size. The superiority of detection efficiency of NaI(Tl) detectors is clear from Fig.II.13 which depicts the absolute efficiencies of NaI(Tl) and Ge(Li) detectors as a function of gamma ray energy with different source-detector geometries [26]. In large detectors the peak-to-total ratio increases measurably as a result of the increased multiple events. Thus NaI(Tl) detectors have a higher peak-to-total ratio than that for germanium detector. The excellent energy resolution of germanium detector can offset the disadvantage of lower efficiency. For very weak gamma ray spectroscopy, sometimes, it is observed that the signal-to-noise ratio is higher in case of Ge(Li) than NaI(Tl) detectors.

In certain cases two NaI(Tl) detectors in coincidence have higher efficiency than a single Ge(Li) detector. So it is difficult to give a single reason for deciding the use of a particular detector in a given situation. One cannot simply discard either of the two detectors, discussed earlier, by pointing out their disadvantages. It is better to have both available to serve nuclear spectroscopy for its rapid development.

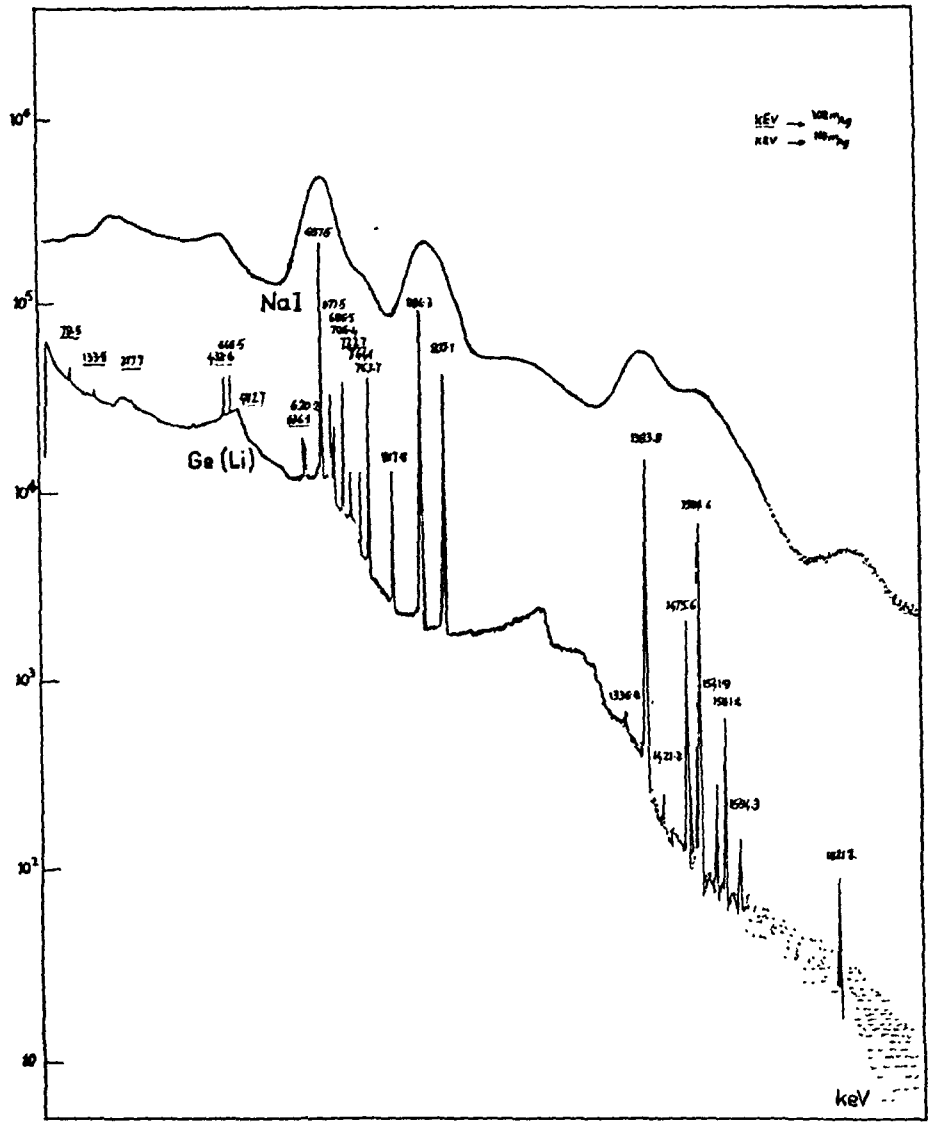

Fig.II.12 Comparative pulse height spectra recorded using a NaI(Tl) detector and a Ge(Li) detector from the decay of ^{108m}Ag and ^{110m}Ag.

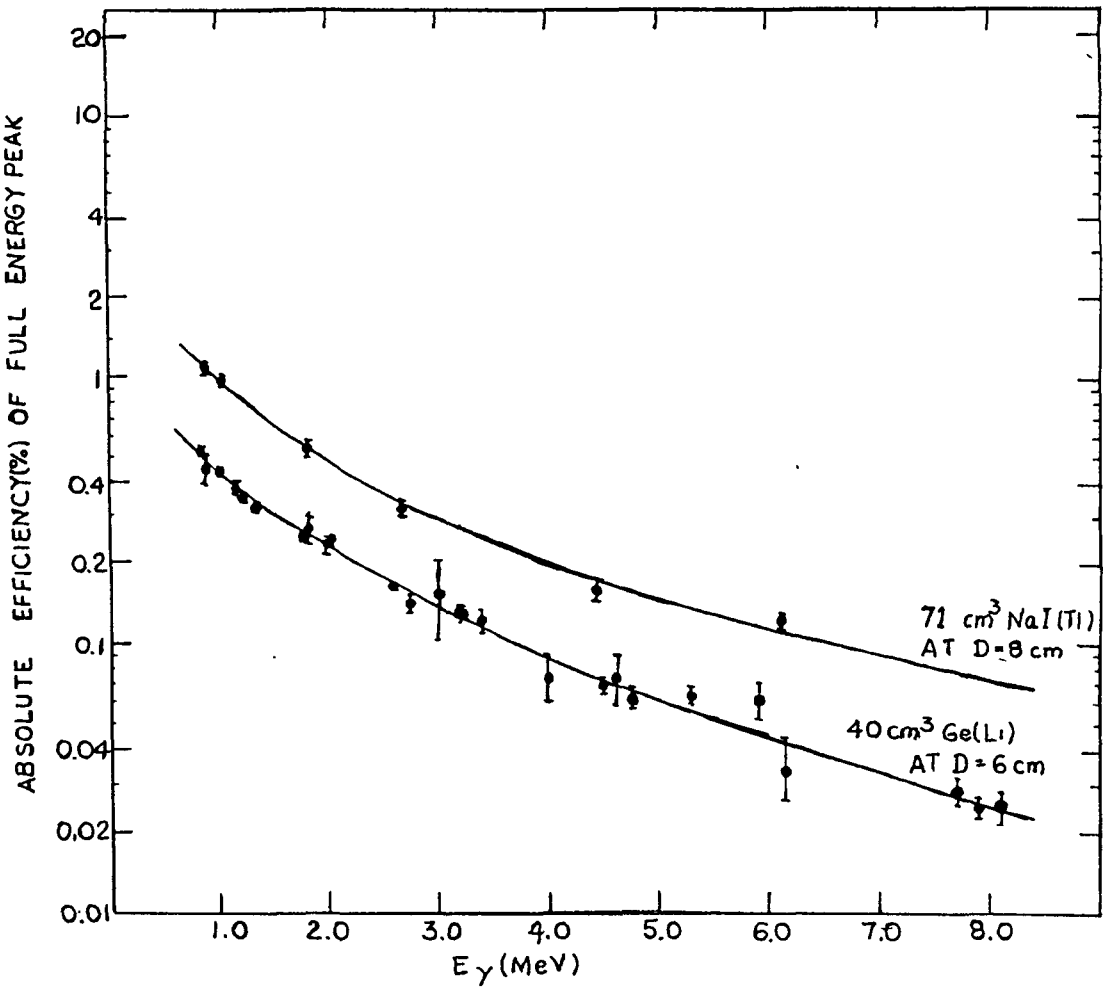

Fig.II.13 A comparison of the absolute FEPE for a NaI(Tl) detector and a Ge(Li) detector as a function of gamma ray energy.

References

1. R.Hofstadtor, IEEE Trans.Nucl.Sci., NS-22 (1975) 13

2. G.H.Hilne, J.Nucl.Med., 18 (1977) 867

3. S.S.Kapoor and Ramamurthy, "*Nuclear Radiation and Detectors*", Willey Eastern Ltd. New Delhi

4. R.Muller and D.Meader, "*Single Crystal Spectroscopy*", chapter VII in "*Scintillation Spectroscopy of γ-radiation*", (S.M.Shaforth, ed.) Gorden and Breach NewYork 1967

5. G.F.Knoll, "*Radiation Detection and Measurement*", Second edition, John Wiley & Sons, New York

6. R.J.D.Beattie and J.Byrne, Nucl.Instr.and Meths., 104 (1972) 163

7. R.W.Perkins, Nucl.Instr.and Meths., 33 (1965) 71

8. C.M.Davison, in "*Alpha-Beta and Gamma-Ray Spectroscopy*", (K.Seigbahm ed. Vol 1 (1965), North-Holland Publications, Amsterdam

9. R.D.Evans, "*The Atomic Nucleus*", (1955) McGraw-Hill, New York

10. W.Heitler, "*The Quantum Theory of Radiations*", (1954) Third edition, Oxford University Press, London and New York

11. W.D.Davis, J.Appl.Phys., 29 (1958) 231

12. E.M.Pell, J.Appl.Phys., 31 (1960) 291

13. D.V.Freck and Wakefield, Nature, 193 (1962) 669

14. G.L.Miller, IEEE Trans. Nucl.Sci., NS-19 (1) (1972) 251

15 A.J.Tavendale, IEEE Trans.Nucl.Sci., NS-12 (1) (1965) 255

16. W.L.Hansen, Nucl.Instr.and Meths., 94 (1971) 377

17. W.L.Hansen and B.V.Jarret, Nucl.Instr.and Meths., 31 (1964) 301

18. F.S.Goulding and R.H.Pehl, in "*Nuclear Spectroscopy and Reactions*", part A (Joseph Cerney ed.) p.320

19. J.Llacer, Nucl.Instr.and Meths., 98 (1972) 259

20. Ch.Meixner, Nucl.Instr.and Meths., 119 (1974) 521

21 J.M.Palms, R.E.Wood and O.H.Pucket, IEEE Trans.Nucl.Sci., NS-15 (3) (1968) 397

22. A.Owens, Nucl.Instr.and Meths., A238 (1985) 473

23. R.S.Mowatt, Nucl.Instr.and Meths., 70 (1969) 237

24. L.A.McNelles and J.L.Campbell, Nucl.Instr.and Meths., 109 (1973) 241

25. R.Singh, Nucl.Instr.and Meths., 136 (1976) 543

26. C.Rolfs and A.E.Litherland, in "*Nuclear Spectroscopy and Reactions*", part C (Joseph Cerney ed.) p.149

CHAPTER III

NEUTRON ACTIVATION ANALYSIS AND FULL ENERGY PEAK EFFICIENCY OF 157 cm^3 HPGe AND 2"X2" NaI(Tl) DETECTORS

III.1 INTRODUCTION

Neutron Activation Analysis (NAA) technique, which is based on the quantitative detection of gamma radioactivity produced in samples by neutron bombardment, was used here for : (i) the study of half lives of certain nuclei, namely, ^{116}In, ^{27}Mg, ^{51}Ti and ^{28}Al (obtained respectively by bombarding ^{115}In, ^{27}Al, ^{51}V and ^{28}Si with neutrons), (ii) a study of elemental analysis of some samples such as SRM 1633a and coinage metal and, (iii) a reinvestigation of relative intensities of gamma rays emitted by ^{116m}In. In order to measure gamma ray transition

intensities an accurate determination of FEPE with photon energy is of significant importance. So we have determined the FEPE of a 157 cm^3 coaxial HPGe detector and that of a 2"x2" NaI(Tl) detector. An empirical calculation of the FEPE of the 157 cm^3 co-axial HPGe detector from manufacturers data has also been done. Moreover we have checked the validity of some analytical functions for the FEPE of 2"x2" NaI(Tl) detector. Finally we studied the variation of the resolution of the gamma detectors (157 cm^3 HPGe,3"x3" and 2"x2" NaI(Tl)) with photon energy. In this chapter we shall give the details of the techniques used, apparatus, measurements and the subsequent analysis.

III.2 NEUTRON ACTIVATION ANALYSIS (NAA)

Neutron Activation Analysis (NAA), as a technique , was developed by Hevesy and Levy [1] in 1936 when they used neutrons from a Ra-Be source to activate rare earth elements for the detection of Dysprosium and Europium (see ref [2]). This was done after the observation of radioactive capture of thermal neutrons by Lea [3] and Amaldi *et.al* [4] in 1933. The outbreak of world war II in September 1939 gave a boost to reactor research,and indirectly to NAA. Till the early 1950's this method was utilised only in a few laboratories in the world.

The NAA technique is based on the interaction of neutrons with an isotope of interest giving rise to a radioactive product nuclide whose concentration can be estimated with the help of a suitable detector by measuring the characteristic radiations

emitted by the product(s). In principle, any of the neutron sources can be used for the bombardment of the sample by neutrons but here we have used a 5 Ci ^{241}Am-Be source for the analysis involving slow/thermal and fast neutrons.

Thermal neutrons interact with nuclei predominantly through (n,γ) reaction. However, fast neutrons, interact with nuclei mainly through (n,p), (n,α) (n,n',γ) or (n,2n) reaction. If the product nucleus is radioactive its later decay can be detected and used for activation analysis [2]. Most of these radioactive nuclei, β-decay with definite half lives, finally emitting gamma rays, whose energies are characteristics of the de-exciting nuclei.

III.2.1 Experimental Set up

Details of the HPGe detector and its associated electronics, the neutron source and the entire experimental arrangement are discussed in the following sections.

III.2.1a. *HPGe Detector and Associated Electronics*

An EG & G Ortec GEM series 157 cm^3 HPGe co-axial detector was used for doing the present gamma measurements. This HPGe detector system consisted of

(i) a semiconductor detector element

(ii) cryostat and liquid nitrogen dewar and

(iii) associated electronics.

(i) Detector Element

This GEM type HPGe closed end coaxial detector employed p-type high purity germanium as detector element with a diffusion of lithium at the outer surface. The detector crystal was 69.6mm in length and 55mm in diameter. The end cap to crystal was 3mm and the thickness of the aluminium window was 1.27mm. It has an inactive layer of germanium having a thickness of 0.7mm. The basic detector element configuration for the detector is shown in Fig.III.1. Because of its closed end coaxial configuration it has excellent charge collection and timing performance. The detection capacity of photon energies varied from 40 keV to 10 MeV.

The original resolution and relative efficiency of the detector were 1.85 keV and 32% at 1332 keV respectively, but both deteriorated with time (detector was being used for $(n,n'\gamma)$ measurements). The FWHM reached a value of 11.65 keV while the FEPE reduced by nearly 8%, as compared to the original values at the same energy (viz 1332 keV) due to neutron damage as reported by Sudarshan and Singh [5].

(ii) Detector Cryostat and Dewar

The cryostat dewar configuration keeps the detector element in a high vacuum and close to liquid nitrogen temperature. The dewar functions as a reservoir for liquid nitrogen while the cryostat provides a path for heat transfer between the detector element and dewar. The cryostat is mounted on the liquid nitrogen dewar of capacity 30 litres as shown in Fig.III.2. In both the dewar and cryostat the cold inner parts are insulated from the outer surfaces by vacuum. The cryostat contains a mount for

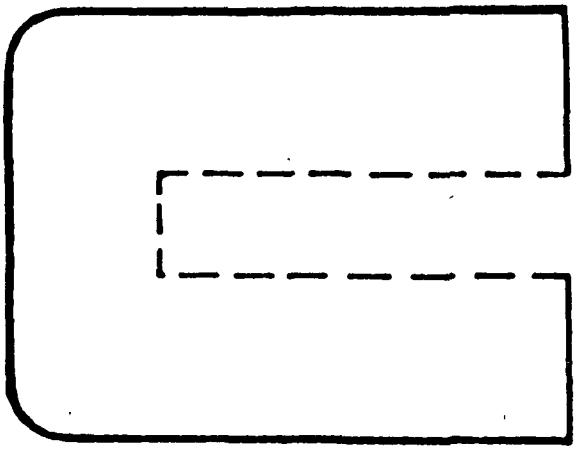

Fig.III.1 GEM series, p-type co-axial HPGe detector.

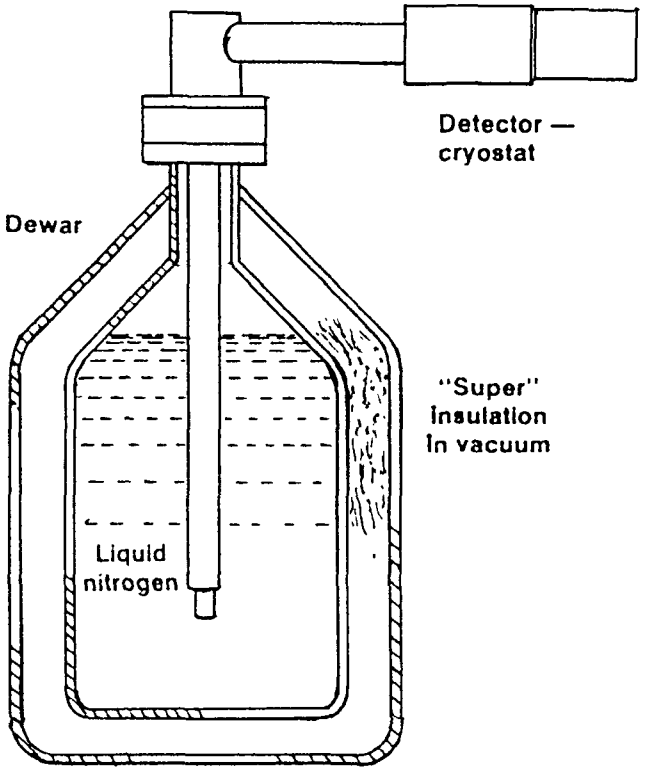

Fig.III.2 Common horizontal configuration of the Cryostat and liquid nitrogen Dewar for a HPGe detector.

detector element and associated electronic components.

(iii) Associated Electronics

The block diagram of the experimental set-up, using HPGe coaxial detector, for gamma ray energy measurements from a radioactive source is given in Fig.III.3. The essential components of the set-up are detector, power supply, pre-amplifier, amplifier, multichannel analyser and the printer. A positive bias of 2.5 kV was applied to the HPGe detector.

Absorption of a photon from the radioactive source by the detector produces a current pulse at the input of the cooled pre-amplifier. Each pulse is integrated by the charge sensitive loop which is essentially an FET input operational amplifier with a capacitive feed back. In this HPGe system, the pre-amplifier is incorporated as a part of the cryostat package so as to keep the pre-amplifier as close to the detector as possible to reduce the capacitance. The input stages of the pre-amplifier are also cooled alongwith the detector to reduce electronic noise.

The signal from the pre-amplfier was fed to the 572 EG & G Ortec amplifier for further processing. This amplifier was adjusted for appropriate gain and shaping time so as to get best signal to noise ratio.

The amplified signal was then fed to the Series 35 Plus Canberra Multichannel Analyser for analysis. This analysed pulse height data in the form of channel number versus counts was then printed out by a fast printer (Centronics GLP II) and used for further analysis.

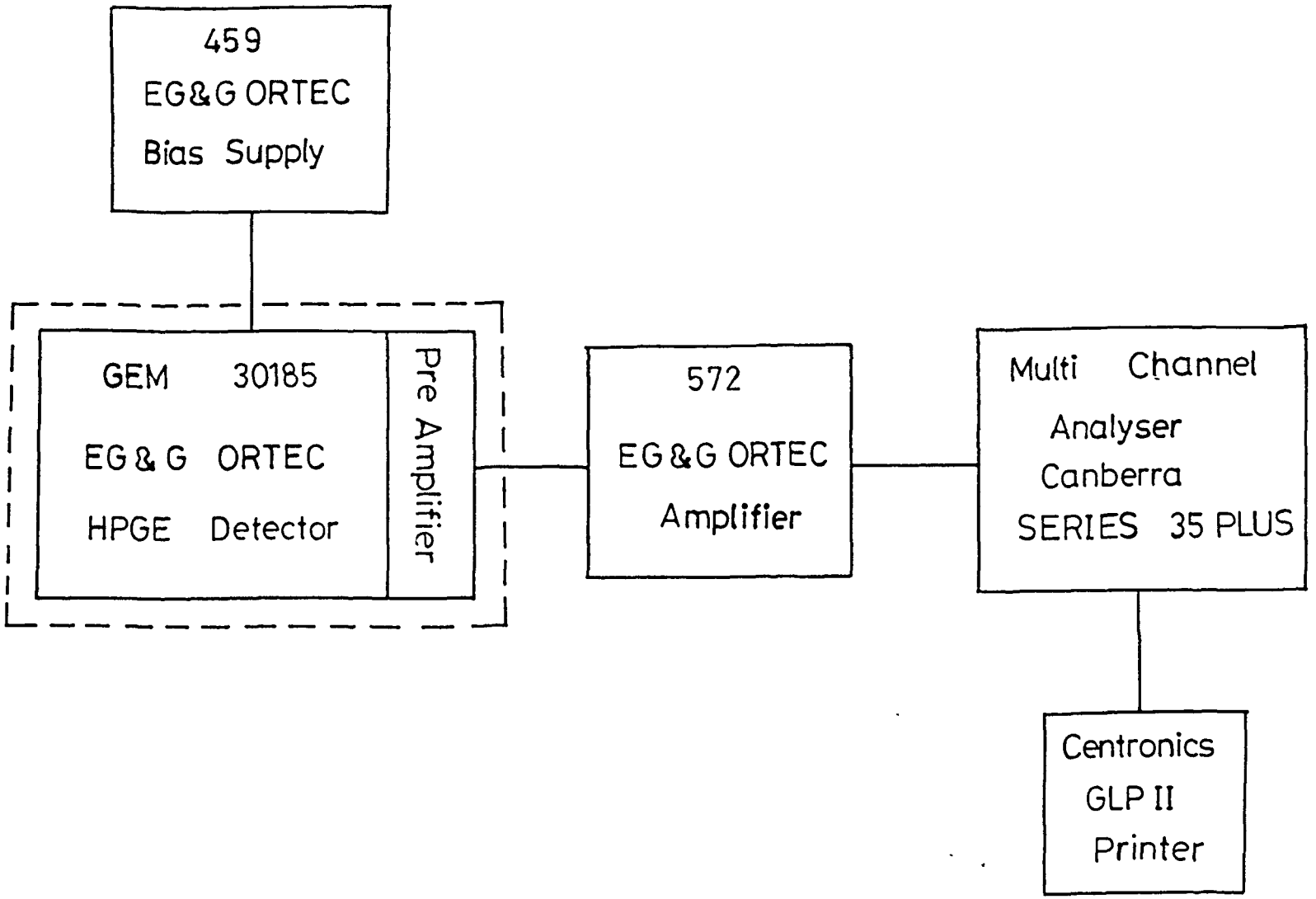

Fig.III.3 Block diagram of the HPGe detector and its associated electronics.

III.2.1b. *The Neutron Source*

We employed a 5 Ci ^{241}Am-Be neutron source, procured from Buchler GmbH, West-Germany, for the present measurements. The ^{241}Am α's produce neutrons as a result of interaction with ^{9}Be as follows

$$^{4}_{2}He + ^{9}_{4}Be \longrightarrow ^{12}_{6}C + ^{1}_{0}n + 5.71 \text{ MeV}$$

The source provided 1.1×10^{7} n/sec and was shielded with borated paraffin wax. The shielded container was cylindrical in shape with a height of 62cm and radius of 27cm. The neutron energy spectrum of the ^{241}Am-Be source is shown in Fig.III.4 [7] (taken from [6]). The various peaks in the spectrum can be analysed in terms of the excited states in which the ^{12}C nucleus is left [8-9] (see ref [6]. The cross sectional view of the neutron source is shown in Fig.III.5 where the plug, attached to the source for handling purpose, can also be seen (taken from ref [6]).

III.2.1c. *Source-Sample and Detector Arrangement*

The experimental set up consisted of an assembly of a 5 Ci ^{241}Am-Be neutron source with a 157 cm^{3} HPGe co-axial detector. The neutron source could be pulled out and lowered into its shielded container with the help of a remote controlled manually operated system. This system consisted of a set of three pulleys, an iron wire, an iron rod, an iron bracket and an operating wheel with a locking arrangement. The iron rod which could be screwed to the source, was connected to the operating wheel by means of an

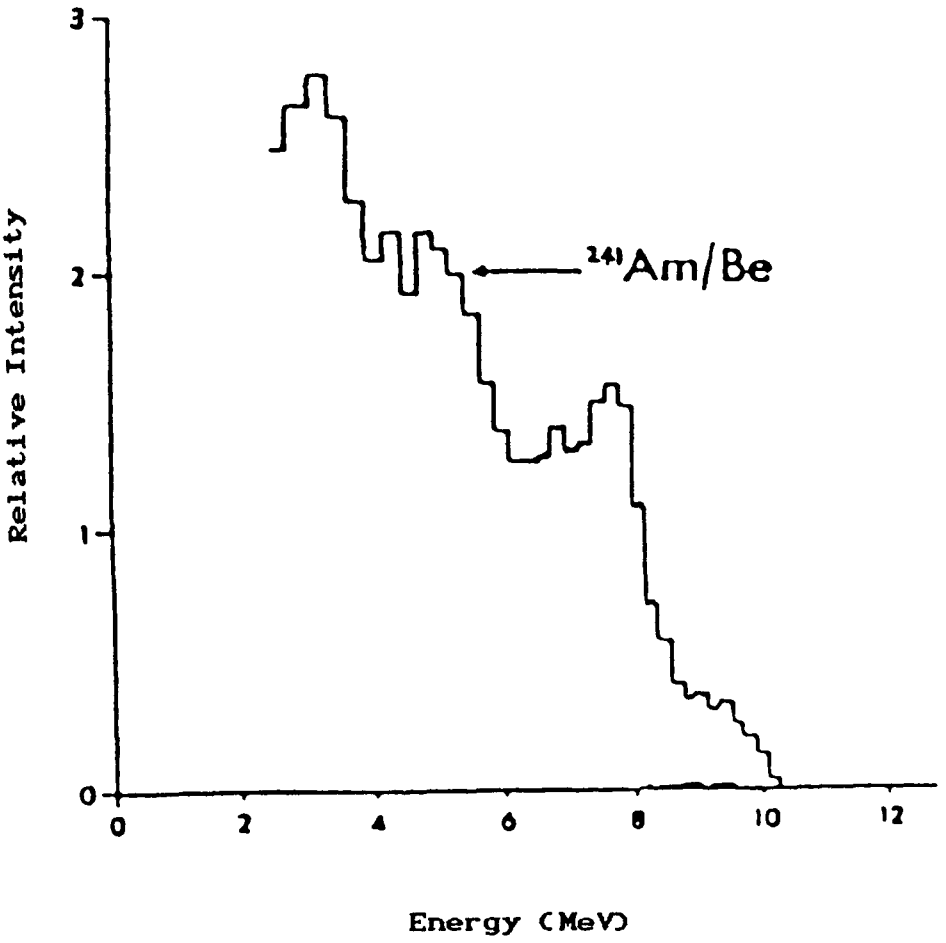

Fig.III.4 Neutron energy spectrum of an ^{241}Am-Be neutron source.

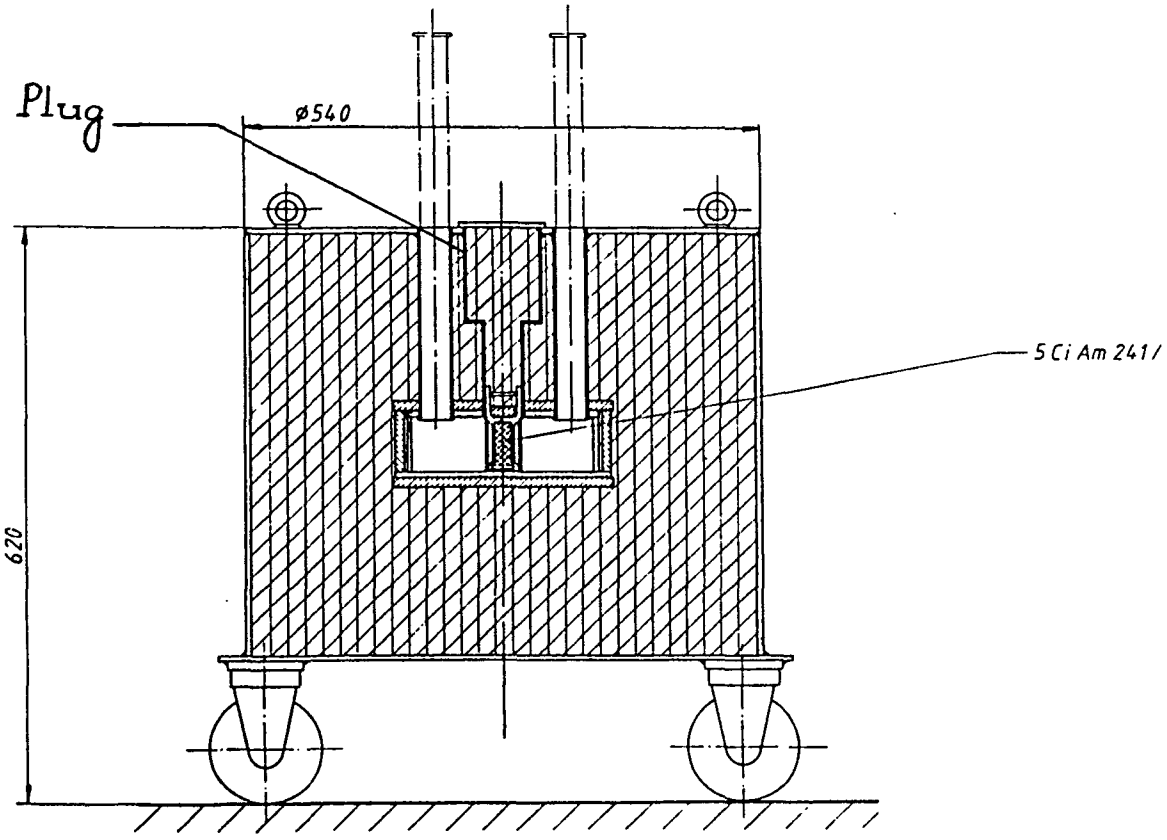

Fig.III.5 A cross sectional view of the ^{241}Am-Be neutron source.

iron wire. The operating wheel, with a locking arrangement, was enclosed in a box which was fixed to the wall of the counting room (see Fig.III.6). The iron bracket (which was fixed to the ceiling above the source) with an iron plate such that the iron wire passes through it, enabling the adjustment of the position of the source, can be seen in Fig.III.6. The pulleys are placed at appropriate positions to enable smooth movement. Thus, by rotating the wheel from the counting room, the source could be easily lifted out of its shielded container and could be fixed at any desired position by locking the operating wheel.

In experiments utilising neutrons it is necessary to use neutron-absorbing shields to confine the neutrons to the irradiation region. In addition to the shielding demanded by the experiment, the investigator requires protection from the neutrons and other radiations. Whenever neutrons are generated in measurable intensities, there is also production of radioactive species. Because of its great penetration, gamma radiation also creates shielding problems. Therefore, one has to pay attention to shielding of the personnel from gamma rays as well.

Considering this shielding factor the neutron source was enclosed in a cabin made of wood about 2.05m in height, 2.74m in length and 1.98m in breadth, with an opening of 1.52m wide and 1.98m high. For neutron shielding, the inner side of the cabin was layered with borated wax bricks (12"x6"x3" in size). The choice of borated wax was due to the large neutron absorption cross section of Boron. Boron captures the low energy neutron produced by the moderation of the neutron flux by hydrogen in the paraffin wax.

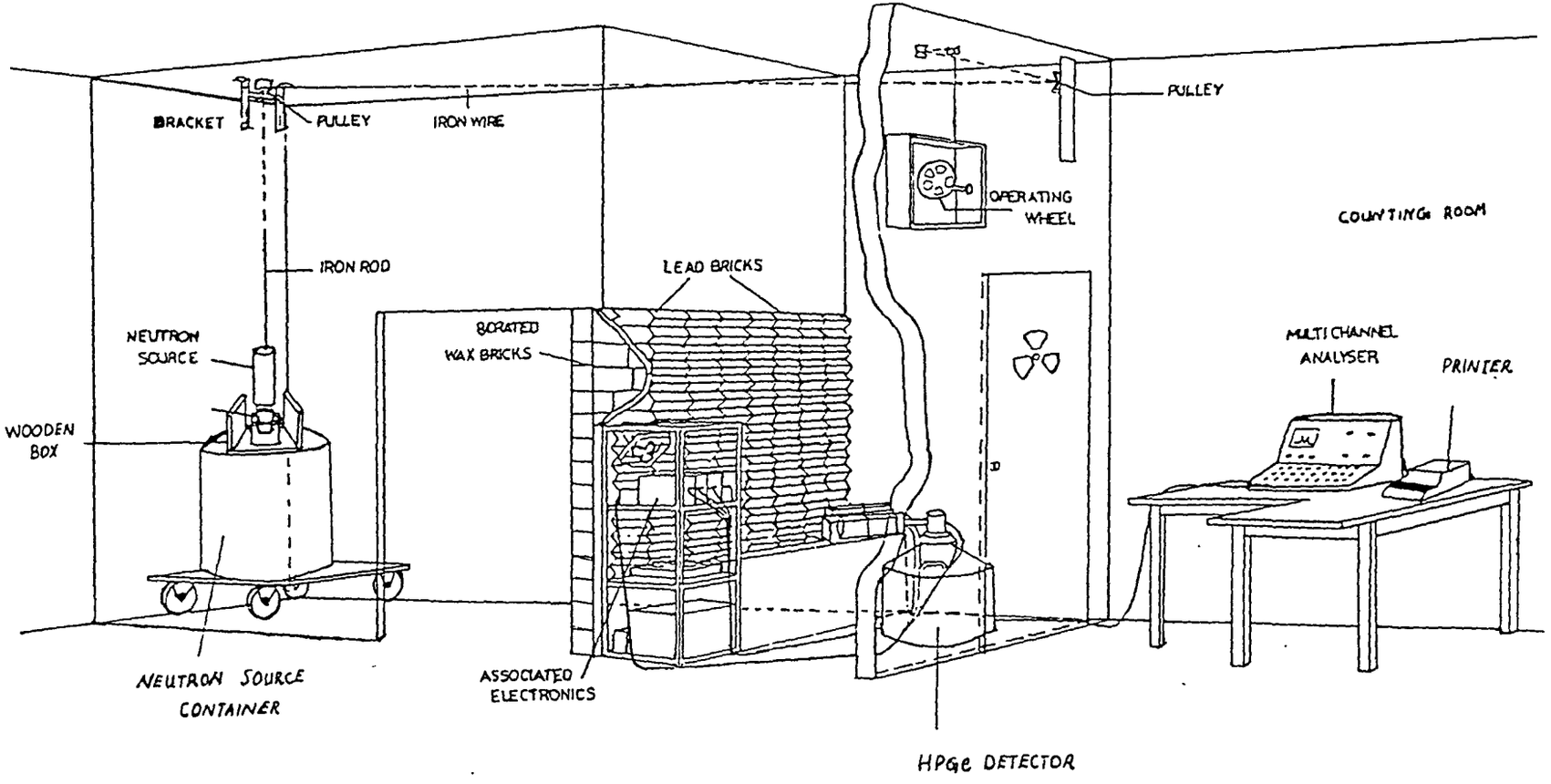

Fig.III.6 A view of the entire experimental set up.

The top side of the cabin was layered with 18cm thick borated plastic bricks and a layer of borated paraffin bricks. In order to prevent the gammas reaching the counting room additional shielding, consisting of lead bricks of thickness 10cm, was provided outside the cabin wall facing the counting room. A movable wooden door filled with borated wax bricks was used to close the opening of the enclosure.

The exposure to radiation was checked by using neutron and gamma dosimeters. It was observed that the shieldings were quite adequate to keep the exposure to radiation well below the permissible limits. Besides, the personnel working are also constantly monitored through the gamma and neutron badge service provided by the Division of Radiological protection, BARC, Bombay.

The 157 cm^3 HPGe detector was placed outside the neutron cabin wall facing the counting room. In order to reduce the gamma background, the detector was surrounded all around by 5cm thick lead bricks except for the face of the detector. The sample was kept in front of the detector for subsequent data collection after irradiation.

A special arrangement was made for irradiating the sample. The sample(for irradiation) was fixed to the end of a small wooden rod (15cm in length) by cellotape. The rod could be tightly fixed in the slots of a wooden stand inside a rectangular box of wood (20cm in length and 10cm in breadth) with the top and both its ends open. The slots of the wooden stand at the two ends of the box were made in such a way so as to keep the rod horizontal. This box could be pushed in and pulled out with 1.0m

long tongs, through a guided path specially made for its proper movements. The guided path prevented the movement of the box side ways and helped to reproduce the geometry. This arrangement is shown in Fig.III.7. A view of the entire experimental arrangement alongwith the neutron shielding is shown in Fig.III.6.

The neutron source was lifted by rotating the operating wheel and could be fixed at the desired position to make the source and sample in the same plane . This position could be fixed by marking on the iron wire with which the neutron source was lifted. After lifting the neutron source, the box with sample at the end of the rod, was pushed in (towards the source till the source-sample distance reaches within $\sim$ 1cm) for irradiation. After the irradiation the box was pulled off from the source and the rod (with the sample) was taken away from the slots for placing in front of the detector for data collection. The source-sample and sample-detector geometry was kept the same for all the measurements. We have assigned $\pm$ 0.5cm as error in the positioning of the source.

We have employed NAA technique for finding the half-lives of certain nuclei, for a study of elemental concentration in some samples, and also for finding the relative intensities of gamma rays emitted by ^{116m}In which are discussed in the following sections.

III.2.2 Half-life Measurement

According to the fundamental law of radioactive decay,

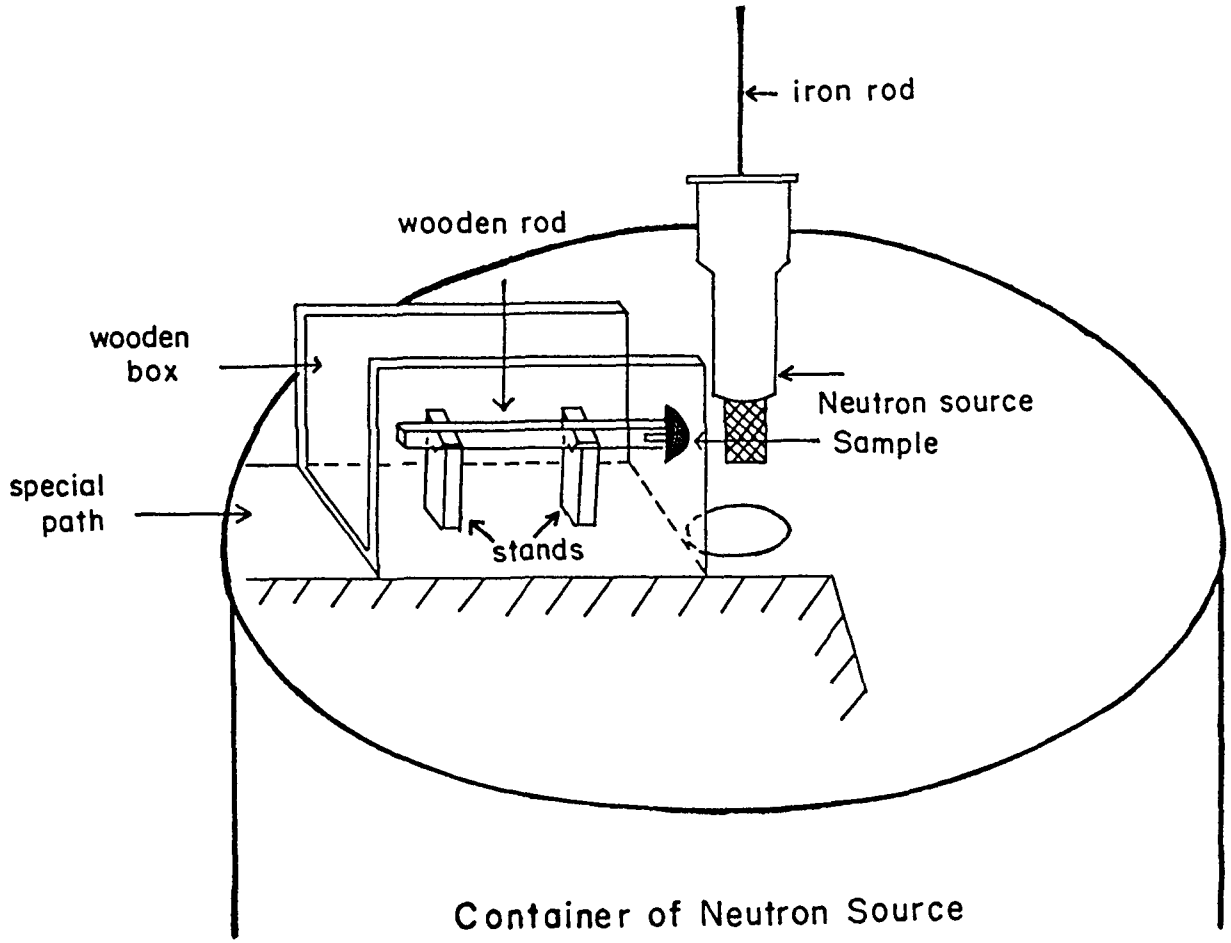

Fig.III.7 Special arrangement made for the irradiation of samples.

$$N = N_o \exp(-\lambda t), \quad (1)$$

where N_o is the number of radioactive nuclei at time t=0, N at time t, and λ is the decay constant. The half-life of radioactive nuclei is defined as the time, $t_{1/2}$, in which the number of nuclei initially present is reduced by a factor of 2. Using eqn.(1) we get

$$t_{1/2} = 0.693/\lambda. \quad (2)$$

During the last two decades or so, the use of short lived isotopes in activation analysis has increased immensely owing to the application of high resolution gamma ray spectroscopy. The present study is based on the following procedure for the measurement of half lives below and above 10 minutes.

Experimental Procedure

The gamma energies of interest in each sample were identified by calibrating the MCA by using a strandard set of gamma sources, procured from the IAEA, Vienna. The gamma sources used for this purpose were ^{22}Na, ^{137}Cs, ^{54}Mn and ^{60}Co.

The samples were sealed in separate polythene bags and irradiated one by one with fast neutrons (except for ^{115}In) from the 5 Ci ^{241}Am-Be source in the arrangement described earlier. The source-sample separation was about 1cm. ^{115}In foil was irradiated by slow neutrons by keeping a 2.5cm thick paraffin disc in between the source and the sample. In this case source sample distance was about 4cm. After irradiation, the sample was placed immediately in front of the 157 cm^3 HPGe detector (at a distance of 5mm) for counting the most prominent gamma rays. Time elapsed for this purpose was noted as delay time (t_d). The gamma spectra were

recorded with the MCA and the data was printed out by a fast printer as follows. The data was collected for a given time and was given a time interval for the data to be printed out. After this time interval the previous data was erased and the data was collected again for the same time. This process continued till the product nucleus decays more or less to the background level. The irradiation time (t_r), collection time (t_c) and time interval (t_i) were chosen in accordance with the information about the half-life of the product nucleus. The background subtracted area of the peak (activity) was plotted against time for all the samples (ie. decay curve) and are shown in Figs.III.8 - III.15

It is seen that the peak areas decreased exponentially with time which is clear from the plots. Half-lives could be obtained from the graph by using the formula,

$$t_{1/2} = \ln(2)(t_2-t_1)/\ln(N_1/N_2), \qquad (3)$$

where N_1 and N_2 are the areas at times t_1 and t_2 respectively. All the experimental parameters and results for each sample are given in Tables III.1 & III.2.

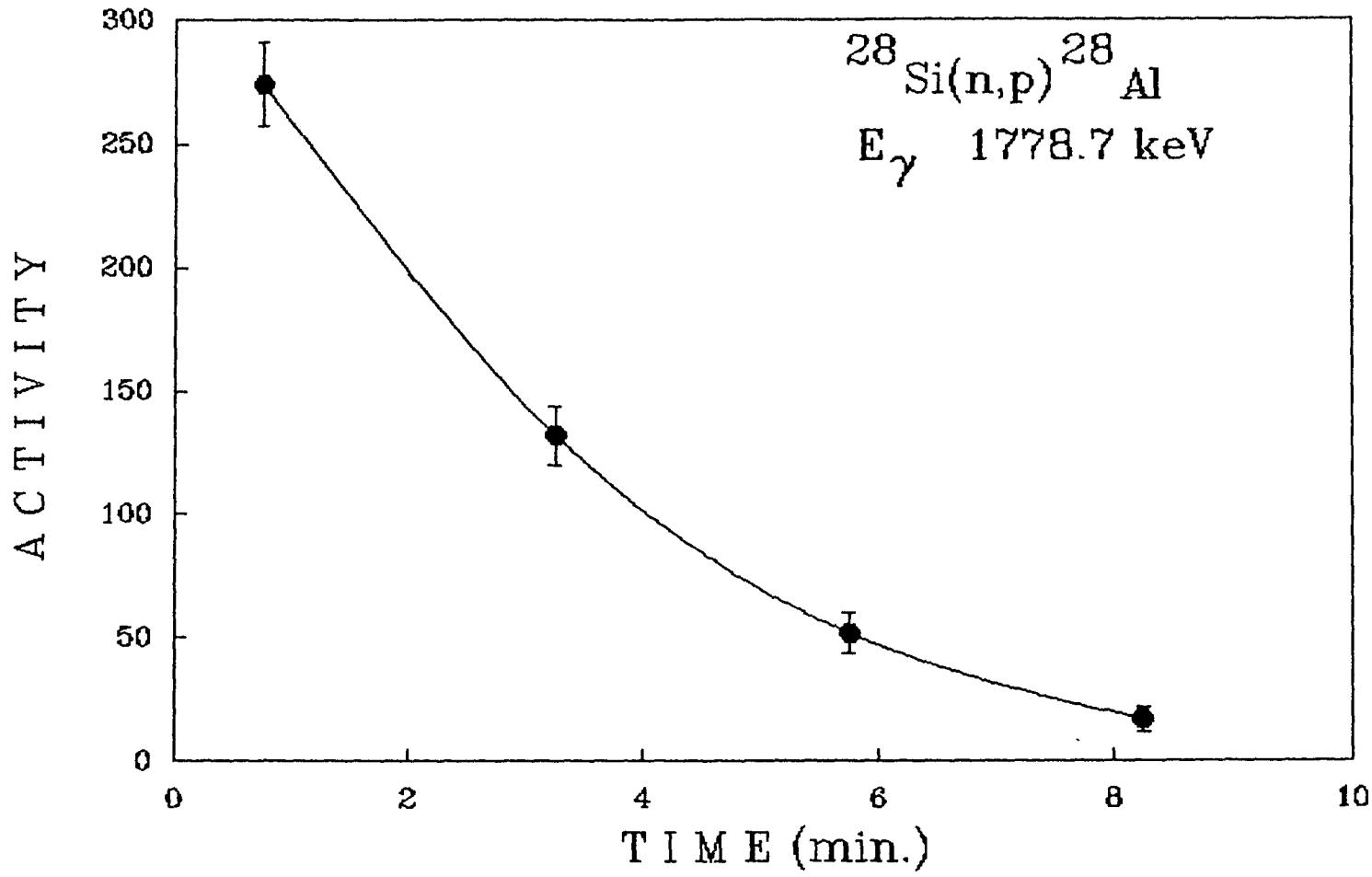

Fig.III.8 Decay curve for ^{28}Si.

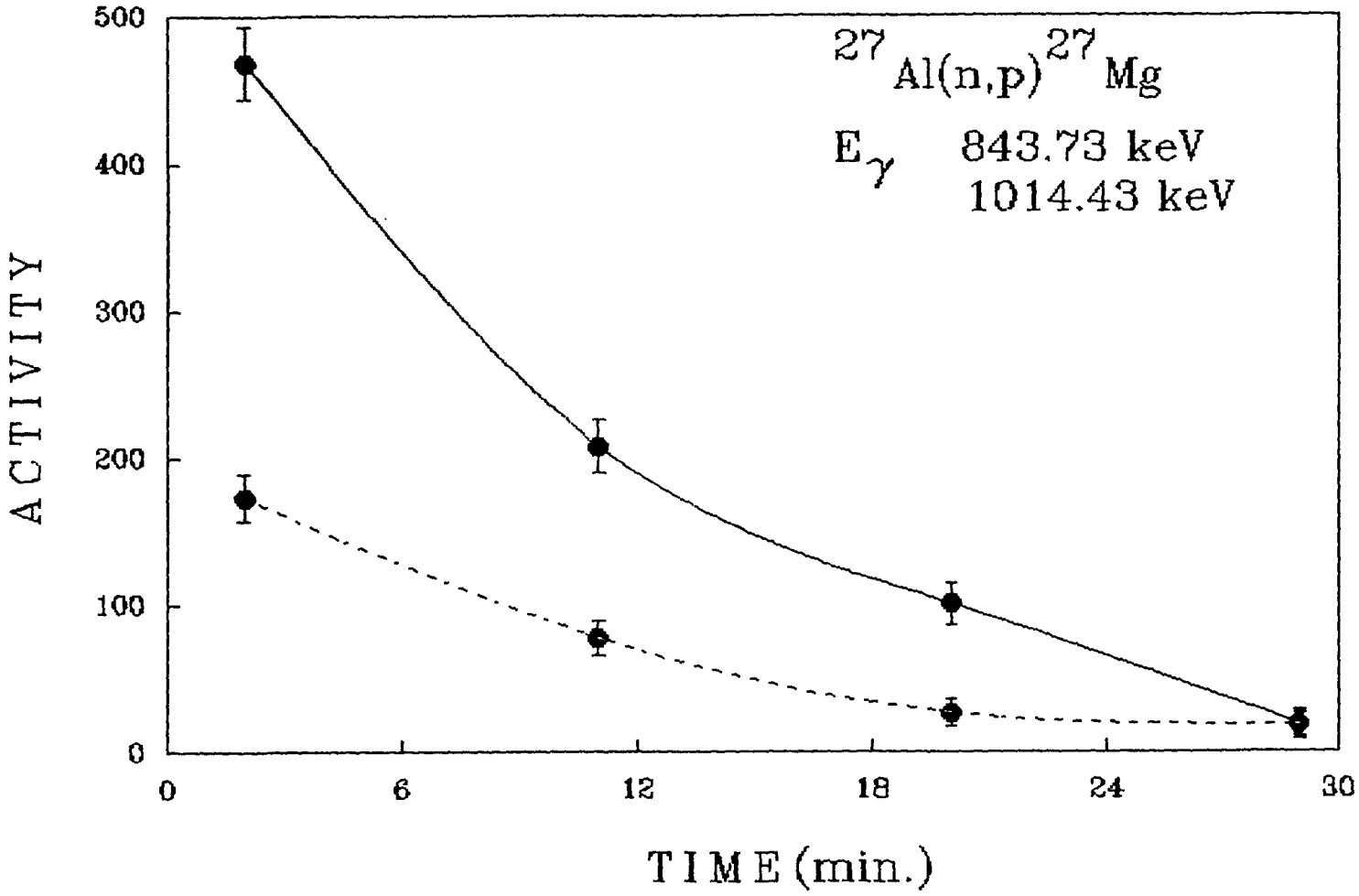

Fig.III.9 Decay curve for ^{27}Al.

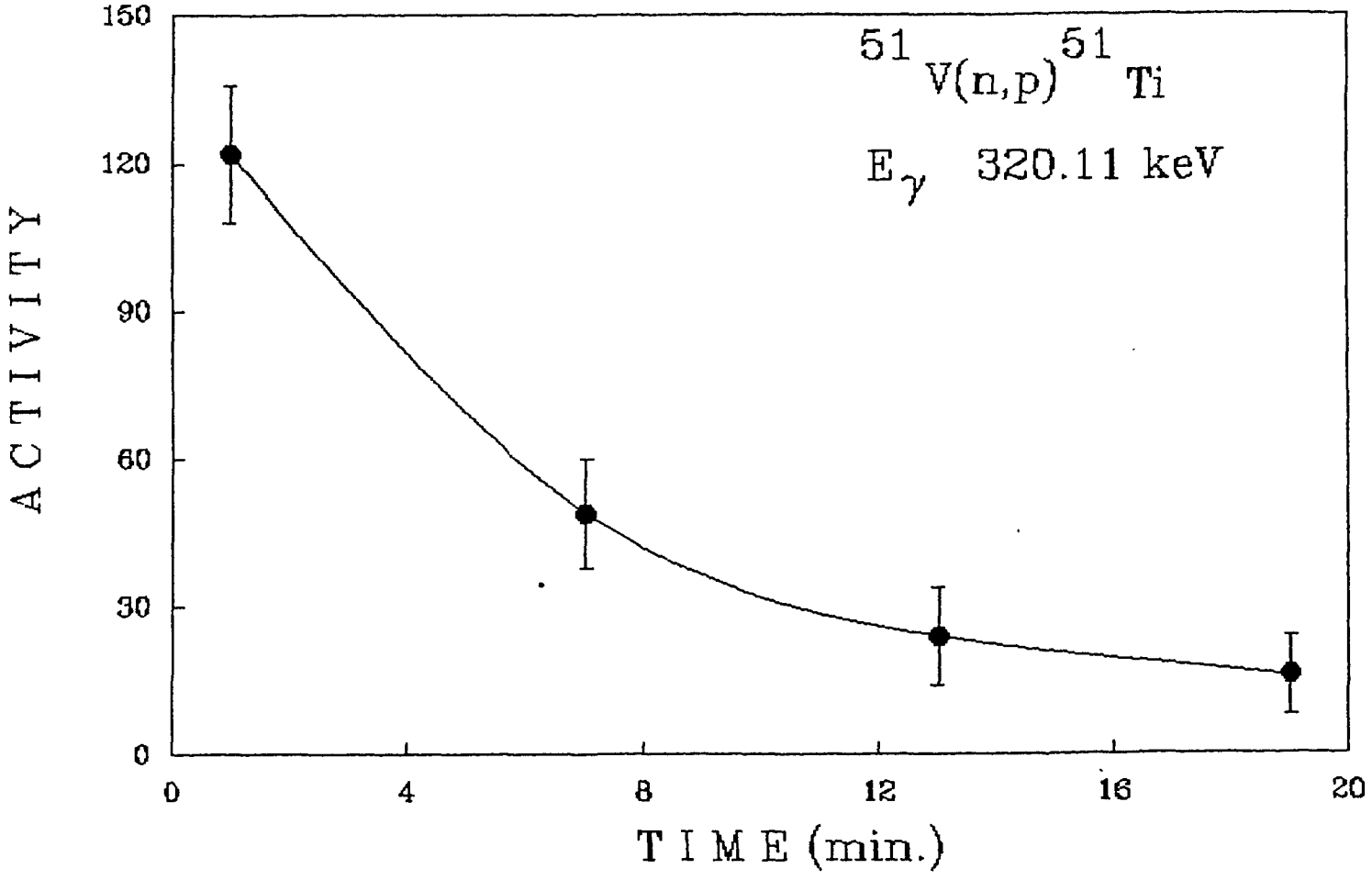

Fig.III.10 Decay curve for ^{51}V.

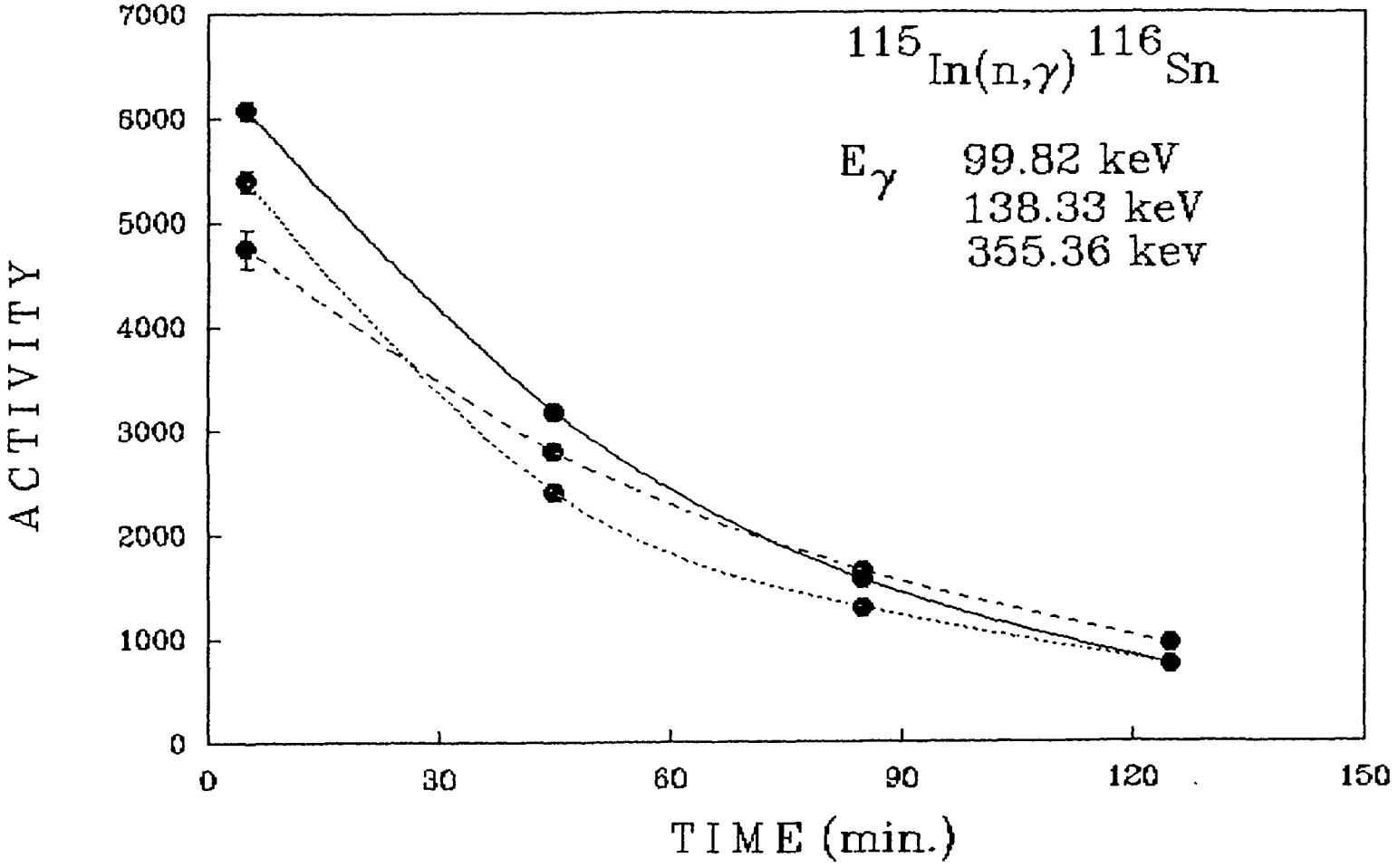

Fig.III.11 Decay curve for ^{115}In.

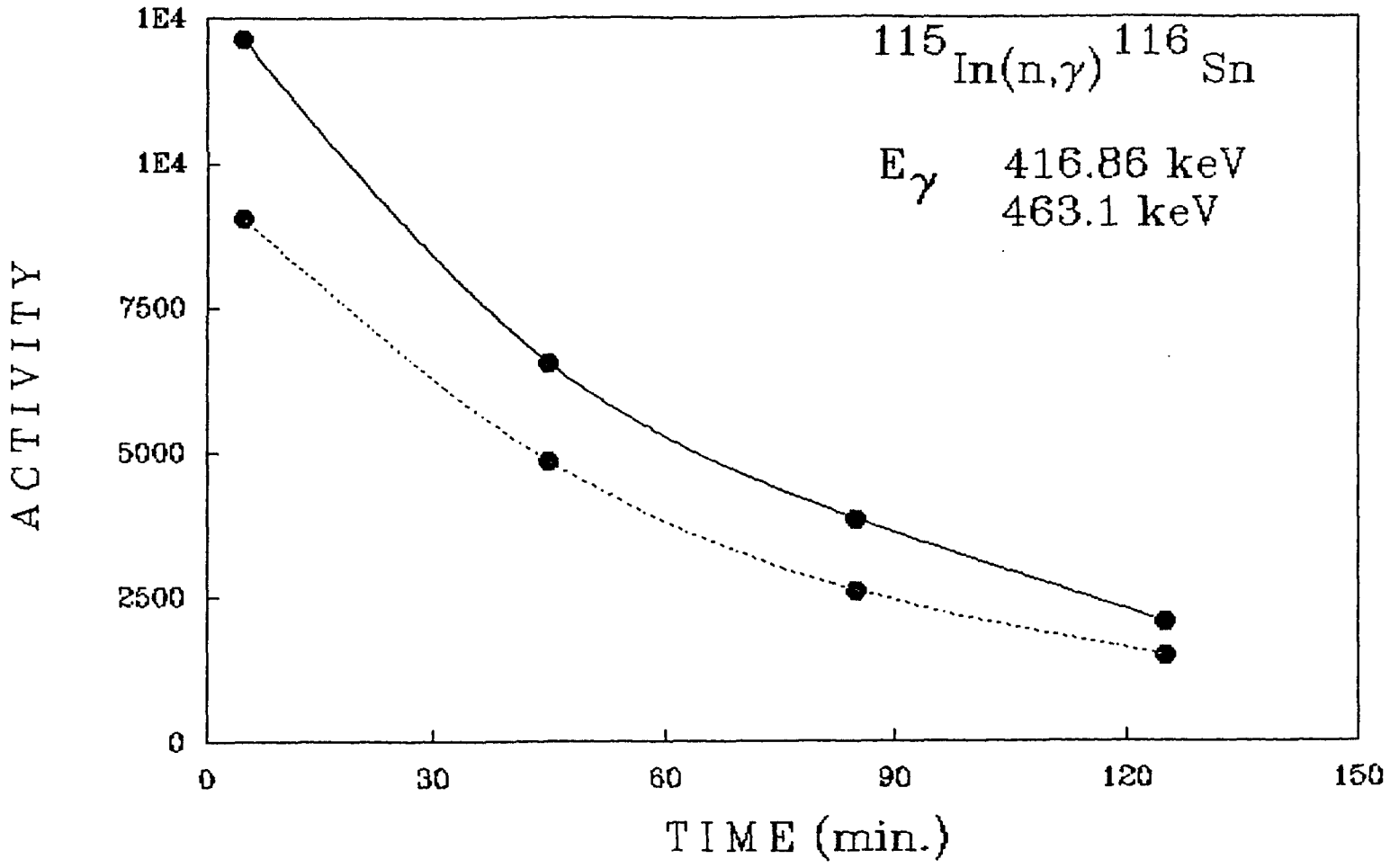

Fig.III.12 Decay curve for ^{115}In.

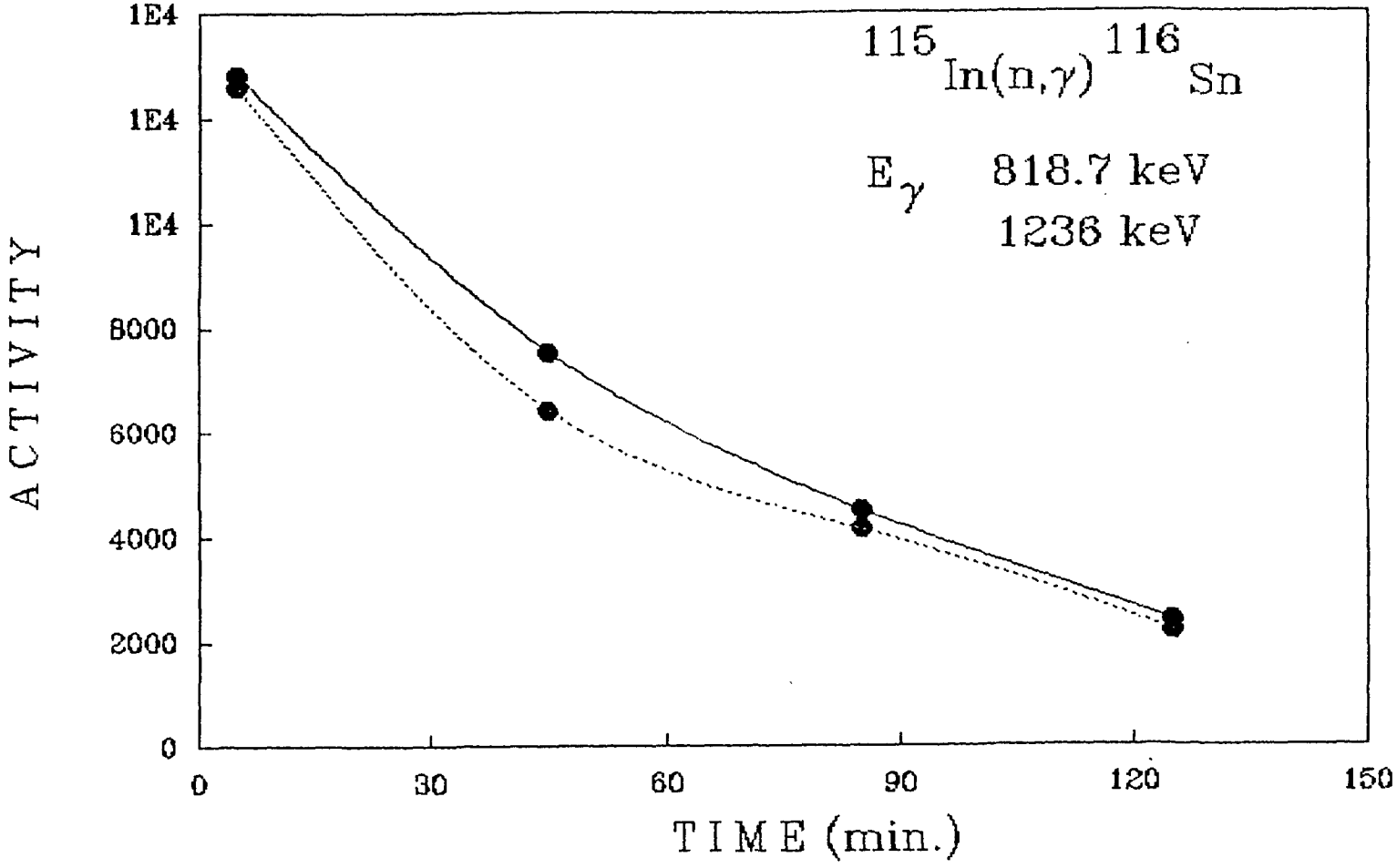

Fig.III.13 Decay curve for ^{115}In.

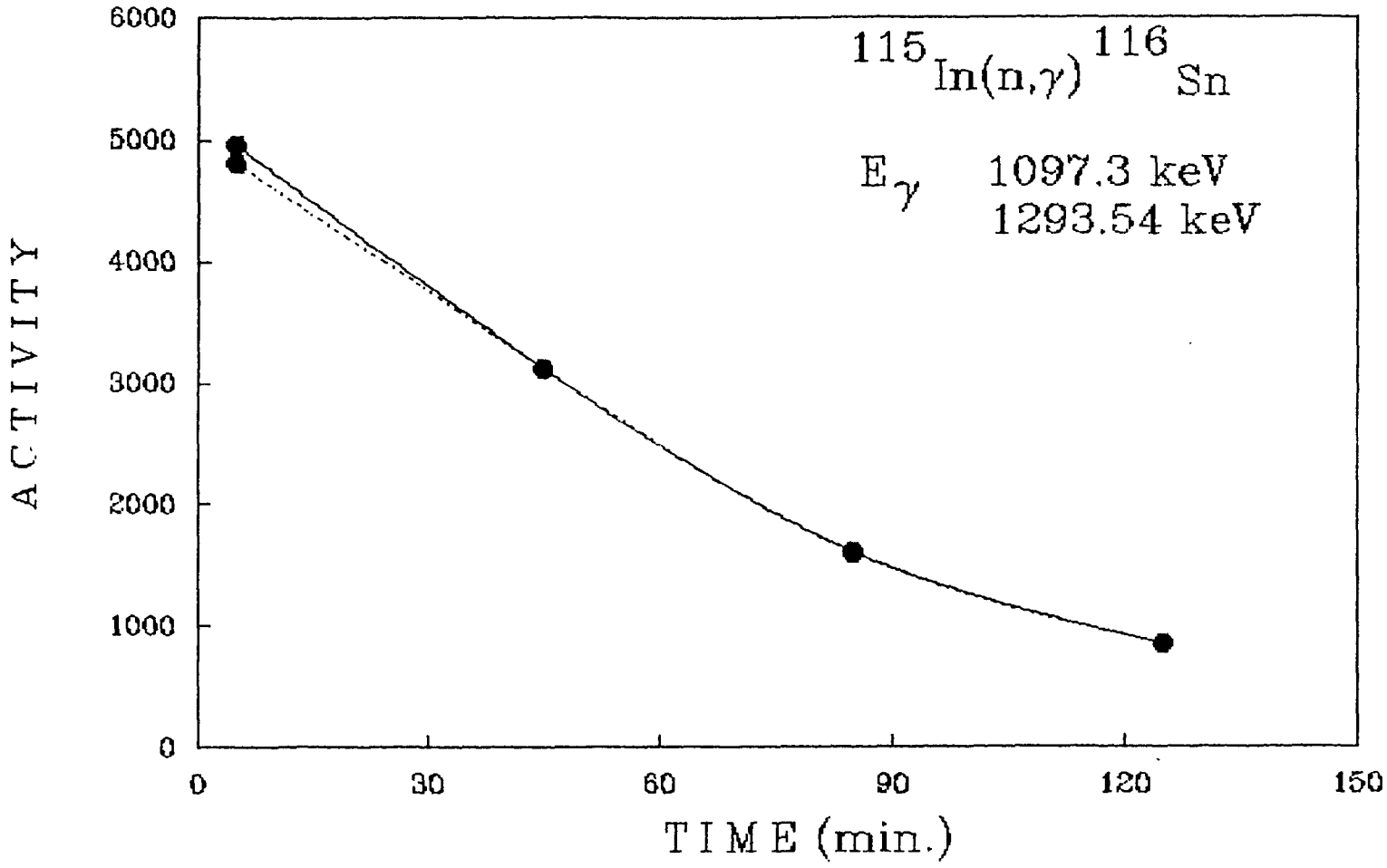

Fig.III.14 Decay curve for ^{115}In.

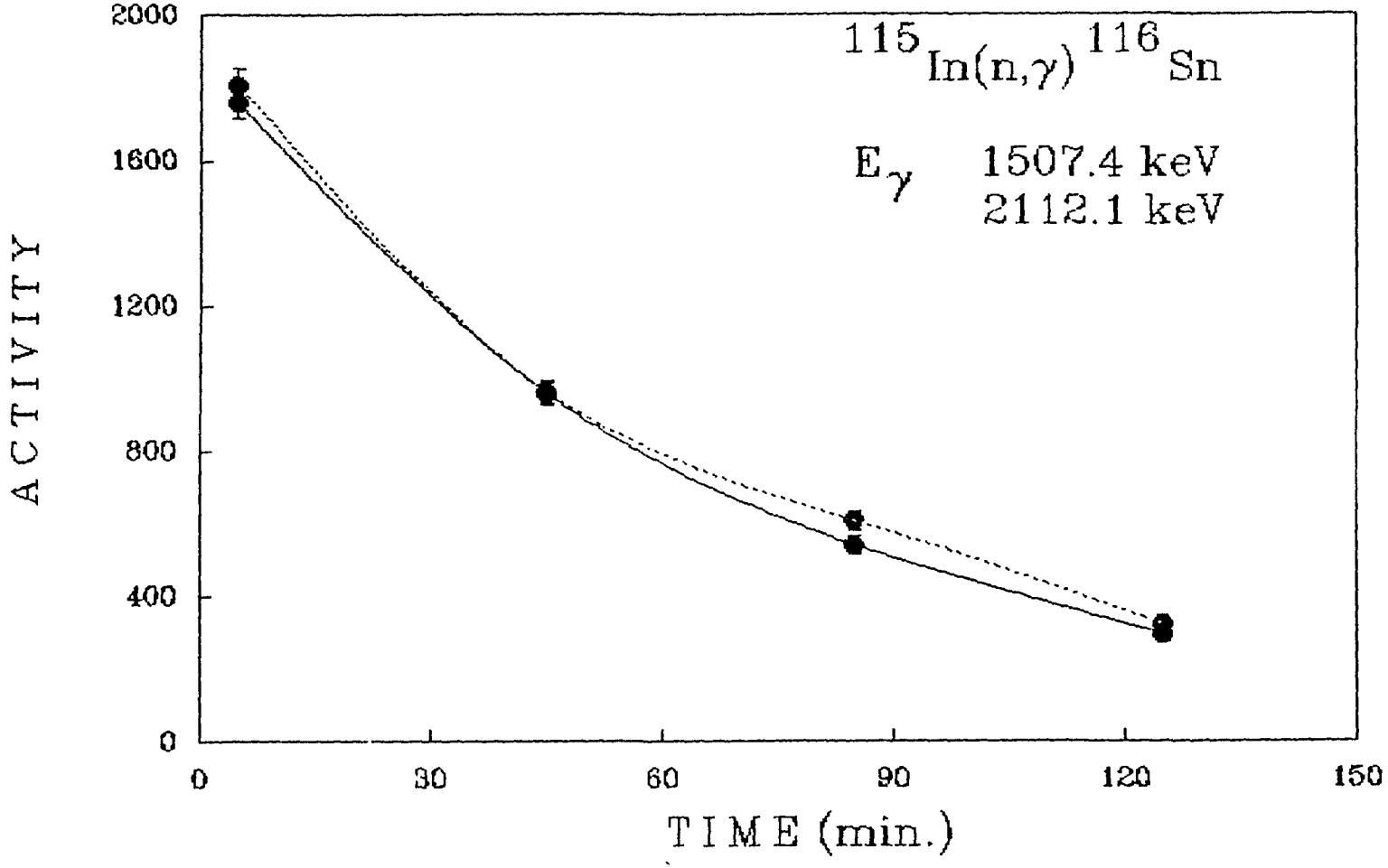

Fig.III.15 Decay curve for ^{115}In.

Table III.1 Table showing the irradiation parameters.

Element	Weight (gm)	Reaction	t_r (min)	t_d (sec)	t_c (min)	t_i (min)
Si	2	$^{28}Si(n,p)^{28}Al$	9	30	1.5	1
Al	2	$^{27}Al(n,p)^{27}Mg$	30	30	4	4
V	4.9	$^{51}V(n,p)^{51}Ti$	20	30	2	4
In	4.59	$^{115}In(n,\gamma)^{116m}In$ $^{116m}In \xrightarrow{\beta^-} {}^{116}Sn$	180	30	60	60

Table III.2 Table showing the decay parameters for the element of interest.

Element	Reaction	E_γ (keV)	$T_{1/2}$ (min)
Si	$^{28}Si(n,p)^{28}Al$	1778.70	2.200±0.4330
Al	$^{27}Al(n,p)^{27}Mg$	843.730	9.600±1.6100
		1014.43	9.400±1.6900
V	$^{51}V(n,p)^{51}Ti$	320.110	5.70±0.62800
In	$^{115}In(n,\gamma)^{116m}In$	99.8200	54.998±2.890
	$^{116m}In \xrightarrow{\beta^-} {}^{116}Sn$	138.830	54.998±2.648
		355.360	55.988±3.200
		416.860	54.99±2.8000
		463.100	54.99±2.8700
		818.700	54.99±3.3100
		1093.30	54.00±2.6000
		1236.00	54.440±1.700
		1293.54	55.00±2.4000
		1507.40	54.50±3.0000
		2111.10	54.00±3.1700

III.2.3 Elemental Analysis

Elemental analysis can be classified into two parts. *Trace elemental analysis* involves the determination of the concentration of the elements that are present in different systems in the range of parts per million (ppm) or parts per billion (ppb). *Bulk elemental analysis* deals with the determination of concentrations of elements that are present in large quantities at least $\sim$ 1% or more.

Basic Principle

The activation of the nuclei of the sample elements results in the production of radioactive isotopes which can be detected and measured by their nuclear radiations. Thus with an exact knowledge of nuclear characteristics the concentration of the element can be determined.

When an incident particle (x) reacts with a stable nucleus (X) it leads to the production of a radioactive product (Y^*), which decays alongwith a non-radioactive product(Y) according to the reaction

$$x + X \xrightarrow{Y^*} Y + y + Q, \qquad (4)$$

where Q is the Q-Value of the reaction. The activity of the nuclide (Y^*) is given by (taken from [2])

$$D(t) = N \sigma \phi \, (S.F) \, (D.F), \qquad (5)$$

where N is the number of atoms of the target nucleus present in sample (atoms/cm^2) and is given by

$$N = m \theta N^{O}/A,$$

where m : as the mass of the element (in gms.),

θ : is the fractional abundance of the isotope of interest,

N^{o} : is the Avogadro's number,

A : is the atomic weight of the element.

And σ : is the activation cross section (barns),

ϕ : is the bombarding neutron flux (neutrons/cm^2/sec),

S.F : is the saturation factor and is given by

S.F = $1 - \exp(0.693\ t_r/t_{1/2})$ and

D.F : is the decay factor and is given by

D.F = $\exp(-0.693\ t_d/t_{1/2})$,

with $t_{1/2}$: as half-life of element,

t_r : as irradiation time and

t_d : as delay time.

By the examination of (S.F) it is observed that irradiation for a period of about 2-3 half-lives is sufficient for all practical purposes. It is relatively easy to employ weighed amounts of known pure substances as reference standards. In order to avoid the measurement of σ and ϕ it is better to irradiate both the sample and the standard in the same geometry.This keeps other experimental parameters also the same. Then one can compare the activity of the standard with unknown sample.

If A_s and A_u are the areas of the peaks of the gamma rays of interest for standard and unknown sample, respectively, for a given collection time and M_s and M_u are the weights of the standard and the unknown sample respectively, a comparision of the two via eqn.(5) yields

$$M_s/M_u = A_s/A_u, \qquad (6)$$

where all other quantities are the same and can be cancelled out. Therefore,

$$M_u = M_s A_u / A_s. \qquad (7)$$

From this, M_u can be calculated and hence the weight, in percentage, of the sample can be easily found out.

Experimental Procedure

The Experimental set up, irradiation procedure and calibration of the system are same as discussed in section III.2.2. The above mentioned principle has been used for finding the concentration of Al and Si in coal fly ash and Al in a twenty paise coin (for a comparative study). For this, 2 gms of Al and Si powder ($\sim$ 100% pure) were taken as standards and packed in polythene packets. The unknown sample, coal fly ash, (SRM 1633 which contains both Al and Si), was also packed in a polythene packet and subjected to irradiation and counting separately for finding Al and Si concentrations. The irradiation time, delay time and collection time for the standard and unknown samples were the same.

A 20 paise coin was also packed in a polythene sheet and subjected to irradiation and counting, exactly in the same way as the standard Al powder. From the collected data for a given time the area of the peak of the gamma ray energies of interest were found out and the weight in percentage of the element in the sample were calculated using eqn.(7). The value thus obtained agreed well with the values given for SRM for Al and Si in coal flyash [10]. In case of the 20 paise coin also, the results obtained for the concentration of Al matched reasonably well

(within the experimental errors) with that quoted in ref [11]. All theexperimental parameters and the results obtained are given in Table III.3.

Table III.3 Table showing the parameters used for and the results otained from the analysis of NIST standard and Coinage metal.

Element	Weight in gms		E_γ	Concentration in %	
	Standard	Sample	(keV)	Certified	obtained
SRM NO: 1633a					
Al	2	5	843.73	14.3±1.0	10.17±3.2
			1014.43		12.00±2.1
Si	2	5	1778.7	22.8±0.8	21.38±3.8
Coinage Metal					
Al	2	2.2	843.73	95.0	90.18±7.7
			1014.43		89.40±8.6

The time of irradiation, delay time and counting time in the case of Aluminium was 30 mins, 30 sec and 5 minutes while for Silicon these values were 10 mins, 30 secs and 1.25 minutes respectively.

III.2.4 The ^{115}In (n,γ) Reaction

Neutron irradiation is one of the simplest ways to activate a sample. The resulting gamma activity can be studied by gamma ray spectroscopy. The interaction of slow neutrons with the nuclei, through (n,γ) reactions, renders the original element radioactive having mass number one higher than earlier, which subsequently undergoes β-decay with definite half-life. Finally they emit gamma rays corresponding to the particular de-exciting nucleus. The activity of the product nuclide depends largely on the value of neutron capture cross section. The present measurement has been carried out for finding the relative intensity of gamma rays emitted by ^{116m}In by activating ^{115}In through (n,γ) reactions. The process of activation and decay can be represented as,

$$^{115}_{49}In + ^{1}_{0}n \longrightarrow ^{116m}_{49}In^{*} \xrightarrow{\beta^-} ^{116}_{50}Sn + \gamma \ . \qquad (8)$$

The decay of $^{116}In^{*}$ obeys the usual radioactive law,

$$N = N_0 e^{-\lambda t}$$

For the measurement of gamma ray intensities an accurate determination of the FEPE of the detector is required. The determination of the FEPE of the detector will be discussed in detail in the next section.

In short, the efficiency of a detector is defined as

$$\epsilon = \frac{\text{Number of pulses recorded in the full energy peak}}{\text{Number of radiation quanta incident on the detector}}$$

The intensity of the gamma rays incident on the detector can be written as,

$$\text{Intensity} = \text{Yield} / \text{Efficiency} \qquad (9)$$

where yield = Peak area /second and

the full energy peak area can be calculated using the formula

$$A = \sum_{n_1}^{n_2} C_n - (C_{n_1} + C_{n_2}) \frac{(n_2 - n_1)}{2}, \qquad (10)$$

where C_n is the total counts under the full energy peak and C_{n_1} and C_{n_2} are the minimum counts on either side of the peak corresponding to the channel numbers n_1 and n_2.

Experimental Procedure

The experimental set up and calibration procedure were the same as discussed in section III.2.2. The Indium foil (having 99.77% ^{115}In) was irradiated for three hours with slow/thermal neutrons by placing a 2.5cm thick paraffin disc in between the source and the foil with the help of the arrangement specially made for the irradiation. After the irradiation the data was collected for a given time. From this spectrum the area under the peak of the gamma ray of interest was calculated using eqn.(10). A set of standard gamma sources was used for the efficiency determination . The efficiency data were least squares fitted to the analytical function of McNelles and Campbell [12]

$$\varepsilon = (a_1/E_\gamma)^{a_2} + a_3\exp(-a_4E_\gamma) + a_5\exp(-a_6E_\gamma) + a_7\exp(-a_8E_\gamma), \qquad (11)$$

where a's are the parameters. This equation was used without the

last term [13] (as discussed in section III.5). The fitted efficiency (see Fig.III.18) values were then used to determine the intensity using eqn.(9).

Here the relative intensities were calculated with respect to the intensity of 1293.54 keV gamma ray. The energy levels of ^{116}Sn have been determined recently by various authors [14-19]. In particular, the levels of ^{116}Sn can be reached via the decay of ^{116m}In or by the decay of ^{116}Sb. The present work was a reinvestigation of gamma ray spectra associated with the decay of ^{116m}In (which was verified by finding the half-life of ^{116m}In) and to find the relative intensities. The gamma ray energies and their relative intensities with respect to 1293.54 keV gamma ray are given in Table III.4. The partial decay scheme of ^{116m}In is also given in Fig.III.16 (taken from [17]).

Table III.4 Table showing the gamma energies and the comparison of their relative intensities with those cited in literature for ^{116m}In decay.

E_γ (keV)	Relative intensities of γ-rays (%) *				
	Present work	Ref[9]	Ref[10]	Ref[11]	Ref[12]
138.830	4.16±0.6140	3.8	4.00	4.70	4.700
355.360	0.82±0.0840	0.8	0.85	0.78	1.000
416.860	23.12±3.202	32	33.0	29.0	40.00
463.100	0.705±0.080	0.6	0.89	0.77	0.000
818.700	13.85±1.460	15	14.0	12.3	18.00
1093.30	68.95±8.120	56	49.0	59.0	64.00
1293.54	100±9.37300	84	82.0	84.0	100.0
1507.40	12.103±1.25	12	15.0	9.90	16.00
1752.40	2.55±0.2720	2	1.70	2.30	2.100
2112.10	14.396±1.68	16	18.0	15.7	22.00

* Intensities with respect to the 1293.54 keV gamma ray

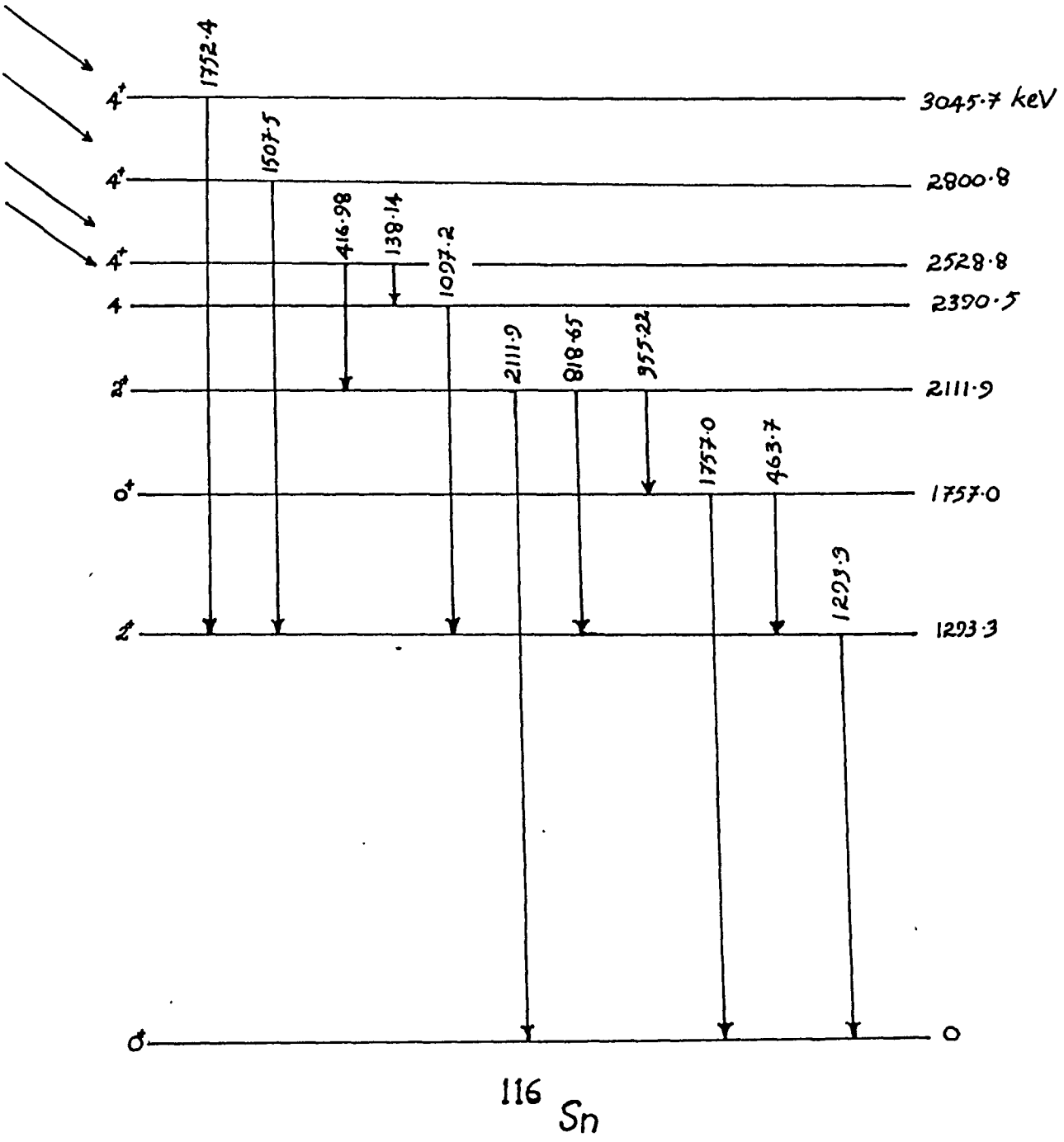

Fig.III.16 Partial decay scheme of ^{116m}In.

III.3 DETERMINATION OF THE FULL ENERGY PEAK EFFICIENCY (FEPE) OF 157cm^3 HPGe AND 2"X 2" NaI(Tl) DETECTORS

The intensity measurement of gamma ray transitions in nuclei with gamma detectors depend on their FEPE. For many purposes the accurate determination of the photon intensities can be of great value than the determination of energy. Thus the determination of the FEPE values as a function of gamma ray energy with high accuracy is very important.

HPGe detectors are increasingly being preferred to NaI(Tl) detectors for most gamma ray spectroscopy experiments because of their better energy resolution characteristics. One drawback in using HPGe detectors is their low efficiency compared to NaI(Tl) detectors. Precise definition of the active size of the NaI(Tl) detector is possible while in case of HPGe detectors it is difficult due to diffused boundaries. Consequently Monte-Carlo calculation of FEPE values often do not give accurate results. Therefore, experimental approach is usually adopted in finding the FEPE of a detector.

The experimental determination of FEPE at discrete energy values with accuracies of one percent or so is a simple but tedious procedure. Usually the FEPE is experimentally determined by employing a set of standard gamma ray sources of known strength which cover a wide range of energies. The energy spectra of emitted gamma rays were often analysed by determining the areas under the photopeak (full energy peak). Energy Cyclotron Centre (VECC), Calcutta. It is also possible to calculate (empirically)

the FEPE of this detector by knowing its dimensions and gamma absorption coefficients.

The experimental determination of the FEPE depends on the following factors

(i) geometry,

(ii) quality of reference (standard) sources used,

(iii) corrections like disintegration scheme and behaviour of the associated electronic equipment,

(iv) method employed to determine the peak area.

For the 157 cm^3 HPGe and 2"x2" NaI(Tl) detector it was possible to determine the FEPE in a fixed source-detector geometry by using a source mount made of perspex, fabricated at the VECC, Central workshop, Calcutta. Gamma ray standard sources used to determine the FEPE consisted of ^{241}Am, ^{57}Co, ^{60}Co, ^{137}Cs, ^{54}Mn, ^{22}Na, ^{133}Ba and ^{152}Eu. Their details are given in Table III.5.

The electronics associated with the HPGe detector was the same as discussed in section III.2.1a, while that of NaI(Tl) detector consisted of a high voltage bias supply, pre-amplifier (EG & G Ortec Model No. 113) and an EG & G Ortec 570 spectroscopy amplifier.

The area of the gamma ray peak could be calculated by the spectrum analysis programme (APPLE) [20] procured from Variable Energy Cyclotron Centre (VECC), Calcutta or manually using the formula given in eqn.(10).We employed both the methods to cross check the calculated areas.

To determine FEPE of the detector one has to relate the number of pulses counted to the number of photons incident on the

detector. The intrinsic efficiency of a detector can be determined (taken from [6]) as follows,

$$\varepsilon = \frac{\text{Number of pulses recorded in the detector}}{\text{Number of radiation quanta emitted by the source}} \times \frac{4\pi}{\Omega}$$

i.e $$\varepsilon = \frac{A/t}{Na\phi}\left[\frac{4\pi}{\Omega}\right], \qquad (12)$$

where A = Area of the photopeak (full energy peak),

t = counting time,

N = present strength of the source at the start of the experiment and is given by,

$$N = N_0 \exp\left(-0.693\ T/T_{1/2}\right),$$

where N_0 = initial strength of the source,

T = time elapsed from the time of fabrication of the source till the start of the present experiment and

$T_{1/2}$ = half-life of the corresponding source,

a = abundance of the emitted gamma ray,

Ω = solid angle subtended by the detector at the source and is written as

$$\Omega = \pi r^2/d^2,$$

where r = the radius of the detector and

d = the source to detector distance

and ϕ = the factor accounting for the absorption of the incident gamma rays .

For the HPGe detector,

$$\phi = \exp\{-(\mu_{Al}x_{Al} + \mu_{Ge}x_{Ge})\} \text{ and}$$

for NaI(Tl) detector,

$$\phi = \exp\{-(\mu_{Al}x_{Al})\},$$

where μ_{Al} and μ_{Ge} are the absorption coefficients of Al and Ge while x_{Al} and x_{Ge} are their respective thicknesses.

Experimental Procedure

The block diagram of the experimental set up of the HPGe detector has already been given in Fig.III.3 (section III.2.1) and that for NaI(Tl) is given in Fig.III.17. The specified bias was applied to the detectors and allowed to stabilise for at least an hour or so. The calibration of the detector system was done by using the standard calibration gamma ray sources (^{241}Am, ^{60}Co, ^{57}Co, ^{137}Cs and ^{22}Na). For FEPE determination all the available standard calibration gamma ray sources were used. The sources were placed on the source mount at a fixed distance (see Table III.6) in front of the detector one by one and the data were taken separately for an appropriate time (see Table III.7). The FEPE of the detector at each gamma ray energy was determined after calculating the area under the corresponding gamma peak and substituting the same in eqn.(12). All the parameters used for determining the FEPE of both detectors are given in Tables III.5-III.8. The experimentally determined FEPE data points for these detectors were fitted to the analytical function proposed by McNelles and Campbell [12] using eqn.(11) as modified by Singh [13] (as discussed in section III.5) and are shown in Figs.III.18 and III.19 (to obtain better fits some of the low energy ε values were excluded as can be seen in Fig.III.18). The parameters are given in Table III.13. The yield, intensity and the FEPE values alongwith their errors (for both HPGe and NaI(Tl) detectors) are given in Tables III.9 and III.10, respectively.

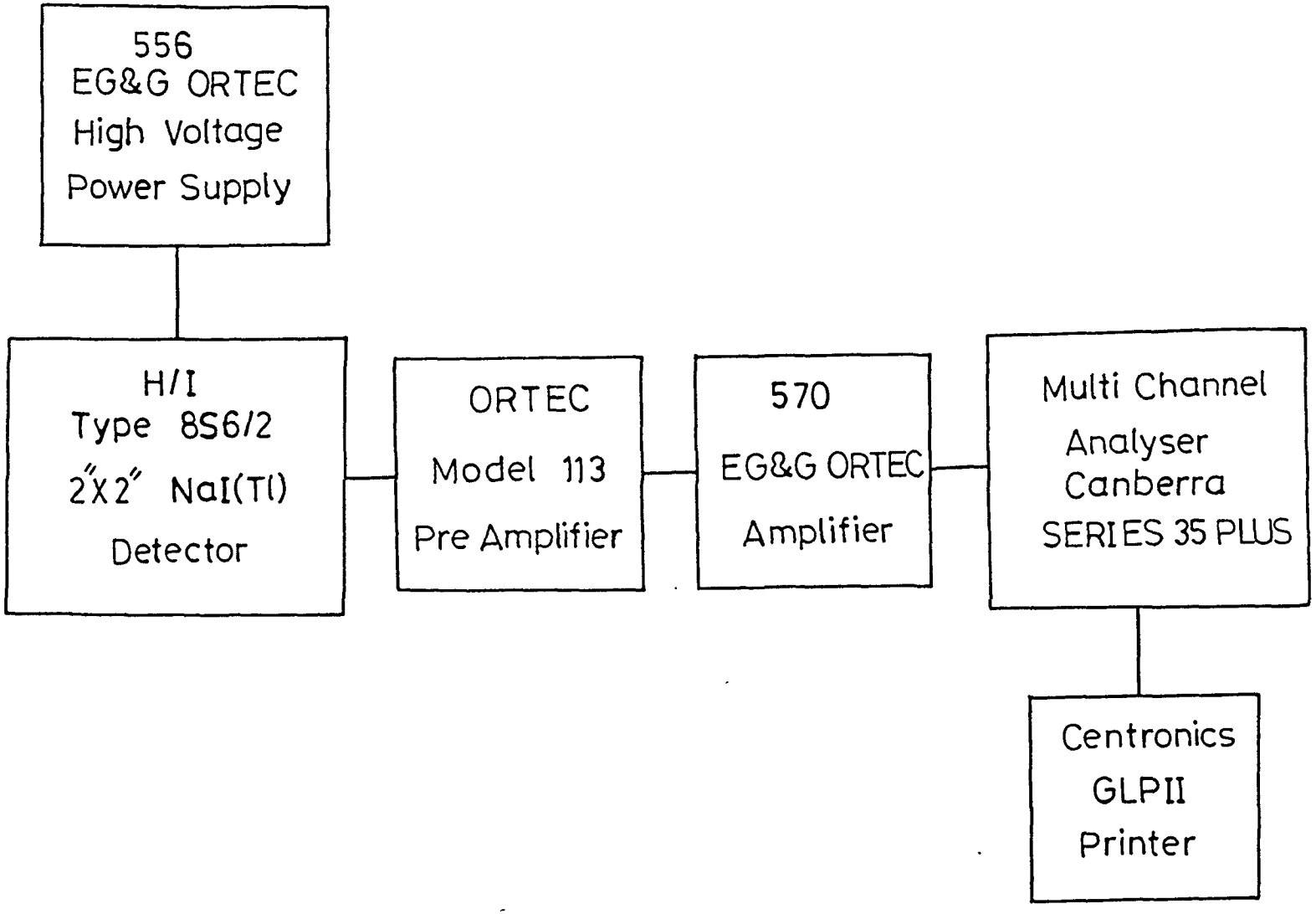

Fig.III.17 Block diagram of the NaI(Tl) detector and its associated electronics.

Table III.5 Details of the standard gamma sources used for the determination of the efficiency of 157 cm^3 HPGe and 2"x2" NaI(Tl) detectors.

Radio-Nuclide	E_γ (keV)	$T_{1/2}$ (days)	Percentage per disintegration	Activity (KBq)
^{241}Am	59.537±0.00100	(1.58±0.002) x10^5	36.00±0.30000	394.5±1%
^{57}Co	122.063±0.0030	271.77±0.050	85.59±0.19000	422.9±1%
	136.476±0.0030		10.58±0.08000	
^{22}Na	511.006±0.0020	950.34±0.130	-	
	1274.54±0.0200		99.94±0.02000	420.0±1%
^{137}Cs	661.645±0.0090	11009±11.000	84.600±0.5000	359.0±1%
^{54}Mn	834.827±0.0210	312.5±0.5000	99.976±0.0002	285.3±1%
^{60}Co	1173.238±0.004	1925.2±0.400	99.8700±0.060	461.50±1%
	1332.501±0.005		99.9800±0.009	
^{133}Ba	80.997±0.00500	3848±1.10000	34.00±0.80000	319±1.50%
	276.397±0.0120		7.100±0.10000	
	302.851±0.0150		18.3300±0.220	
	356.005±0.0170		62.300±0.7000	
	383.851±0.0150		8.9200±0.0900	
^{152}Eu	121.779±0.0030	4931±15.0000	28.3700±0.240	358.60±2%
	244.693±0.0050		7.5100±0.0600	
	344.272±0.0070		26.5800±0.180	
	411.111±0.0110		2.2340±0.0130	
	443.979±0.1000		3.12100±0.018	
	778.89±0.01600		12.9600±0.070	
	867.38±0.03000		4.1600±0.0600	
	964.05±0.03000		14.6200±0.060	
	1085.83±0.0300		10.1600±0.050	
	1112.08±0.0400		13.5600±0.060	
	1408.03±0.0300		20.580±0.0900	

[Data taken from IAEA, Vienna, Certificate No.EMS-A2,dated 28.06.1983.]

Table III.6 Table showing the dimensions of the gamma ray detectors.

Detector	Crystal		Thickness of		Source-detector
	Length (mm)	Radius (mm)	Al (mm)	Ge (mm)	distance (cm)
HPGe	69.6	27.5	1.27	0.7	5.0
NaI(Tl)	50.8	25.4	2.54	0.0	9.8

Table III.7 Table showing the collection time and elapsed time used in the case of HPGe and NaI(Tl) detectors for efficiency calculation.

Source	HPGe		NaI(Tl)	
	collection time (sec)	elapsed time (T) (days)	collection time (sec)	elapsed time(T) (days)
^{241}Am	100	5177.52	100	5356.75
^{57}Co	600	5177.52	1000	5356.76
^{22}Na	200	5177.52	1200	5356.79
^{137}Cs	100	5177.52	200	5356.71
^{54}Mn	3600	5177.52	15000	5356.81
^{60}Co	150	5177.52	900	5356.66
^{133}Ba	200	5177.52	400	5356.84
^{152}Eu	500	5177.52	2000	5356.87

Table III.8 Table showing the absorption coefficients (μ) for Al and Ge at different energies.

E_γ (keV)	μ_{Al} (cm^{-1})	μ_{Ge} (cm^{-1})
59.53700	0.7550	10.950
80.99700	0.5400	5.0000
121.7790	0.4060	2.0500
122.0630	0.4060	2.0500
136.4760	0.3850	1.6500
244.6930	0.3050	0.7500
276.3970	0.2900	0.6700
302.8510	0.2800	0.6200
344.2720	0.2655	0.5680
356.0050	0.2625	0.5500
383.8510	0.2550	0.5230
411.1110	0.2475	0.4970
443.9790	0.2377	0.4750
661.6450	0.2000	0.3840
778.8900	0.1850	0.3526
834.8270	0.1781	0.3425
867.3800	0.1750	0.3360
964.0500	0.1663	0.3175
1085.830	0.1563	0.2960
1112.080	0.1539	0.2910
1173.238	0.1500	0.2840
1274.540	0.1438	0.2710
1332.501	0.1406	0.2650
1408.030	0.1369	0.2575

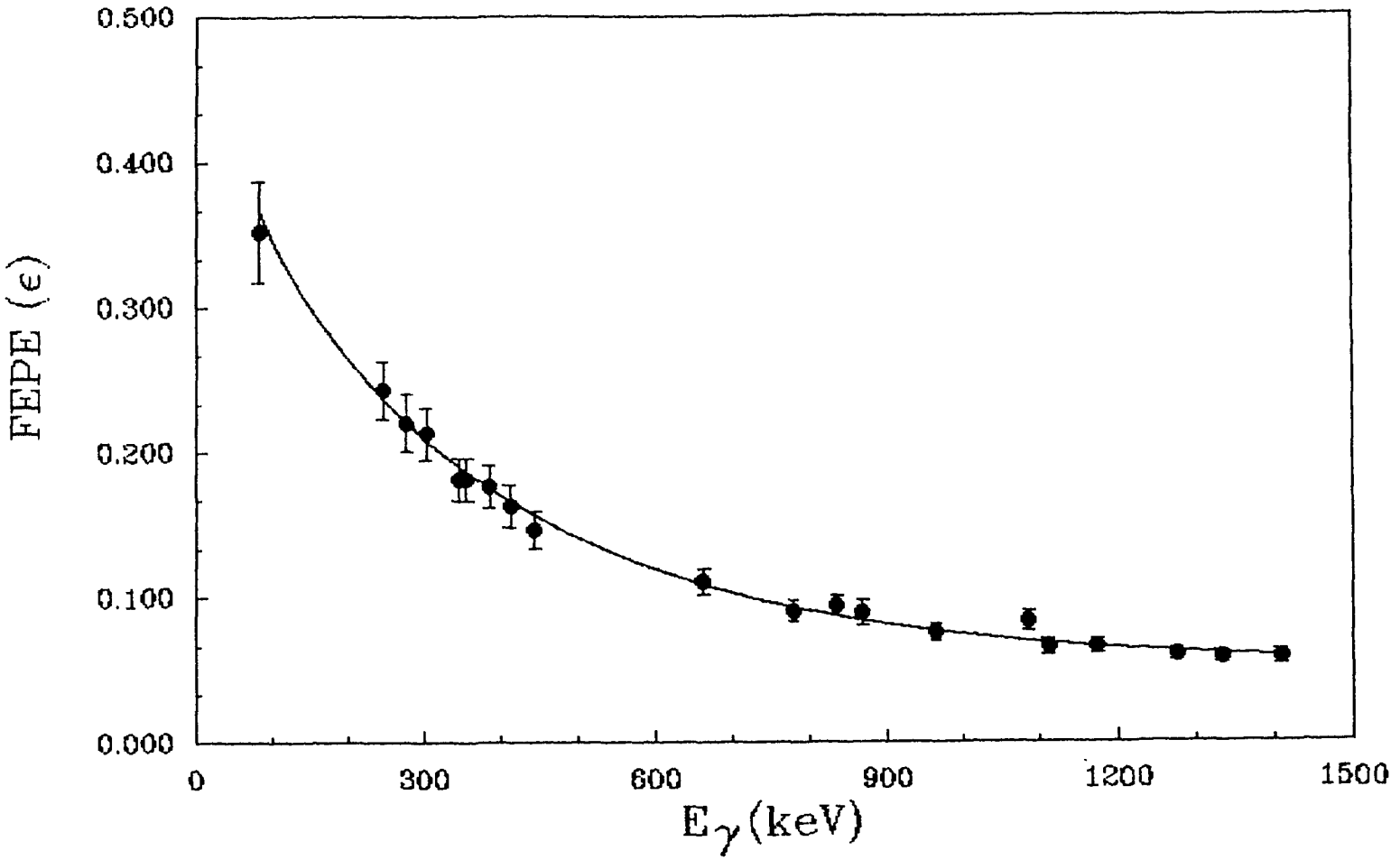

Fig.III.18 Least-Square fit of the FEPE data of the 157 cm^3 HPGe co-axial detector to eqn.(11) (without the last term).

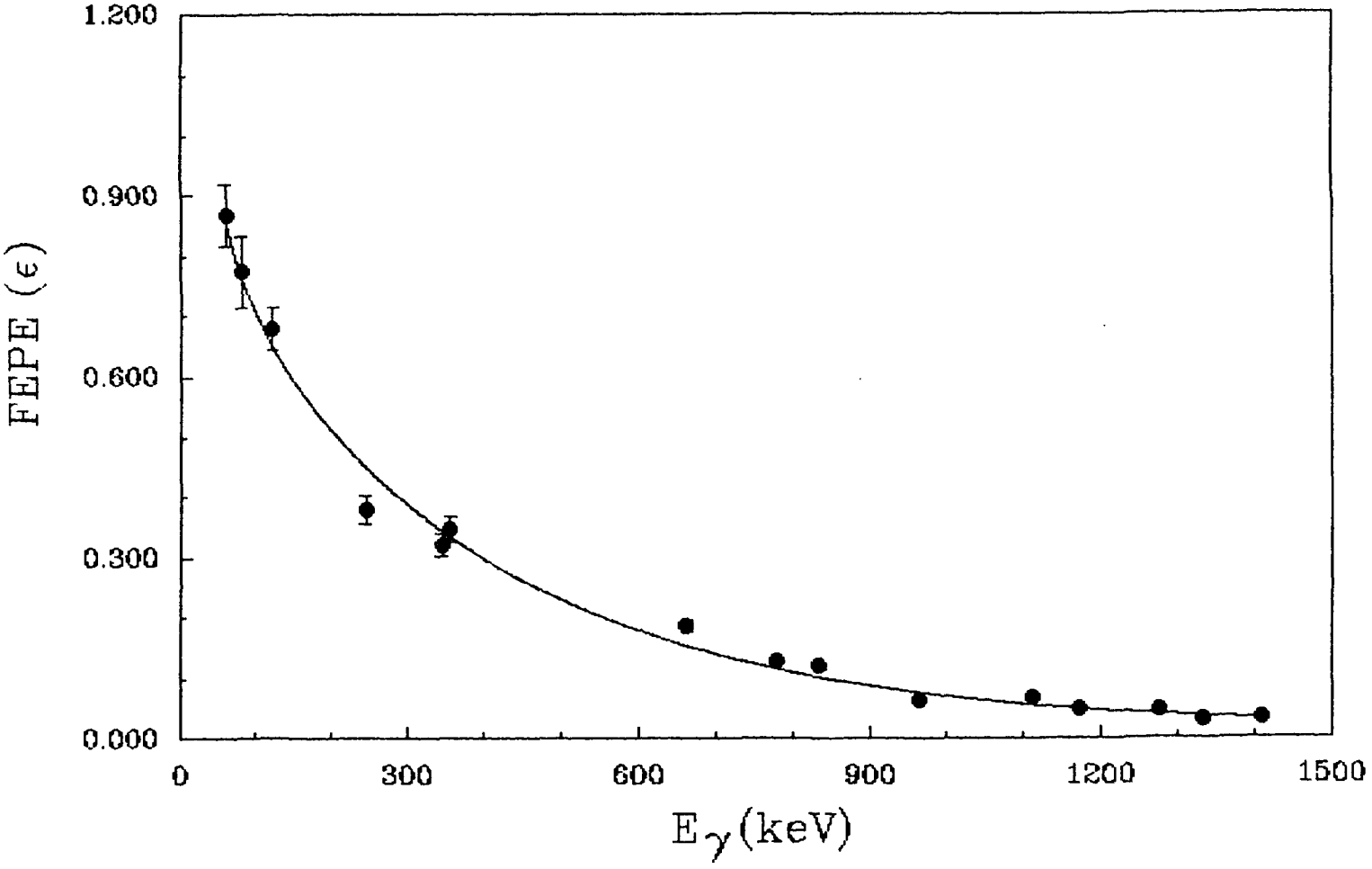

Fig.III.19 Least-Square fit of the FEPE data of the 2"x2" NaI(Tl) detector to eqn.(11) (without the last term).

Table III.9 Table showing the yield, intensity, efficiency and the error in ε of HPGe detector at different energies.

E_γ (keV)	Yield (Y)	*Intensity (I)	Efficiency (ε)	$\Delta\varepsilon$
59.5370	961.5370	4497.134	0.21382	0.019406
80.9970	1311.803	3720.123	0.35262	0.034812
121.779	1715.949	4735.988	0.37153	0.029811
122.063	51.94800	114.6870	0.45296	0.032167
136.476	6.043000	14.61800	0.41334	0.043511
244.693	338.4220	1390.858	0.24332	0.020095
276.397	239.8250	1085.838	0.22086	0.019526
302.851	601.1550	2816.699	0.21343	0.017816
344.272	910.0700	5010.825	0.18162	0.014431
356.005	1752.055	9641.828	0.18172	0.014753
383.851	244.4170	1384.428	0.17655	0.014732
411.111	69.23300	424.2170	0.16321	0.014265
443.979	87.09200	594.3020	0.01465	0.012543
661.645	2123.980	19151.49	0.11091	0.008405
778.890	224.1120	2467.137	0.09084	0.007302
834.827	19.71200	208.3590	0.09461	0.006561
867.380	72.24900	806.2920	0.08961	0.008452
964.050	215.8770	2840.476	0.07600	0.005599
1085.83	166.7470	1979.442	0.08423	0.006758
1112.08	175.2220	2643.507	0.06628	0.005269
1173.238	1055.613	15922.085	0.06629	0.004499
1274.54	410.8270	6760.958	0.06076	0.004048
1332.501	941.1000	15979.902	0.05889	0.003968
1408.03	235.5980	4030.251	0.05846	0.004561

*Intensity = number of gammas incident on the detector.

Table III.10 Table showing the yield, intensity, efficiency and the error in ε of NaI(Tl) detector at different energies.

E_γ (keV)	Yield (Y)	*Intensity (I)	Efficiency (ε)	$\Delta\varepsilon$
59.537	2012.43	2317.899	0.868212	0.051877
80.997	946.824	1221.452	0.775162	0.059153
121.779	798.308	1251.302	0.637982	0.038078
122.063	17.3330	25.49400	0.679865	0.035643
244.693	126.425	332.0910	0.380695	0.022671
344.272	377.768	1176.638	0.321057	0.018732
356.005	782.856	2253.963	0.347324	0.020719
661.645	832.240	4434.417	0.187677	0.009786
778.89	74.2620	574.8850	0.129176	0.007597
834.827	49.8030	41.06000	0.121297	0.006221
964.05	41.3230	648.8280	0.063687	0.003934
1112.08	41.5760	601.9750	0.069011	0.004192
1173.238	177.473	3565.698	0.049772	0.002237
1274.54	69.3850	1472.224	0.047129	0.002237
1332.501	143.928	4434.417	0.032457	0.001457
1408.03	30.6030	914.0120	0.033482	0.002024

*Intensity = number of gammas incident on the detector.

III.4 EMPLOYMENT OF A NEW METHOD FOR CALIBRATING THE HPGe DETECTORS

Ray Gunnik [21] has developed a method for determining the FEPE of a coaxial germanium detector by using the manufacturer's specifications. By examining the FEPE curve of a large number of detectors of various sizes for developing a calibration method, he found a model that viewed the 50 keV to 4 MeV calibration curve in energy regions: ≤ 90 keV, 90 to 200 keV and > 200 keV. We have employed the same method here for determining the FEPE values of our 157 cm^3 HPGe detector. These values have been compared with the experimentally obtained values.

Procedure

(i) 50-90 keV Region

By ignoring the source to detector distance, FEPE for 157 cm^3 HPGe coaxial detector in this energy region is determined by the equation,

$$\varepsilon_E = \varepsilon_o \exp\{-(\mu_{Al}\, x_{Al})\} \exp\{-(\mu_{Ge} x_{Ge})\}, \qquad (13)$$

where, ε_E = observed detector FEPE,

ε_o = ideal FEPE (with no absorption),

μ_{Al} and μ_{Ge} are the absorption coefficients of Al and Ge and x_{Al} and x_{Ge} are their corresponding thicknesses. The values of μ_{Al}, μ_{Ge}, x_{Al} and x_{Ge} are known and is presented in Table III.8. Therefore, only one FEPE point is needed to completely characterise the FEPE curve in this region.

(ii) The > 200 keV Region

In this region it is observed that the logarithm of the

efficiency is a linear function of the logarithm of the energy. After using a number of analytical functions a polynomial expression of the following form (when energies are expressed in MeV) was obtained,

$$\ln \varepsilon_E = \sum_{j=1}^{6} a_j (\ln E)^{j-1}, \qquad (14)$$

where, a_j's are the higher order coefficients (non linearity coefficients) and are described using the following equations.

$$a_1 = \ln (0.0053 + 0.01157\ \varepsilon_{1.33}),$$

where $\varepsilon_{1.33}$ is the efficiency at 1.33 MeV (using a ^{60}Co source) as quoted by the manufacturer (%);

$$a_2 = 0.06\ [1-(D/H)^2] - 1.742 + 0.1872\ \ln(0.785\ H\ D^2),$$

where D and H are the detector's diameter and the height respectively;

$$a_3 = 0.539 - 0.01611\ V + 1.566\times10^{-4}\ V^2 - 5.01\times10^{-7}V^3,$$

where V is the detector volume;

$$a_4 = -0.13595 + 1.239\times10^{-3}\ V - 6.088\times10^{-6}\ V^2,$$

$$a_5 = -0.2239 + 6.3\times10^{-3}\ V - 5.895\times10^{-5}\ V^2 + 1.852\times10^{-7}V^3,$$

$$a_6 = -0.04057 + 1.606\times10^{-3}\ V - 1.416\times10^{-5}\ V^2 + 4.292\times10^{-8}V^3.$$

By knowing $\varepsilon_{1.33}$, D, H and V of the detector a_j's can be easily found out. Using all the a_j's in eqn.(15), which is the expanded form of eqn.(14), one can calculate the FEPE at energies greater than 200keV.

$$\ln \varepsilon_E = a_1+a_2(\ln E)+a_3(\ln E)^2+a_4(\ln E)^3+a_5(\ln E)^4+a_6(\ln E)^5 \qquad (15)$$

(iii) The 90-200 keV Region

The FEPE curve in this region can be obtained by interpolating the above two regions by considering the equation,

$$\ln\varepsilon_E = A_1 + A_3[4.816 \ln E + \ln E^2]. \quad (16)$$

Here ε_E for the two boundary points can be determined from eqns.(13) and (15). The parameters A_1 and A_3 can be found easily by solving the two equations with two boundary FEPE points.

Results and Discussion

The above mentioned method greatly reduced FEPE calibration effort. We have determined the FEPE points for all the three regions, and they are given in Table III.11 alongwith the experimentally obtained values. In this method the number of measurement points needed for constructing the FEPE curve is reduced. These FEPE data points are plotted as a function of energy and is shown in Fig.III.20. The points with error bars in Fig.III.20 represent the experimentally obtained FEPE values. Detector dimensions and all the non-linear coefficients that were used in the calculations are given in Table III.12. We have taken $\varepsilon_{1.33}$ ($\sim$ 5.9%) from experimental data instead of taking it from manufacturers data. This is because the efficiency of the detector had greatly reduced due to neutron damage (as discussed in section III.1.1.)

Table III.11 Table showing the parameters used in efficiency calculation of the HPGe detector by empirical method.

Equation Number	Parameters
(15)	$V = 157\ cm^3$
	D = 5.50000 cm
	H = 6.96000 cm
	a_1= -2.6089777
	a_2= -0.7633243
	a_3= -0.0690529
	a_4= -0.0914901
	a_5= 0.02884550
	a_6= 0.02863800
(16)	A_1= -9.3323025
	A_3= -1.9385188

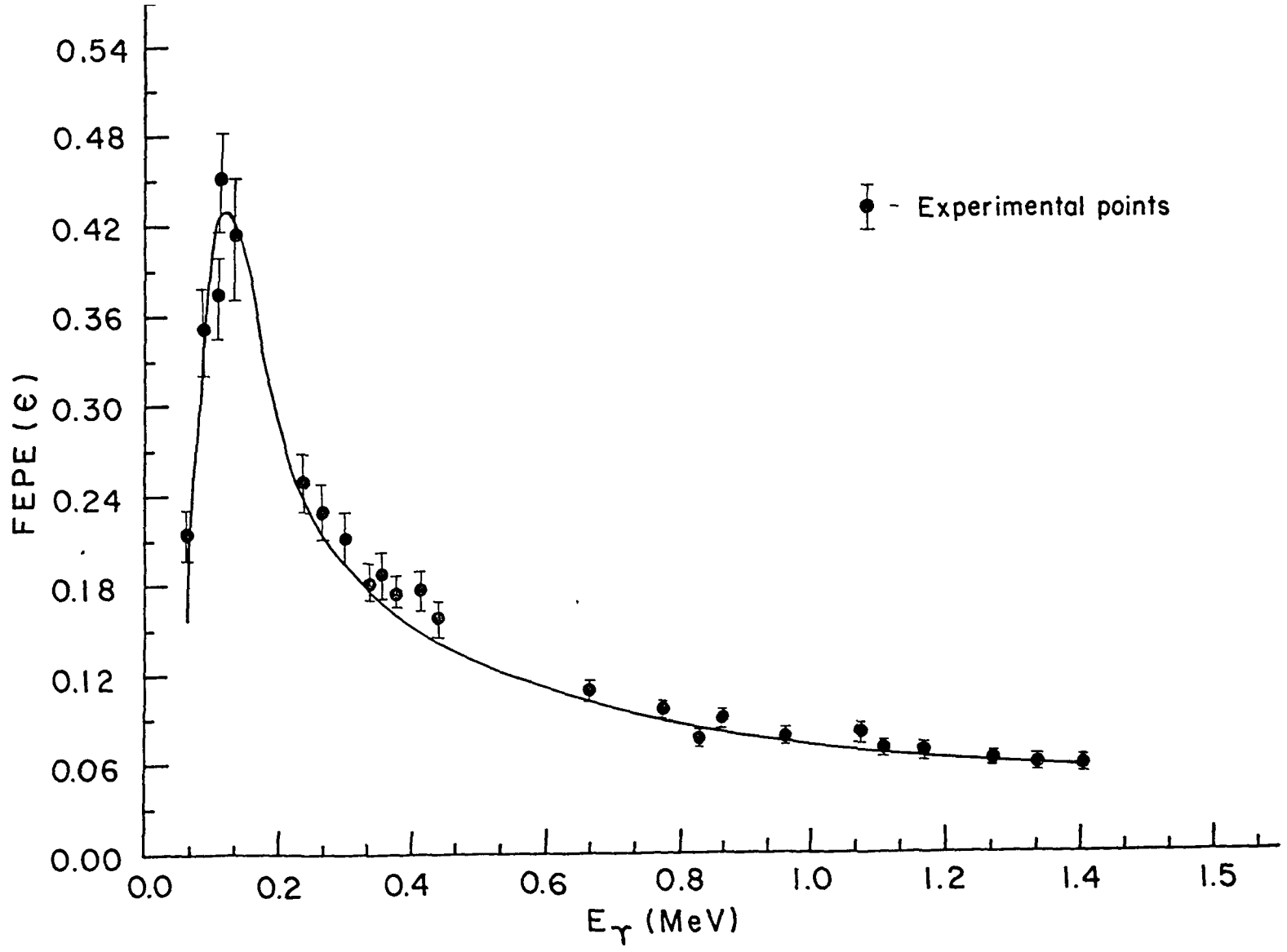

Fig.III.20 The calculated FEPE curve (solid line) of a 157 cm^3 coaxial HPGe detector as a function of the gamma ray energy.

Table III.12 Table showing the efficiency of HPGe detector (obtained by both experimental and empirical method) at different energies.

E_γ (keV)	Efficiency(ε)	
	Experimental	Empirical
0.059537	0.21382	0.15441
0.080997	0.35262	0.30641
0.121779	0.37153	0.43144
0.122063	0.45296	0.43158
0.136476	0.41334	0.42305
0.244693	0.24332	0.23201
0.276397	0.22086	0.20828
0.302851	0.21343	0.19191
0.344272	0.18162	0.17123
0.356005	0.18172	0.16624
0.383851	0.17655	0.15569
0.411111	0.16321	0.14684
0.443979	0.01465	0.13762
0.661645	0.11091	0.10041
0.778890	0.09084	0.08893
0.834827	0.09461	0.08434
0.867380	0.08961	0.08196
0.964050	0.07600	0.07589
1.085830	0.08423	0.06909
1.112080	0.06628	0.06782
1.173238	0.06629	0.06502
1.274540	0.06076	0.06085
1.332501	0.05889	0.05868
1.408030	0.05846	0.05607

III.5 LEAST SQUARES FIT OF THE FEPE DATA OF A 2"x2" NaI(Tl) DETECTOR TO THE ANALYTICAL FUNCTIONS

Since the increased detector efficiency compensates for the poor resolution of NaI(Tl) gamma detectors, there is no substitute for its employment in detection of high energy gamma rays. A precise measurement of the gamma ray intensities with gamma detectors necessitates an accurate determination of FEPE, which is one of the important characteristics of the detector. The experimental procedure for determining FEPE are complicated by the need to maintain good geometry and to compensate for absorption effects. The semi-empirical approach provides the potential and accurate way to determine the FEPE. The advantage of this technique is that all geometrical and scaling factors may be treated as the parameters which can be determined empirically.

An investigation to check the validity of various analytical functions to the FEPE of a 3"x3" NaI(Tl) detector has been done by Sudarshan [6]. Here we have studied the validity of some analytical functions for representing the FEPE data of a 2"x2" NaI(Tl) detector in the energy range from 59.5 to 1408.03 keV. In the past they have been employed for the FEPE of the germanium detectors only.

We have determined the intrinsic FEPE of the 2"x2" NaI(Tl) detector (as discussed in section III.3) with overall error of less than 8% . The fitting of the FEPE data thus obtained was done by making use of the following analytical functions. Several convenient analytical functions, whose parameters are to

be regarded as variables to be obtained from a fitting procedure, have been proposed by several investigators [12 & 22-27].

The analytical expressions put forward by Kane and Mariscotti [22] for the FEPE, ε, in the energy range from 59.5 to 1408.03 keV for the 9 cm^3 co-axial Ge(Li) detector, was able to describe the FEPE of our 2"x2" NaI(Tl) detector reasonably well. This analytical function is a two parameter function of the form,

$$\ln \varepsilon = bx + cx^2, \qquad (17)$$

with $x = \ln(1.022/E_\gamma)$,

where E_γ is the gamma ray energy, and b and c are the parameters. Mcnelles and Campbell [12] treated 1.022 also as a parameter to fit the FEPE data of their 25 cm^3 co-axial Ge(Li) detector and obtained a poor fit. Later on Singh [13] obtained a very good fit to the FEPE data from 319.8 to 2598.8 keV to his 38 cm^3 co-axial Ge(Li) detector by treating x as, $x = \ln(a/E_\gamma)$ (a being an additional parameter). With this modified function, the obtained fit for our present detector was quite good for energies from 59.5 to 1408.03 keV which is shown in Fig.III.21.

East [23] proposed an analytical function for describing the FEPE of a 50 cm^3 co-axial Ge(Li) detector using a four parameter expression as

$$\varepsilon = \alpha_1 \exp(\beta_1 E_\gamma) + \alpha_2 \exp(\beta_2 E_\gamma), \qquad (18)$$

where α_1, α_2, β_1 and β_2 are the parameters and obtained a good representation of the FEPE in a limited energy region from 54 to 1332.48 keV. When this function was applied to the FEPE of our 2"x2" NaI(Tl) detector a good fit was acheived in the same energy region which is clear from Fig.III.22.

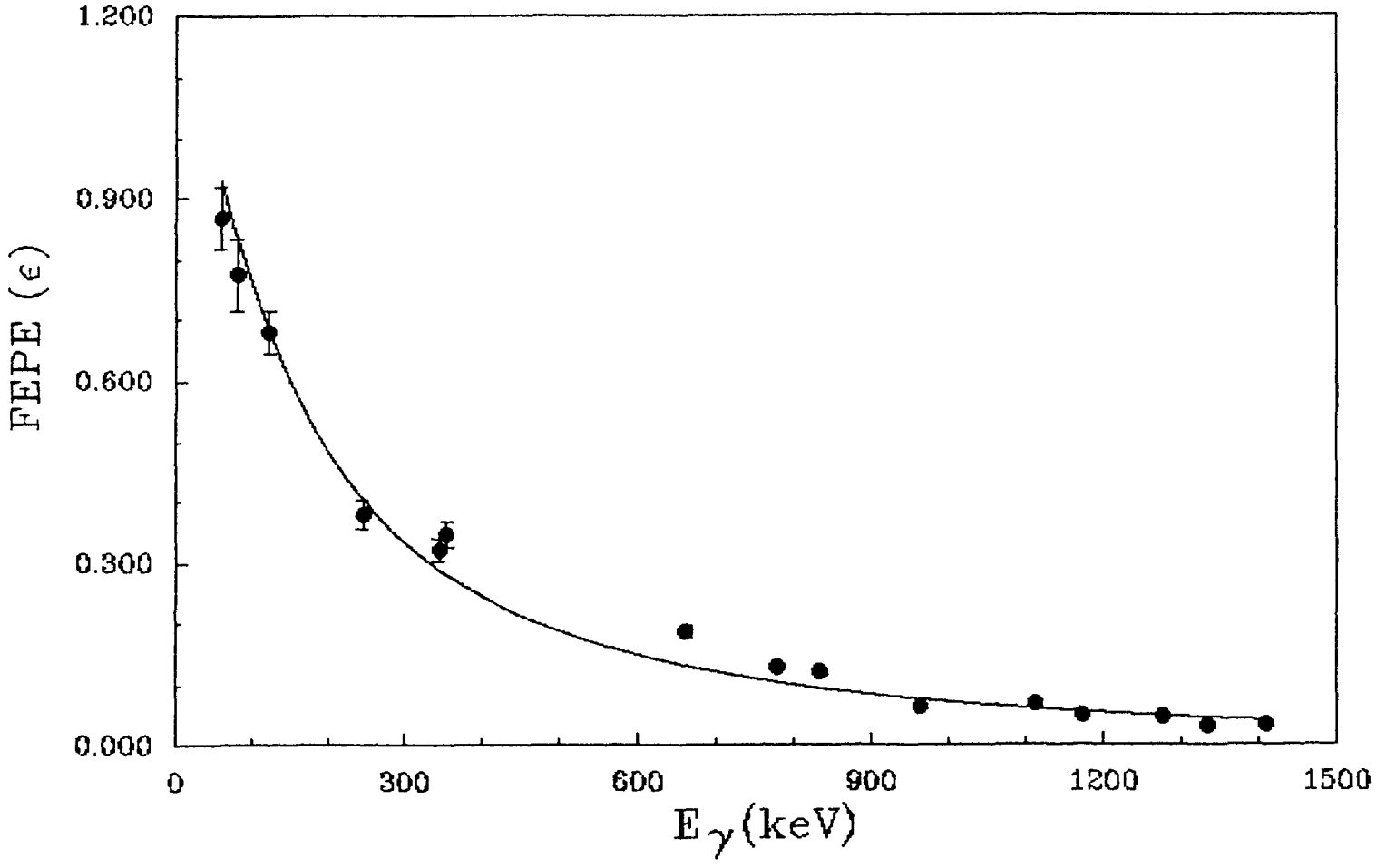

Fig.III.21 Least-Square fit of the FEPE data of the 2"x2" NaI(Tl) detector to eqn.(17).

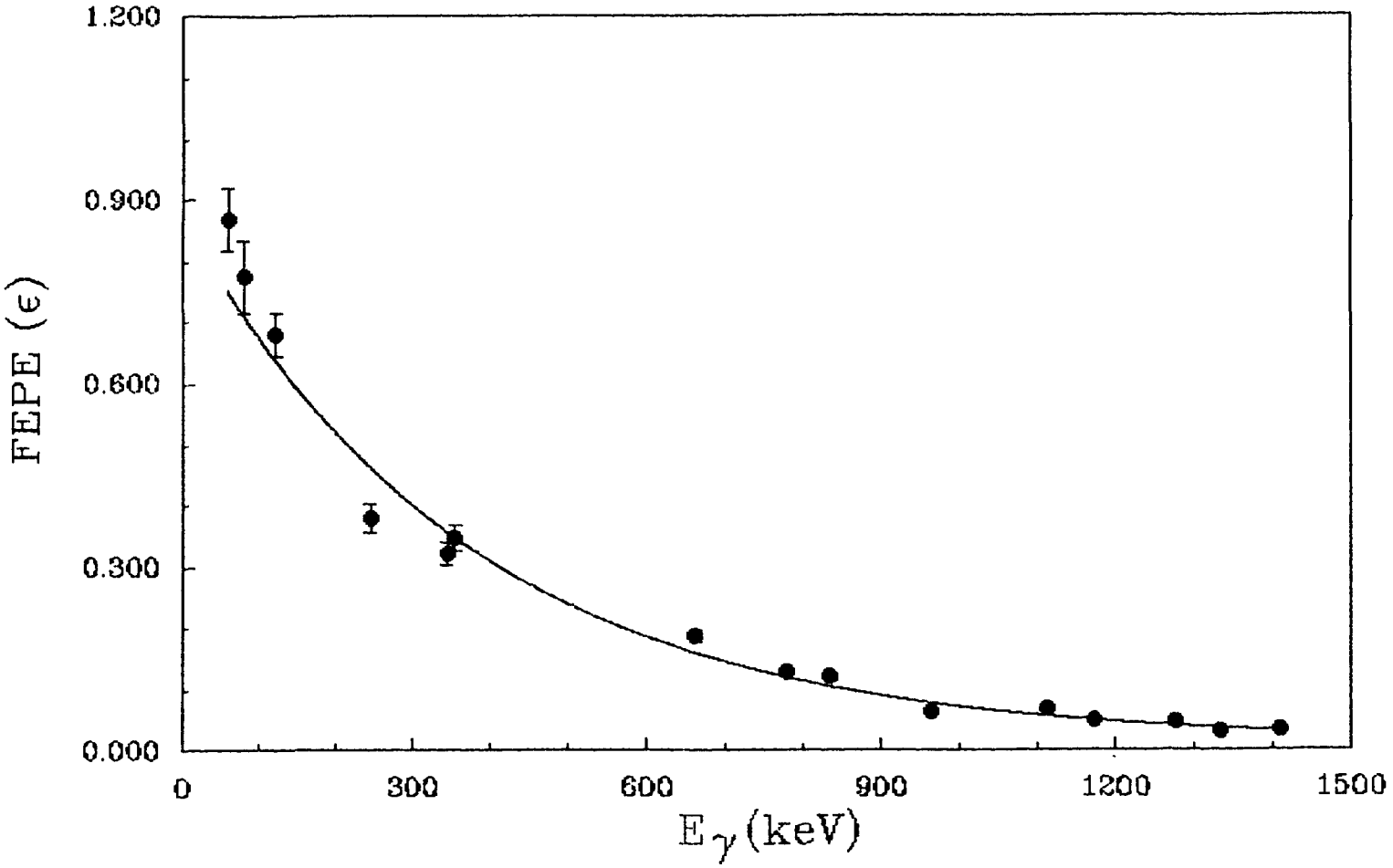

Fig.III.22 Least-Square fit of the FEPE data of the 2"x2" NaI(Tl) detector to eqn.(18).

McNelles and Campbell [12] put forward an eight parameter function for their 25 cm^3 Ge(Li) detector (given by eqn.(11).This gave the best representation for their data. But Singh [13] found that, for his 38 cm^3 Ge(Li) detector, this function, without the last term, gave an excellent fit to the experimental data. So we used the six parameter analytical function to represent the FEPE of the present data and obtained quite a good fit which is shown in Fig.III.23.

Willet [24] suggested a three parameter analytical function, which accounts for the absorption of low energy gamma rays, to represent the FEPE of Ge(Li) detector in an energy range from 392 to 1332.5 keV.

$$\ln(\varepsilon) = A \ln E_\gamma + B (\ln E_\gamma)^2 - C/E_\gamma^3, \qquad (19)$$

where A, B and C are the parameters. This function gave a reasonable description of the efficiency of our detector excluding the region from 244 to 900 keV as can be seen in Fig.III.24.

Gray and Ahmed [25] offered a polylog function and checked it for a number of Ge(Li) detectors in the energy range from 120 to 1850 keV. The polylog function is

$$\varepsilon = [P_1+P_2\ln E_\gamma+P_3(\ln E_\gamma)^2+P_4(\ln E_\gamma)^3+P_5(\ln E_\gamma)^5+P_6(\ln E_\gamma)^7]/E_\gamma \qquad (20)$$

where P's are the parameters. A fairly good fit was obtained (for $E_\gamma \geq 900$ keV) for the FEPE of the present detector with this function as depicted in Fig.III.25.

Hubert et.al [26] suggested the following analytical function for a 174 cm^3 HPGe detector to describe its FEPE from $\sim$ 110 keV to 5 MeV

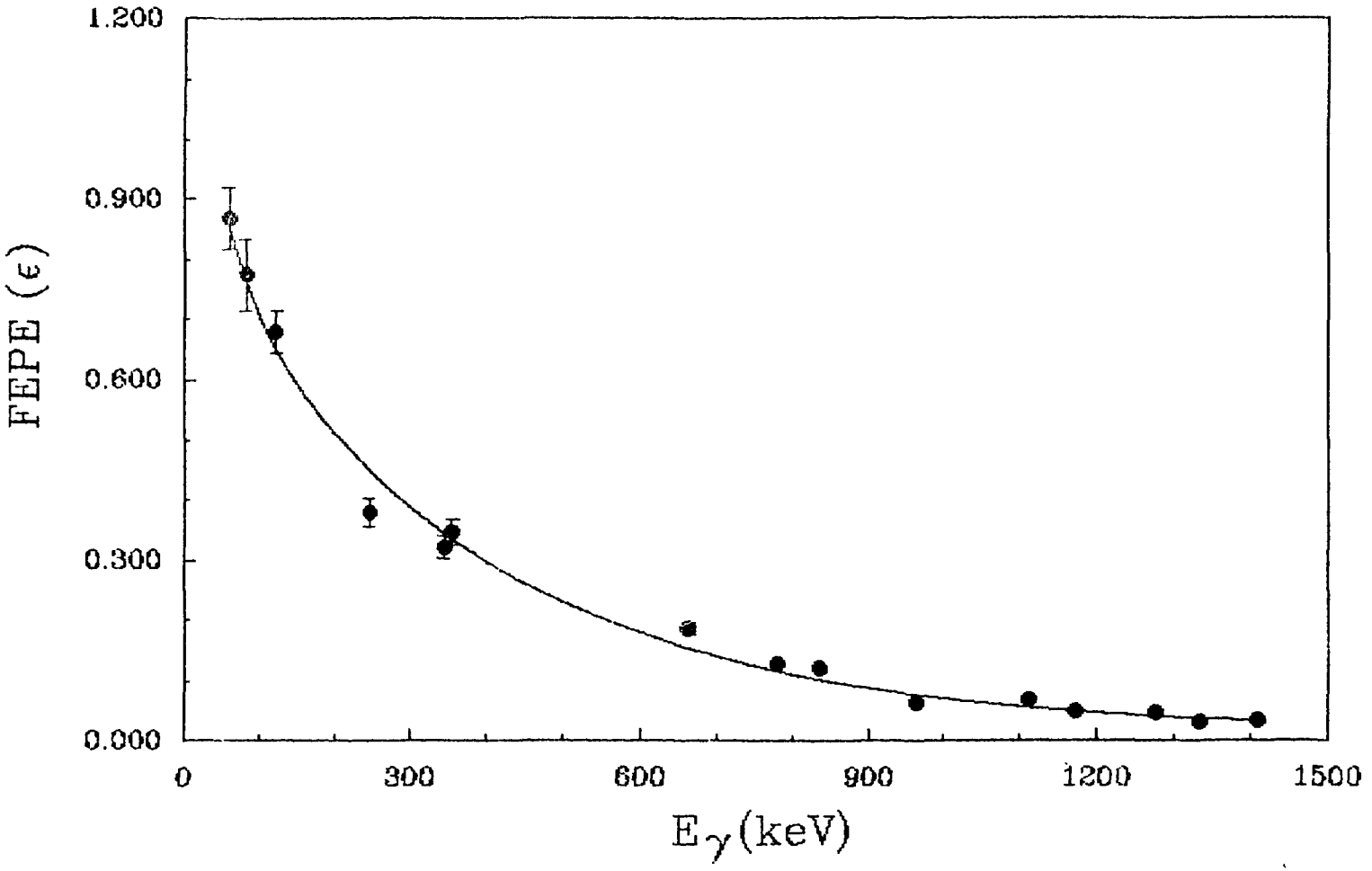

Fig.III.23 Least-Square fit of the FEPE data of the 2"×2" NaI(Tl) detector to eqn.(11) (without the last term).

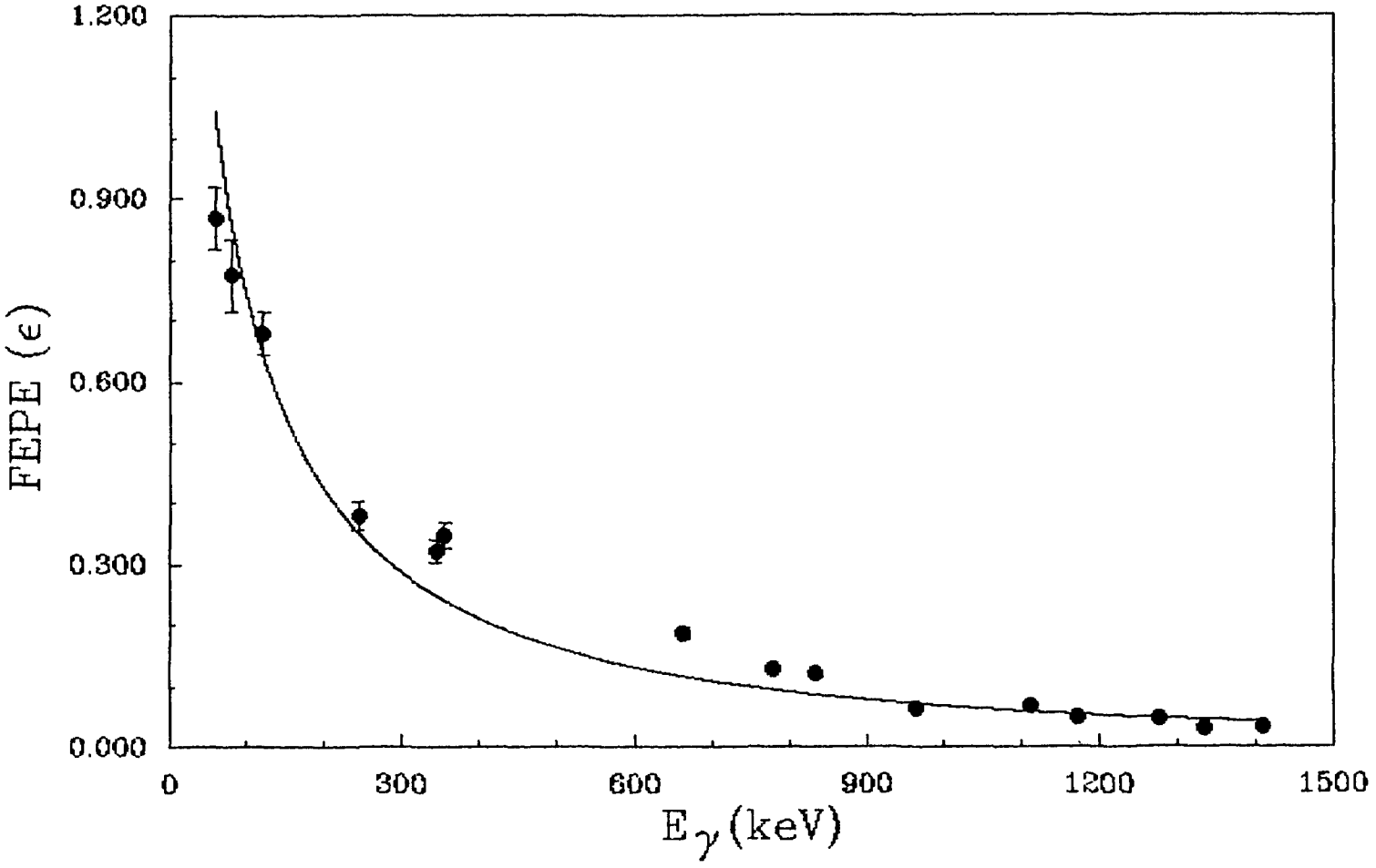

Fig.III.24 Least-Square fit of the FEPE data of the 2"x2" NaI(Tl) detector to eqn.(19).

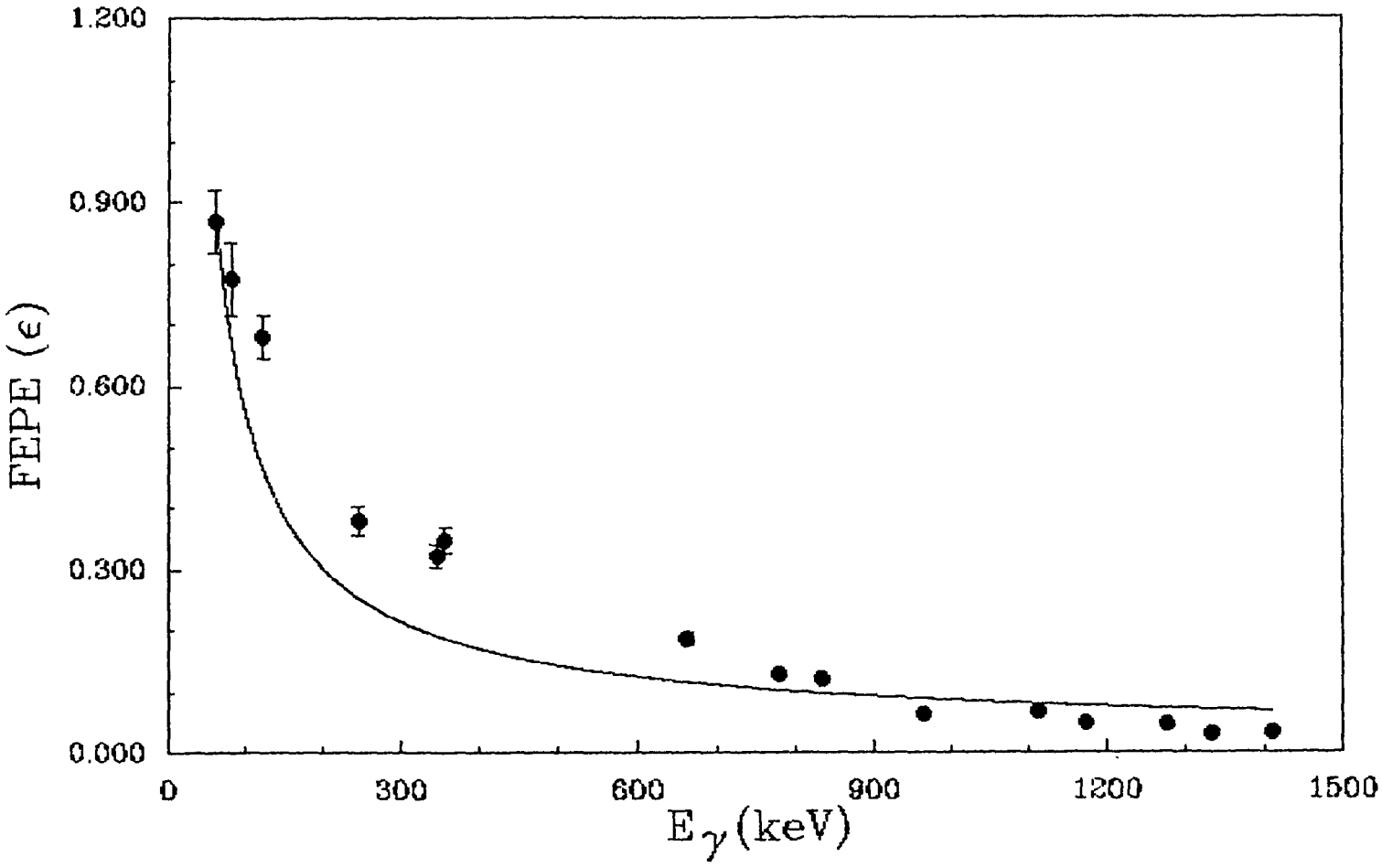

Fig.III.25 Least-Square fit of the FEPE data of the 2"x2" NaI(Tl) detector to eqn.(20).

$$\varepsilon = 10^{-3}\exp\,[8.544 - 0.8581\ln E_\gamma + 0.002701(\ln E_\gamma)^2], \quad (21)$$

we simply re-wrote this equation as

$$\varepsilon = a_1\exp\,[a_2 - a_3\ln E_\gamma + a_4(\ln E_\gamma)^2], \quad (22)$$

with a's as parameters and carried out a fit to our data.

This analytical function gave a poor fit, compared to the other functions, when used to represent FEPE curve of the 2"x2" NaI(Tl) detector. This fit is shown in Fig.III.26. The fit was not as good specially in the region between 150 to 900 keV, as can be noted.

Mitchell [27] constructed a model for describing the gamma ray response function for both scintillation and semi-conductor detectors. The function is

$$\varepsilon = [\phi^n / (1 + \phi^n)]^{1/n}, \quad (23)$$

where $\phi = \exp(\alpha x + \beta x^2)$ and

$$x = 0.1\,[\ln E_\gamma - \ln E_o]$$

E_o, α and β are the parameters and n = 4 for scintillation counter. We treated n also as a parameter and obtained a reasonably good fit and obtained a value of 4.13 for n. This fit is shown in Fig.III.27.

The parameters involved in all these functions as obtained in the present investigation alongwith the χ^2 values and % mean deviations are given in Table III.13.

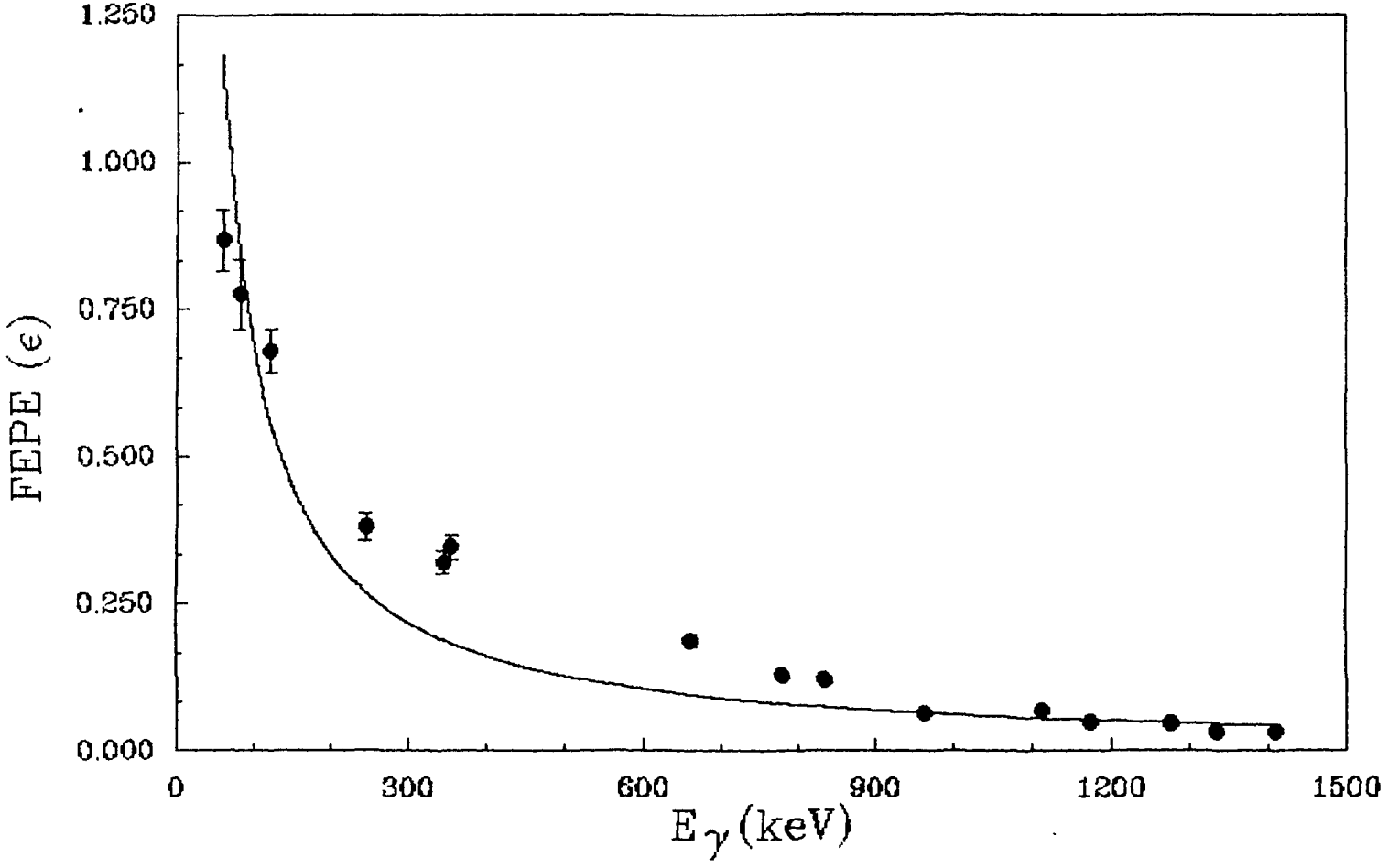

Fig.III.26 Least-Square fit of the FEPE data of the 2"x2" NaI(Tl) detector to eqn.(22).

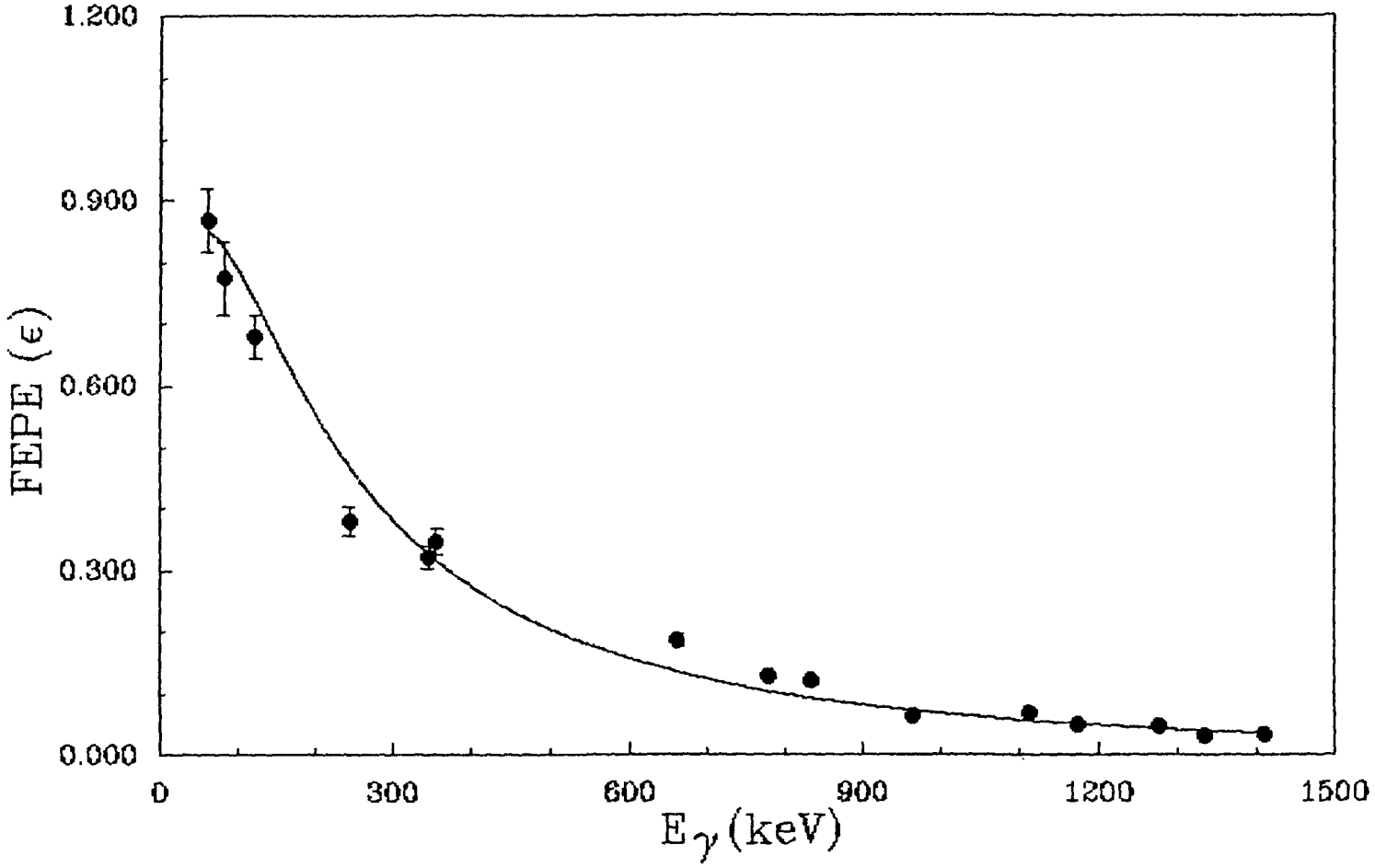

Fig.III.27 Least-Square fit of the FEPE data of the 2"x2" NaI(Tl) detector to eqn.(23).

Table III.13 Table showing the parameters obtained from the LSF of the FEPE data of 2"x2" NaI(Tl) detector to the analytical functions.

Equation Number	Parameters
(17)	$a = 0.356171 \times 10^{2}$ $b = 0.280500 \times 10^{-1}$ $c = -0.228980000$ $\chi^2 = 5.11000 \times 10^{-1}$ % mean deviation = 15.42
(18)	$\alpha_1 = 6.74370 \times 10^{-1}$ $\alpha_2 = 0.10993 \times 10^{-1}$ $\beta_1 = -0.26676 \times 10^{-2}$ $\beta_2 = 0.78150 \times 10^{-4}$ $\chi^2 = 2.53000 \times 10^{-1}$ % mean deviation = 11.1
(11)	$a_1 = 1.65832 \times 10^{1}$ $a_2 = 1.36672000$ $a_3 = 0.79526000$ $a_4 = 0.26680 \times 10^{-2}$ $a_5 = 0.01182000$ $a_6 = 2.22000 \times 10^{-1}$ $\chi^2 = 2.22000 \times 10^{-1}$ % mean deviation = 9.72
(11) (for 157 cm^3 HPGe detector)	$a_1 = 0.35274350$ $a_2 = 0.46092310$ $a_3 = 0.32303680$ $a_4 = 0.2936959 \times 10^{-2}$ $a_5 = 0.3106724 \times 10^{-1}$ $a_6 = -0.3007867 \times 10^{-4}$ $\chi^2 = 5.3833790 \times 10^{-2}$ % mean deviation = 3.82

Table III.13 (contd.)

Equation Number	Parameters
(19)	$A = 0.5881500$ $B = -0.141420$ $C = 0.7857 \times 10^{-2}$ $\chi^2 = 7.7400 \times 10^{-1}$ % mean deviation = 19.77
(20)	$P_1 = 0.508028 \times 10^{2}$ $P_2 = 0.108219 \times 10^{2}$ $P_3 = 0.591420 \times 10^{-1}$ $P_4 = 0.181500 \times 10^{-2}$ $P_5 = -0.19010 \times 10^{-2}$ $P_6 = 0.625000 \times 10^{-5}$ $\chi^2 = 4.210000 \times 10^{0}$ % mean deviation = 42.61
(22)	$a_1 = 0.339500 \times 10^{-3}$ $a_2 = 0.124228 \times 10^{2}$ $a_3 = 0.104406 \times 10^{1}$ $a_4 = 0.134300 \times 10^{-5}$ $\chi^2 = 1.480000 \times 10^{0}$ % mean deviation = 27.18
(23)	$n = 0.413020 \times 10^{1}$ $E_0 = 0.668750 \times 10^{2}$ $\alpha = -0.19152 \times 10^{1}$ $\beta = -2.96345 \times 10^{1}$ $\chi^2 = 3.55000 \times 10^{-1}$ % mean deviation = 12.83

III.6 VARIATION OF MEASURED RESOLUTION WITH GAMMA ENERGY

As mentioned earlier gamma ray spectroscopy have long been dominated by two categories of detectors namely NaI(Tl) and germanium detectors. The superior energy resolution of germanium detectors as compared to NaI(Tl) detectors has already been mentioned in chapter II alongwith the factors affecting the resolution.

Considering the dominance of statistical broadening of the peak among other potential sources, the variation of the resolution with photon energy is given as, (from eqn.(5) in chapter II)

$$\ln R = \ln K - (1/2)\ln E_{\gamma}.$$

We have made graphical representations of the variation of the measured resolution with photon energy for our 157 cm^3 co-axial HPGe detector, and 3"x3" and 2"x2" NaI(Tl) detectors (see Tables III.14-III.16). They are depicted in Figs.III.28-III.30 (similar to Fig.II.1). From these figures it is clear that the non-statistical potential sources like variation in charge collection, effect of electronic noise etc. also contributes to the peak broadening because the slope is not as steep as predicted (see ref [6] of chapter II).

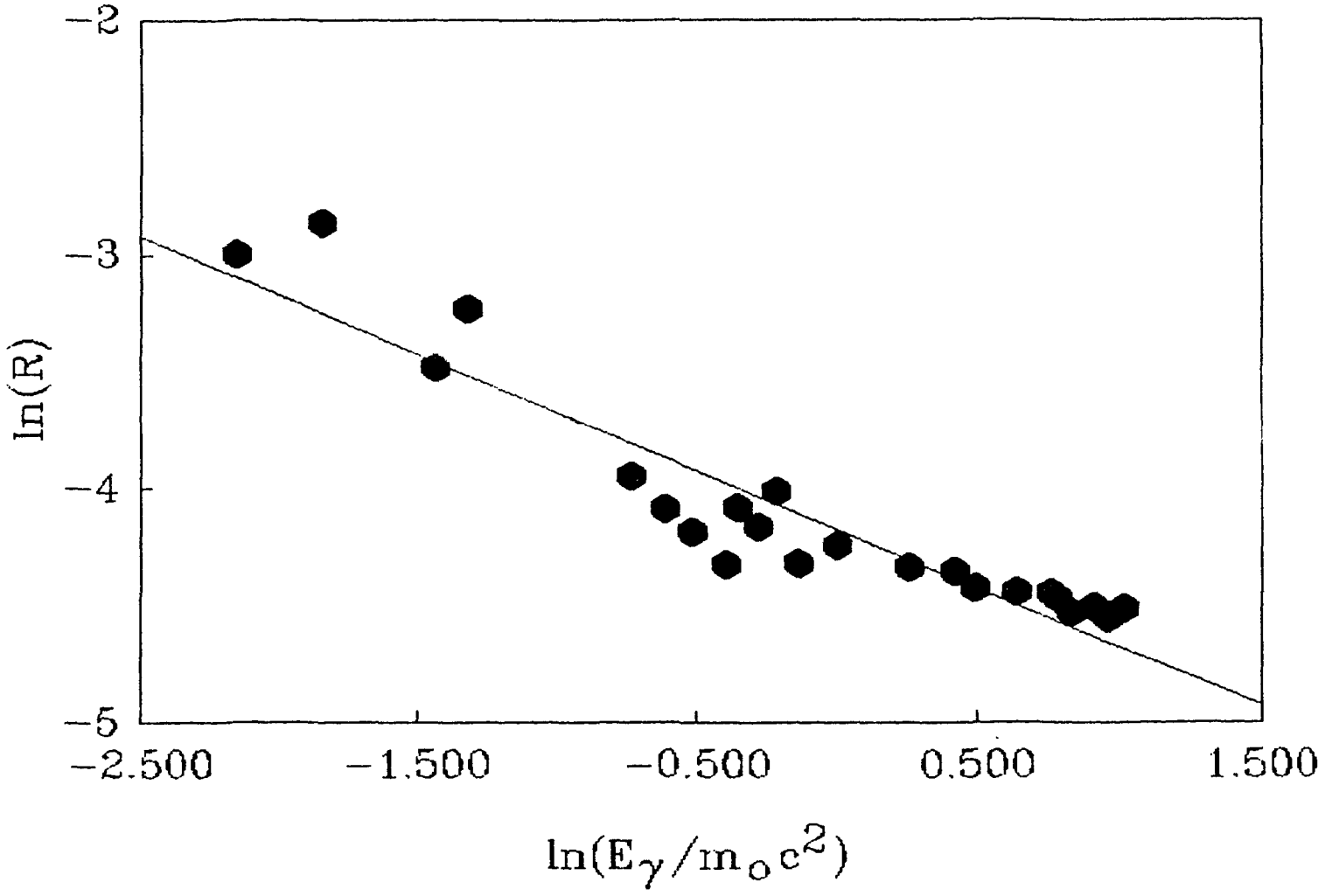

Fig.III.28 Experimentally measured resolution R from a HPGe detector for various gamma ray energies E_γ.

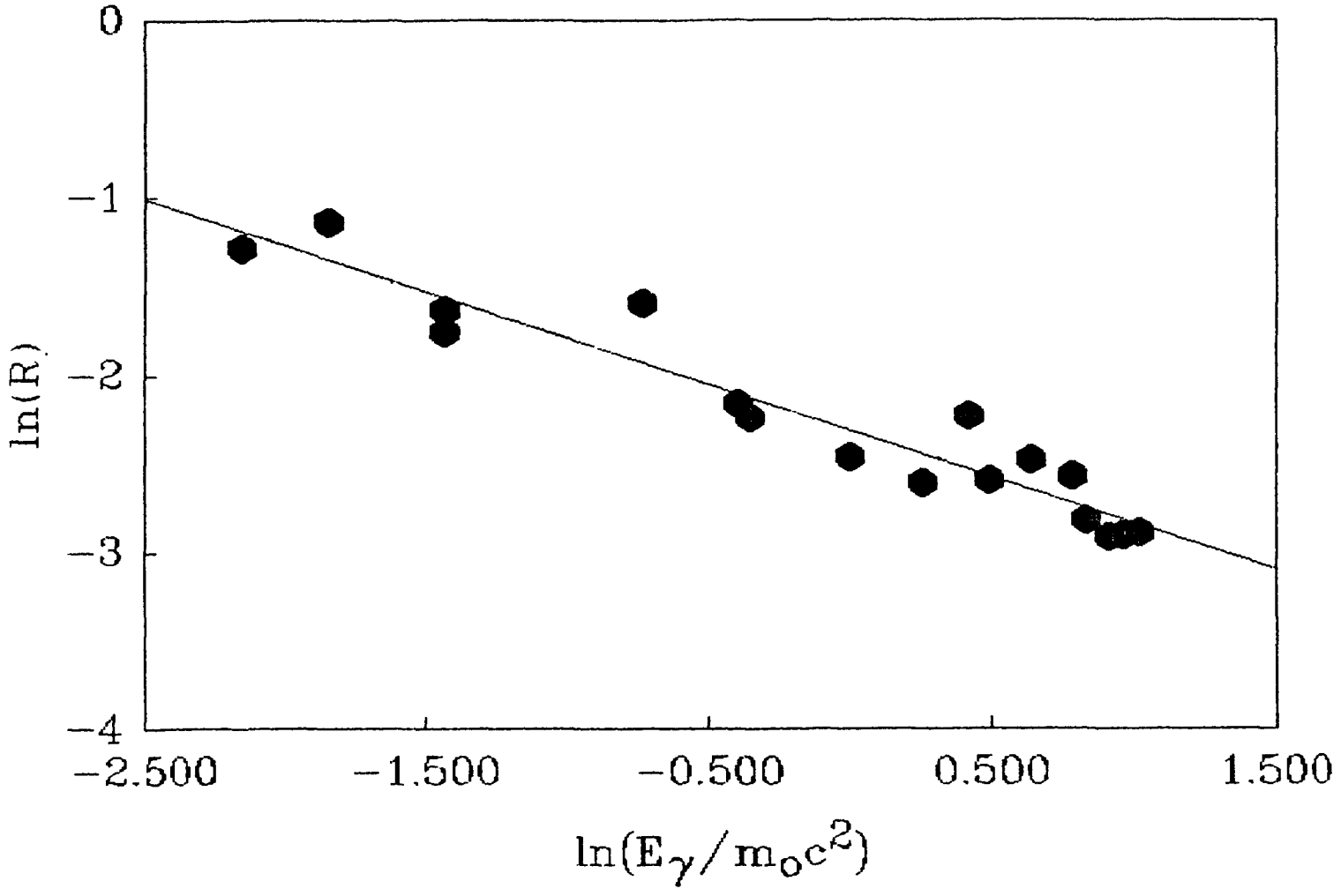

Fig.III.29 Experimentally measured resolution R from a 3"x3" NaI(Tl) detector for various gamma ray energies E_γ.

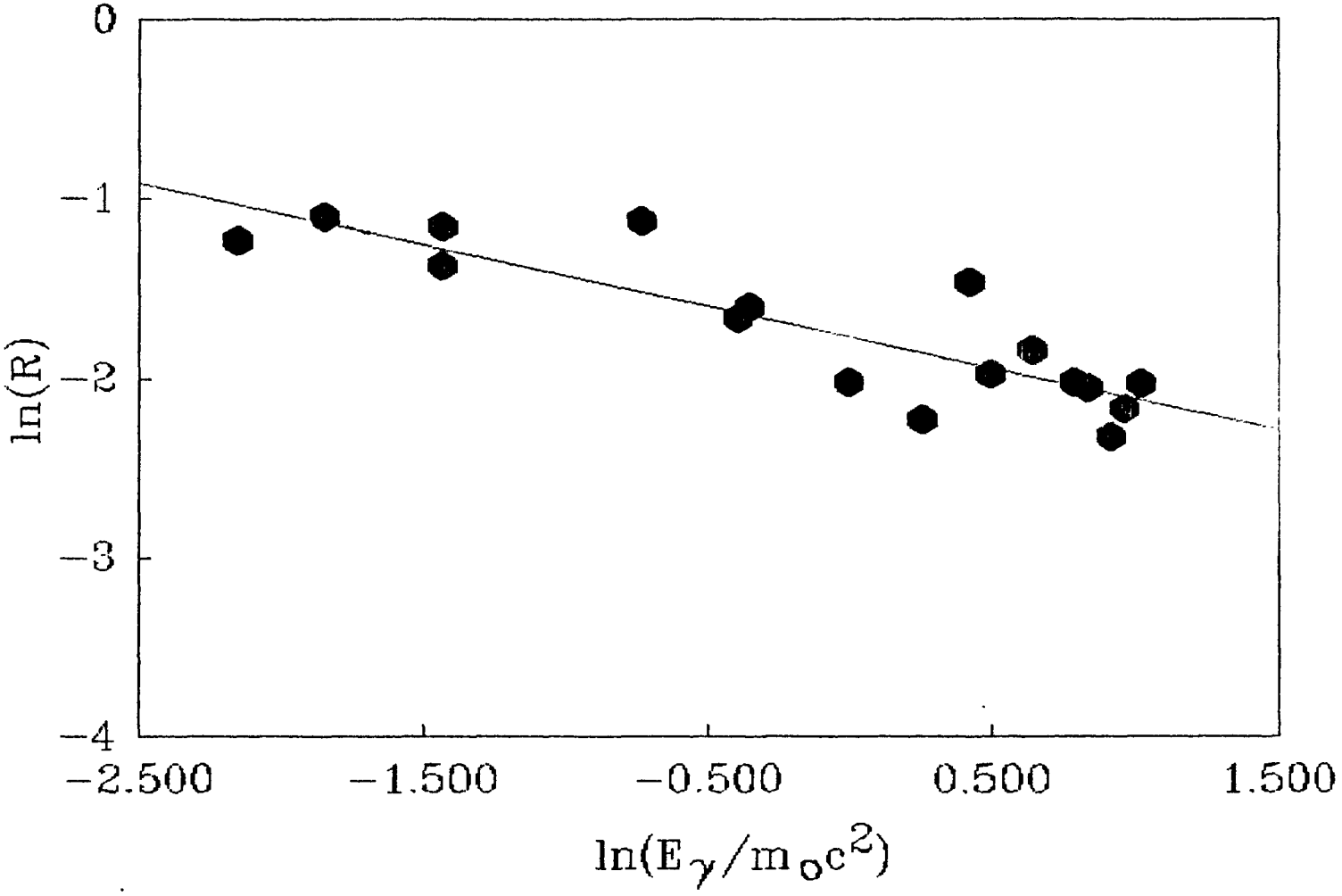

Fig.III.30 Experimentally measured resolution R from a 2"x2" NaI(Tl) detector for various gamma ray energies E_γ.

Table III.14 Table showing the lnR and $\ln(E_\gamma/m_o c^2)$ at different energies for the 157 cm^3 HPGe detector.

E_γ (keV)	ln R	$\ln(E_\gamma/m_o c^2)$
59.5370	-2.99573	-2.14977
80.9970	-2.99373	-1.84195
121.779	-3.48124	-1.43416
122.063	-3.48124	-1.43183
136.476	-3.23212	-1.32022
244.693	-3.94481	-0.73636
276.397	-4.08317	-0.61453
302.851	-4.03044	-0.52312
344.272	-4.32634	-0.39499
356.005	-4.07754	-0.36142
383.851	-4.15888	-0.28612
411.111	-4.01096	-0.21751
443.979	-4.31414	-0.14059
511.006	-4.24276	0.00000
661.645	-4.33511	0.258350
778.890	-4.35119	0.421500
834.827	-4.42227	0.490850
964.050	-4.43823	0.634770
1085.83	-4.44526	0.753730
1112.08	-4.46845	0.777610
1173.238	-4.52541	0.831150
1274.54	-4.50535	0.913970
1332.501	-4.55071	0.958440
1408.03	-4.51085	1.013570

Table III.15 Table showing the lnR and $\ln(E_\gamma/m_oc^2)$ at different energies for the 3"x3" NaI(Tl) detector.

E_γ (keV)	ln R	$\ln(E_\gamma/m_oc^2)$
59.5370	-1.28401	-2.14977
80.9970	-1.33281	-1.84195
121.779	-1.73582	-1.43416
122.063	-1.66945	-1.43183
344.272	-2.16204	-0.39499
356.005	-2.23773	-0.36142
511.006	-2.46254	0.00000
661.645	-2.60542	0.258350
834.827	-2.58953	0.490850
964.050	-2.47539	0.634770
1112.08	-2.56832	0.777610
1173.238	-2.82137	0.831150
1274.54	-2.90822	0.913970
1332.501	-2.90311	0.958440
1408.03	-2.88702	1.013570

Table III.16 Table showing the lnR and $\ln(E_\gamma/m_oc^2)$ at different energies for the 2"x2" NaI(Tl) detector.

E_γ (keV)	ln R	$\ln(E_\gamma/m_oc^2)$
59.5370	-1.22807	-2.14977
80.9970	-1.0986	-1.84195
121.779	-1.17164	-1.43416
122.063	-1.14916	-1.43183
344.272	-1.66208	-0.39499
356.005	-1.59716	-0.36142
511.006	-1.99240	0.00000
661.645	-2.07674	0.258350
834.827	-1.97630	0.490850
964.050	-1.84330	0.634770
1112.08	-2.02155	0.777610
1173.238	-2.04788	0.831150
1274.54	-2.32521	0.913970
1332.501	-2.16871	0.958440
1408.03	-2.02866	1.013570

III.7 CONCLUDING REMARKS

With the advent of semi-conductor gamma ray spectroscopy, the NAA field has entirely changed and thereby the detection of elements in minute quantities has become increasingly popular. The determination of some elements with neutron induced radioactivity is not posible because of unfavourable decay characteristics and low activation cross sections etc. The interference from unwanted activities in a target material which contains several elements can be nullified by selecting proper irradiation time and counting technique with the knowledge of half-lives. An irradiation of 2-3 half-lives is sufficient for all practical purposes to reach the saturated level of induced activity. By tagging the gamma energies the elements could be identified and the concentrations obtained by determining the intensities of the corresponding gamma rays. The results obtained from the half-life measurement, determination of elemental concentration and relative intensity measurements by making use of this technique have shown quite a good match with the pre-investigated values.

We have determined the FEPE of a 157 cm^3 HPGe and that of a 2"x2" Na(Tl) detector by using a set of standard calibrated gamma ray sources covering a wide energy range. It is evident from the two sets of FEPE data that the FEPE of large volume HPGe detector is less than that of a relatively small NaI(Tl) detector. Of course, a part of the reduction of FEPE of our HPGe detector is also because of the neutron damage it had suffered. We have

calculated the FEPE of the same HPGe detector by using a pre-determined value and observed that the calculated values are quite close to the experimental ones. This method has greately reduced the number of measurement points needed for determining the efficiency curve. We have investigated the applicability of some analytical functions for the FEPE of a 2"x2" NaI(Tl) detector in the energy range from 59.5 to 1408.03 keV. It is clear from examining the FEPE curves obtained, that the analytical functions which were used for representing the FEPE data of germanium detectors can be used well for representing the FEPE of the NaI(Tl) detectors. The best fit could be obtained with the analytical functions of McNelles and Campbell [12], and East [22]. Finally, the variation of the energy resolution of the three (157 cm^3 HPGe, 3"x3" and 2"x2" NaI(Tl)) detectors with gamma energy shows the expected trend.

References

1. G.V.Hevesy and H.Levy, Kgl.Danske.Videnskab.Mat.Fys.Medd., 14 (5) (1936) 3
2. V.R.Rao, Ph.D. Thesis "*Study of an External Beam Irradiation System for Liquids in Charge Particle Activation Analysis*", NEHU, Shillong, (1990) (unpublished)
3. D.E.Lea, Nature, 133 (1934) 24
4. E.Amaldy, O.D.Agostino, E.Fermi, B.DonteCorvo and E.Serge, Recerca Sc., 2 (1934) 467 Cit.Anal.Chem., 40 (1968) 1990
5. M.Sudarshan and R.Singh, Meas.Sci.Technol., 2 (1991) 1192
6. M.Sudarshan, Ph.D. Thesis " *Bulk Elemental Analysis by Neutron Inelastic Scattering and Efficiency of Gamma Detectors*", NEHU, Shillong (1991) (unpublished)
7. Techniches Bullettin, 76/7, June 1929 Amsterdam Buchler
8. K.W.Geiger and Van der Zwan, Nucl.Instr. and meths., 131 (1975) 315
9. A.Kumar and P.S.Nagaraja, Nucl. Instr. and Meths., 140 (1977) 175
10. NIST Standards, Certificate of Analysis- Standard Reference Material (SRM - 1633a)
11. R.J.Batra, A.N.Garg and R.C.Sinvhal, Indian Journal of Technology, 27 (1989) 289
12. L.A.McNelles and J.L.Campbell, Nucl.Instr. and Meths., 109 (1973) 241
13. R.Singh, Nucl.Instr. and Meths., 136 (1976) 543
14. N.L.DaCosta et.al., Nuova Cimento, 50B (1967) 345
15. P.Fettweis and J.Vervier, Z.Phys., 201 (1967) 465

16. G.Garcia-Bermudez et.al., Phys.Rev., C9 (1974) 1060

17. F.Pleiter, Nucl.Phys., A184 (1972) 443

18. F.Pleiter, Z.Phys., 24 (1970) 244

19. F.Pleiter, Nucl.Instr.and Meths., 108 (1973) 503

20. Spectrum Analysis code developed by S.R.Banerjee, VECC, Calcutta (unpublished)

21. Ray Gunnik Nucl.Instr.and Meths., *Physics Research*, A299 (1990) 372

22. W.R.Kane and M.A.Mariscotti, Nucl.Instr. and Meths., 56 (1967) 189

23. L.V.East, Nucl.Instr. and Meths., 93 (1971) 193

24. J.B.Willet, 1971 *Radioactivity in Nuclear Spectroscopy* ed. J H Hamilton (New York, Gordon and Breach) p.1317

25. P.W.Gray and A.Ahmed, Nucl.Instr. and Meths., 237 (1985) 577

26. F.Hubert et.al, Z.Phys., A333 (1989) 237

27. D.G.Mitchell et.al, Nucl.Instr. and Meths., A276 (1989) 547